NAVAL POSTGRADUATE SCHOOL

MONTEREY, CALIFORNIA

THESIS

THE INFLUENCE OF PROTECTIVE POUCHES ON TROPICAL CYCLOGENESIS IN THE CARIBBEAN SEA

by

Meredith A. McKaig

December 2021

Thesis Advisor:	Michael T. Montgomery
Co-Advisor:	Mark A. Boothe
Second Reader:	Scott Powell

THIS PAGE INTENTIONALLY LEFT BLANK

REPORT DOCUMENTATION PAGE			*Form Approved OMB No. 0704-0188*

1. AGENCY USE ONLY *(Leave blank)*	**2. REPORT DATE** December 2021	**3. REPORT TYPE AND DATES COVERED** Master's thesis

4. TITLE AND SUBTITLE THE INFLUENCE OF PROTECTIVE POUCHES ON TROPICAL CYCLOGENESIS IN THE CARIBBEAN SEA	**5. FUNDING NUMBERS**
6. AUTHOR(S) Meredith A. McKaig	
7. PERFORMING ORGANIZATION NAME(S) AND ADDRESS(ES) Naval Postgraduate School Monterey, CA 93943-5000	**8. PERFORMING ORGANIZATION REPORT NUMBER**
9. SPONSORING / MONITORING AGENCY NAME(S) AND ADDRESS(ES) N/A	**10. SPONSORING / MONITORING AGENCY REPORT NUMBER**

11. SUPPLEMENTARY NOTES The views expressed in this thesis are those of the author and do not reflect the official policy or position of the Department of Defense or the U.S. Government.

12a. DISTRIBUTION / AVAILABILITY STATEMENT Approved for public release. Distribution is unlimited.	**12b. DISTRIBUTION CODE** A

13. ABSTRACT (maximum 200 words)

This paper is an investigation of the formation of tropical cyclones in the Caribbean Sea. The research is aimed to investigate the question of whether the formation of tropical cyclones in this area occurs by a different process than in the open ocean? This study is focused on three named late-season storms from the 2020 Atlantic Hurricane season, Gamma, Zeta, and Iota, and investigates the mechanisms behind their formation, with particular focus on the effects of the Okubo-Weiss variable and Dunkerton, Montgomery, and Wang's 2009 marsupial paradigm. This paper investigates the differences in formation of these tropical cyclones through a retrospective examination of the precursors of the storms in a co-moving framework, looking at the evolution of pouches as described in the marsupial paradigm. This study also provides a comparison of the mechanisms that formed these hurricanes, with Iota forming from a tropical wave, Gamma forming from the interaction of a tropical wave and a low-level strip of relative vorticity that rolled up, and Zeta forming from the interaction of a tropical wave and a Central American Gyre.

14. SUBJECT TERMS tropical cyclone, TC, hurricanes, marsupial paradigm, MP, Okubo-Weiss, OW, pouch, prediction, Caribbean Sea, 2020 Hurricane Season,	**15. NUMBER OF PAGES** 107
	16. PRICE CODE

17. SECURITY CLASSIFICATION OF REPORT Unclassified	**18. SECURITY CLASSIFICATION OF THIS PAGE** Unclassified	**19. SECURITY CLASSIFICATION OF ABSTRACT** Unclassified	**20. LIMITATION OF ABSTRACT** UU

NSN 7540-01-280-5500

Standard Form 298 (Rev. 2-89)
Prescribed by ANSI Std. 239-18

THIS PAGE INTENTIONALLY LEFT BLANK

Approved for public release. Distribution is unlimited.

THE INFLUENCE OF PROTECTIVE POUCHES ON TROPICAL CYCLOGENESIS IN THE CARIBBEAN SEA

Meredith A. McKaig
Lieutenant Commander, United States Navy
BS, United States Naval Academy, 2011

Submitted in partial fulfillment of the
requirements for the degree of

MASTER OF SCIENCE IN METEOROLOGY AND PHYSICAL OCEANOGRAPHY

from the

NAVAL POSTGRADUATE SCHOOL
December 2021

Approved by: Michael T. Montgomery
Advisor

Mark A. Boothe
Co-Advisor

Scott Powell
Second Reader

Wendell A. Nuss
Chair, Department of Meteorology

THIS PAGE INTENTIONALLY LEFT BLANK

ABSTRACT

This paper is an investigation of the formation of tropical cyclones in the Caribbean Sea. The research is aimed to investigate the question of whether the formation of tropical cyclones in this area occurs by a different process than in the open ocean? This study is focused on three named late-season storms from the 2020 Atlantic Hurricane season, Gamma, Zeta, and Iota, and investigates the mechanisms behind their formation, with particular focus on the effects of the Okubo-Weiss variable and Dunkerton, Montgomery, and Wang's 2009 marsupial paradigm. This paper investigates the differences in formation of these tropical cyclones through a retrospective examination of the precursors of the storms in a co-moving framework, looking at the evolution of pouches as described in the marsupial paradigm. This study also provides a comparison of the mechanisms that formed these hurricanes, with Iota forming from a tropical wave, Gamma forming from the interaction of a tropical wave and a low-level strip of relative vorticity that rolled up, and Zeta forming from the interaction of a tropical wave and a Central American Gyre.

THIS PAGE INTENTIONALLY LEFT BLANK

TABLE OF CONTENTS

THIS PAGE INTENTIONALLY LEFT BLANK

LIST OF FIGURES

THIS PAGE INTENTIONALLY LEFT BLANK

LIST OF ACRONYMS AND ABBREVIATIONS

ACE	Accumulated Cyclone Energy
AEW	African Easterly Wave
AFB	Air Force Base
AWP	Atlantic Warm Pool
CAG	Central American Gyre
CL	Critical Latitude
ELI	ENSO Longitude Index
ENSO	El Niño Seasonal Oscillation
GFS	Global Forecast System
GIS	Geographic Information System
GOES	Geostationary Operational Environmental Satellite
GOM	Gulf of Mexico
IR	Infrared
MDR	Main Development Region
MJO	Madden Julian Oscillation
MP	Marsupial Paradigm
NHC	National Hurricane Center
OW	Okubo-Weiss parameter
QGIS	Quantum Geographic Information System
RH	Relative Humidity
RI	Rapid Intensification
SSHWS	Saffir-Simpson Hurricane Wind Scale
SST	Sea Surface Temperature
TC	Tropical Cyclone
TD	Tropical Depression
TPW	Total Precipitable Water
TS	Tropical Storm
TUTT	Tropical Upper Tropospheric Trough
WGS	World Geodetic System

THIS PAGE INTENTIONALLY LEFT BLANK

ACKNOWLEDGMENTS

I would like to express my deepest gratitude for my advisory team, Dr. Michael T. Montgomery and Mr. Mark Boothe, for guiding me through this process and lending their experience and expertise to the problem. Thank you both for your tireless help and advice, especially in the final stages of the thesis experience.

Thank you also to Dr. Scott Powell for your help in making this paper both more readable and scientific. Your comments have been invaluable in improving this thesis.

I am also extremely grateful for my family, specifically my mom, Ilene McKaig, and my sister, Libby McKaig, who have been very supportive of my efforts here at NPS.

THIS PAGE INTENTIONALLY LEFT BLANK

I. INTRODUCTION

A. SYNOPSIS

Hurricanes have caused problems for people in the Americas for hundreds of years. Though they were not necessarily well understood in the Age of Sail, they were known hazards to ships and coastlines, endangering lives and livelihoods with their wrath. Today, there has been significant advancement in the prediction and tracking of such storms, but there are still times when the meteorological community has struggled to predict the effects of these storms in a timely manner.

Forecasting of Tropical Cyclones (TC) has been greatly improved from the advancements in the understanding of how tropical cyclones form. In his pioneering work, William Gray (1975) established the six "Primary Genesis Parameters" of low-level cyclonic relative vorticity, the presence of the Coriolis Effect, low vertical wind shear, sea surface temperature (SST) above 79°F in at least 200 feet of water depth, a vertical gradient in Θ_e that supports deep convection, and sufficient relative humidity in the middle troposphere to support genesis (Gray 1975). These parameters were supplemented by the work of Dunkerton, Montgomery, and Wang with the Marsupial Paradigm (MP) conceptual model (Dunkerton et al. 2009). Using operational global analysis data together with NASA TRMM data on precipitation rate, this work established that it is also necessary for a quasi-closed recirculating region (or protective "pouch") to form around the center of the disturbance in order to facilitate the growth of a storm as opposed to generic widespread convection without any organization. When a disturbance is viewed in a pre-storm relative (or co-moving) framework, the pouch within the wave trough region strongly resembles a "Kelvin cat's-eye" circulation. A Kelvin cat's eye is what an observer sees when moving at the wave speed. In this co-moving frame, a recirculating vortex, which is isolated from its surroundings becomes evident. The vortex and the tow exterior nodes in the co-moving streamlines resemble the shape of a cat's eye. A Kelvin cat's eye can exist in any fluid flow, but the presence of one in the tropical atmosphere is hypothesized to be necessary for the formation of a

tropical cyclone from easterly waves or other wave-like disturbances in monsoonal environments.

As can be seen in Figure 1, the pouch forms along the pressure trough region of a tropical wave and serves to protect the disturbance from the adverse effects of environmental vertical wind shear and dry air entrainment. Oftentimes, pouches are only visible in the co-moving framework. The co-moving framework allows the streamlines to be analyzed with respect to how they are affecting the precursor disturbance from the pre-storm's frame of reference (Dunkerton et al. 2009).

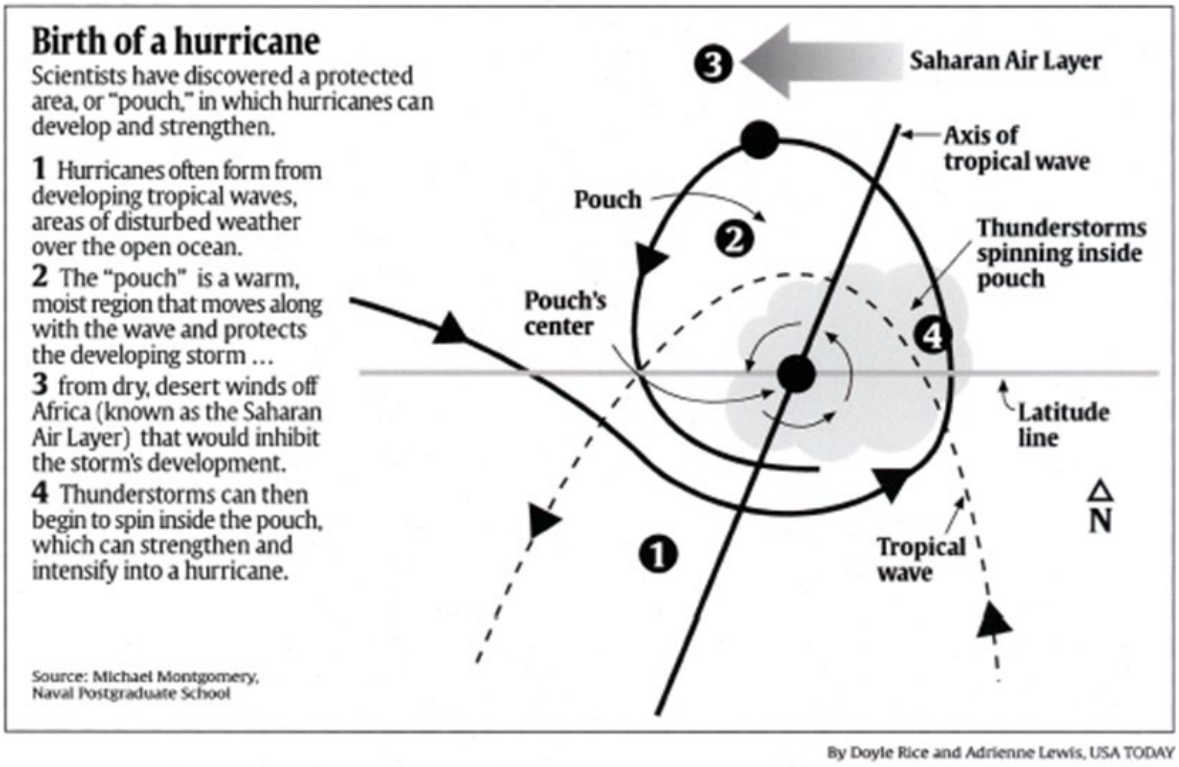

A graphical depiction and description of a pouch forming and growing a promotive environment for tropical cyclone formation. The trough axis, critical latitude (labeled "Latitude line"), and tropical wave are all visible.

Figure 1. Graphic depiction of the Marsupial Paradigm.
Source: Rice (2008).

There are three hypotheses associated with the marsupial paradigm. The first hypothesis states that the precursor to a cyclone develops a Kelvin cat's eye due to the

interaction of the parent wave and its critical latitude (CL), which is defined as where "the intrinsic wave frequency goes to zero" (Dunkerton et al. 2009). The critical latitude is "the locus of points where this low-frequency zonal wind matches the zonal phase speed of the wave" (Dunkerton et al. 2009), where low-frequency is determined to mean that the period of the wave is greater than nine days (Dunkerton et al. 2009). The critical latitude is expressed mathematically as seen in equation (1).

$$c = \mathbf{k} \bullet \mathbf{U} \tag{1}$$

In this equation the critical latitude is "defined as the location where c = U" (Dunkerton et al. 2009), where the time-mean flow is **U**, (often approximated by the zonal component of the mean vector wind for near-westward traveling disturbances), the wave phase speed in the wave's propagation direction is c, and **k** is the unit wavevector. This Kelvin cat's eye develops into a "pouch," which largely encloses an area of nearly zero mean relative flow.

The small mean relative flow allows for the aggregation of cloud-enhanced, low-level, cyclonic vorticity near the so-called "sweet spot" of the wave trough and thereby enhanced cyclonic rotation (Dunkerton et al. 2009) This so-called "bottom-up development" of the cyclonic rotation provides a buffer against straining and shearing deformations that would otherwise rip the vortex apart (Dunkerton et al. 2009).

The second hypothesis states that the Kelvin cat's eye formation of the parent wave provides a semi-closed environment in which convection moistens the atmosphere and protects the nascent cyclone from detrimental factors in the external environment (such as vertical wind shear), in effect a protective pouch (Dunkerton et al. 2009) In effect, the pouch both shelters the precursor disturbance and allows the convection to further moisten the pouch and grow (Dunkerton et al. 2009).

The third hypothesis is that the parent wave maintains or enhances the wave amplitude from the vortical eddies in the wave that are augmented by diabatic heating, which is more in areas where phase speed is low (Dunkerton et al. 2009).

When taken together, in simple terms the marsupial paradigm says that in order for a tropical cyclone to grow from a precursor disturbance, the precursor disturbance must first develop a Kelvin cat's eye pouch that protects the nascent disturbance from a hostile environment outside the pouch, particularly from the mechanical effects of horizontal and vertical wind shear and adverse thermodynamical effects associated with dry air (Dunkerton et al. 2009). This pouch allows for deep convection to develop that both enhances cyclonic vorticity within and moistens the air column. These processes are especially favored near the center (or sweet spot) of the pouch. The wave that generates the pouch is maintained and/or strengthened by the diabatic eddies within the pouch (Dunkerton et al. 2009).

The effects and presence of these pouches can be observed by plotting the relative vorticity (ζ) and Okubo-Weiss parameter (hereafter OW) (Dunkerton et al. 2009). Vorticity is defined as "a vector measure of local rotation in a fluid flow, defined mathematically as the curl of the velocity vector" (American Meteorological Society [AMS] 2014).

$$\zeta = \nabla \times \mathbf{u} \tag{2}$$

In Equation (2), vorticity is denoted by the Greek letter ζ, and the velocity vector is given by the boldface variable **u**. This study uses relative vorticity, which is the tendency of a parcel to spin relative to the Earth, which itself is spinning in the absolute frame. Since the storm formation instances examined in this thesis occurred in the Northern Hemisphere, the association of positive vorticity with cyclonic (counterclockwise) flow will be used throughout. For clarity purposes, as one of the storms investigated was Hurricane Zeta, this study will always refer to relative vorticity as such vice the colloquial term "zeta." Unless otherwise stated, vorticity will be taken to mean the vertical component of the three-dimensional vector quantity. Relative vorticity is a key quantity because it is an indication of the spin of a fluid particle and the cyclonic rotation indicated by positive vorticity is a necessary ingredient in a burgeoning tropical cyclone.

OW is defined as "a measure of the shape-preserving component of a vortical flow in comparison to (i) the shape-destroying component associated with shearing

deformation, and (ii) straining deformation" (Dunkerton et al. 2009). Mathematically, for purely horizontal flow, OW is given by the square of the relative vertical vorticity minus the squares of the horizontal strain and shear deformations.

$$OW = \zeta^2 - S_1^2 - S_2^2 = (V_x - U_y)^2 - (U_x - V_y)^2 - (V_x + U_y)^2 \quad (3)$$

In equation (3), ζ denotes the relative vertical vorticity, S1 denotes the horizontal strain deformation, and S2 denotes the horizontal shear deformation (Dunkerton et al. 2009). In plain language, the OW can be described as a measure of a fluid parcel's tendency to spin around a vertical axis when the effects of shear and strain are removed, which gives a clearer view of what is occurring within a protected pouch. Similar to how the air inside and above the bed of a moving pickup truck is protected from the overall flow around the truck, the pouch protects the air parcels within it from the shearing and straining processes that would otherwise inhibit the formation of a tropical cyclone. In this way, when the OW of a tropical wave is evaluated, the regions which help preserve the vortical shape can be differentiated from the regions that are unfavorable for the development and organization of deep convection. Upon analysis, regions that demonstrate positive OW denote areas where vorticity is dominant vs. negative OW regions where strain is dominant. Therefore, regions with positive OW are beneficial to cyclone development, whereas negative OW regions are not (Dunkerton er al. 2009). These ideas can be taken a step further to show pouch development and strength, as pouches appear as areas of strong positive OW surrounded by approximately closed streamlines. Clearly constructed plots of relative vorticity and OW, in conjunction with the co-moving streamlines and thermodynamic variables such as relative humidity, can then be utilized to determine the nature of the formation of the storm and the underlying processes therein.

B. MOTIVATION

Atlantic tropical cyclones remain a grave threat to U.S. Navy installations, ships, and Sailors. As a service that is located primarily near the ocean, the U.S. Navy is threatened every hurricane season by tropical cyclone activity that has historically

caused billions of dollars of damage to equipment and personnel. In the past decade, there have been $50 million worth of damages caused by Post-Tropical Cyclone Sandy in 2012 at Naval Weapons Station Earle and $3.6 billion worth of damages at Camp Lejeune from Hurricane Florence in 2017 as well as severe damages and impacts to Naval Air Station (NAS) Key West from Hurricane Irma in 2017 (United States Senate 2018). Caribbean-forming hurricanes have historically been difficult to forecast at long lead times because they form so close to land and there is often very little time to prepare for the impact of the storm. An excellent example of this issue is Hurricane Michael in 2018, which, formed and rapidly intensified from an NHC invest to a Category 5 storm making landfall on the Florida panhandle within a five-day span. Hurricane Michael directly caused 16 deaths and approximately $25 billion in damages (Beven et al. 2019), including severely damaging Tyndall Air Force Base (AFB), causing approximately $5 billion in damages on the base alone (United States Senate 2018) and leaving 484, roughly half, of the buildings on the base "destroyed or damaged beyond repair" (Reeves 2019). A similar storm could devastate various naval facilities located on the Gulf of Mexico as well as threaten civilian lives and infrastructure, including strategically critical oil platforms in the Gulf of Mexico. Early detection of such threats would enable the adaptation, preparation, and repositioning of assets to minimize the national security threat and best enable a quick and effective response in the wake of a disaster.

In addition to the fiscal motivation, the Caribbean Sea has been less studied in the tropical cyclone formation realm than the open ocean of the Atlantic. Caribbean-forming storms often form quickly and near to land, giving them compressed timelines in relation to the storms that come from the Atlantic. The unique situation of the late 2020 hurricane season in the Caribbean Sea allowed for an opportunity to study such storms that were very similar in background, both temporally and geographically, but still had significant differences in the formation path.

The goal of this study is to examine similar cases of hurricanes that formed in the Caribbean Sea through the application of the Marsupial Paradigm as a means to understand the mechanisms behind their formation.

This study aims to expand the collective knowledge of the meteorological tropical cyclone community with the eventual goal to enable better predictive capability earlier in the life cycle than we currently have.

C. BACKGROUND TO 2020 SEASON

For this study, we examine three 2020 Atlantic tropical cyclones, specifically Hurricanes Iota, Gamma, and Zeta, all of which formed in the western Caribbean. These three storms all formed as tropical depressions in an area bounded by 10–20N, and 70–85W. These storms were also late-season storms, occurring in October or November, well past the typical peak of the Atlantic hurricane season, which occurs in the middle of September as demonstrated in Chapter 3 of Elsberry et al. (1985).

1. Late Season Conditions of the 2020 Atlantic Hurricane Season

The 2020 Atlantic hurricane season was unusually active, particularly in October and November (Klotzbach et al., 2021). Through a combination of La Niña, the Madden Julian Oscillation (MJO), and "extremely favorable conditions in the Gulf of Mexico and Caribbean," especially anomalously low vertical wind shear and high sea temperatures, conditions were ripe for the later months of 2020 Atlantic hurricane season to be very dynamic, especially in the Caribbean Sea (Klotzbach et al., 2021).

The sea surface temperatures (SST) in the Atlantic Warm Pool (AWP) in July-September 2020 were the "4th warmest on record" (Klotzbach et al. 2021). Since a warm SST is a key ingredient in cyclone formation, this is an indication of an extremely favorable environment for tropical cyclone formation. As is evident in Figure 2, the 2020 Atlantic hurricane season, marked in red in both panels, had anomalously high Accumulated Cyclone Energy (ACE) of nearly 75×10^4 kt^2. The ACE is a measure of how much kinetic energy is being produced over a period of time as it relates to the sustained wind speeds of cyclones, in the area of interest over a time, generally one month or the entire season. It is important to note that because ACE is calculated using a summation over an interval, more intense storms and longer-lived storms both result in higher ACE numbers. When the anomalously high ACE observed in 2020 is combined with a low El Niño Seasonal Oscillation (ENSO) Longitude Index (ELI) of 157°E

indicating a strong La Niña, the indices indicated that the ingredients were present for a record-breaking hurricane season. The ELI is simply an index that describes the location of the Pacific warm pool and characterizes the stage of ENSO at a given point in time, with El Niño events having an ELI greater than 165°E and La Niña events having an ELI lower than 160°E (Williams and Patricola 2018). The importance of La Niña is that it represents an expected increase in hurricane activity in the Atlantic Basin. This is an observable correlation as there is a statistically significant increase in probability of a hurricane strike on the continental United States in La Niña years vice El Niño or neutral years of ENSO (Bove et al. 1998). This comes from the concept of El Niño reducing hurricane activity due to increased vertical wind shear in the Main Development Region (MDR) in the Atlantic (Gray 1984). The Main Development Region is taken to be the area "from ~ 10° to 20°N between the west coast of Africa and Central America," which is where most Atlantic hurricanes form (Goldenberg and Shapiro 1996). As 2020 experienced a strong La Niña event, it is unsurprising that it was a highly active season.

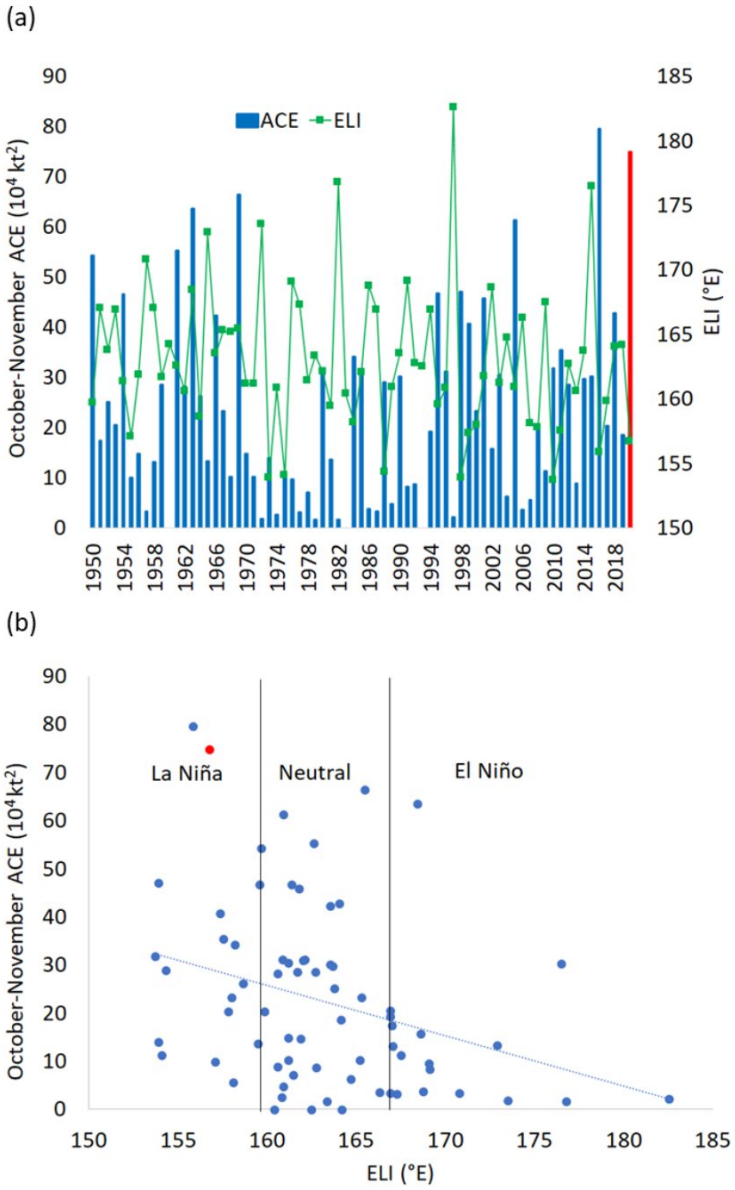

Klotzbach et al. compared the 2020 Atlantic hurricane season in the Caribbean to climatology from 1950-2020. (a) October-November Atlantic Accumulated Cyclone Energy (ACE) from 1950-2020 (blue columns) and the ENSO Longitude Index (ELI, green line). The red column highlights the observed ACE in October-November 2020. (b) Scatterplot of the relationship between October-November ACE and ENSO from 1950-2020 as represented by the ELI. The red dot represents the observed value of the ELI and October-November ACE in 2020, while the blue dashed line represents the regression relationship between the two time series form 1950-2019. Black lines delineate the longitude breakdowns between El Niño and neutral and La Niña conditions, respectively. The 2020 season had anomalously high ACE and low ELI, as seen in (a). Plot (b) depicts the rarity of the combination of both conditions at the same time, as it is an outlier, with only one other season exceeding its extremes of ACE and ELI.

Figure 2. 2020 Caribbean ACE vs. climatology 1979–2020. Source: Klotzbach et al. (2021).

As illustrated by Figure 3, the late-season storms in 2020 primarily formed in the Caribbean Sea and Gulf of Mexico. In panel (a), the October formation locations of all tropical cyclones in the years 1950–2019 were widespread across the Atlantic basin, an effect mirrored in panel (b), which shows the November formation locations of tropical cyclones in the years from 1950–2019. Panels (c) and (d) display the tropical cyclone tracks from October and November 2020 respectively, and it can be clearly seen that the Caribbean Sea and the Gulf of Mexico (GOM) regions were far more active than the open-ocean Atlantic basin in the 2020 season. The unusually conducive conditions in the GOM and Caribbean in 2020 make it a unique opportunity to study the formation of such systems in relatively direct comparisons.

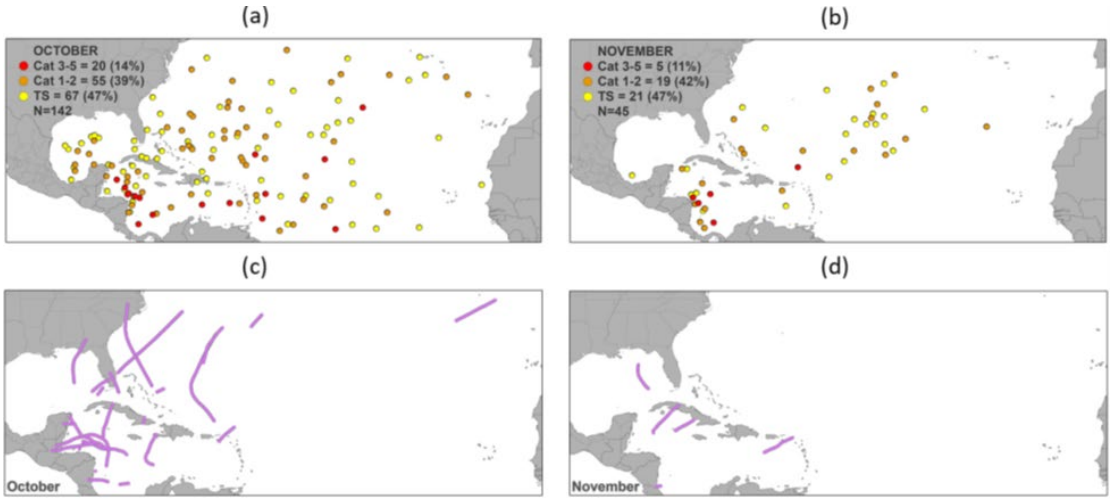

While the formation locations of named storms in October from 1950–2019 is spread well throughout the Atlantic basin (a), the tracks for named storms in October 2020 majorly formed in the Caribbean Sea and the Gulf of Mexico (c). Similarly, though the formation locations of named storms in November 1950–2019 were widespread (b), all of the named storms that formed in November 2020 formed within the Caribbean Sea and the Gulf of Mexico (d).

Figure 3. Formation location and storm tracks in October and November 1950–2019 vs. 2020 Hurricane Season. Source: Klotzbach et al. (2021).

The MJO is often correlated with the tropical cyclone activity of the Atlantic basin (Klotzbach 2010). Generally, when the MJO is in phases 1 or 2 it is more likely that both tropical cyclones and strong tropical cyclones will form in the Atlantic Ocean

than if the MJO is in phases 6 or 7, particularly for storms that reach major hurricane status (Klotzbach 2010). As Figure 4 shows, the MJO for the time period of the life cycles of the storms of interest (October 2 – 18 November) begins in phase 5, then circles around through phases 6, 7, 8 1, and 2. The lower panel of Figure 4 depicts the occurrence of each late-season storm in relation to the velocity potential anomalies between 5°N and 5°S during their life cycles. The velocity potential is "a scalar function with its gradient equal to the velocity vector of u of an irrotational flow" (AMS 2012). Velocity potential is often used in Hovmoller diagrams, such as in Figure 4, to graphically show the evolution and movement of upper-tropospheric divergence, which is generally co-located with deep, moist convection, associated with the MJO over time. That storms were consistently able to develop in the various phases of the MJO is an indication that the MJO was not the primary causal factor in the development of tropical cyclones in the Caribbean Sea in the late 2020 Atlantic hurricane season.

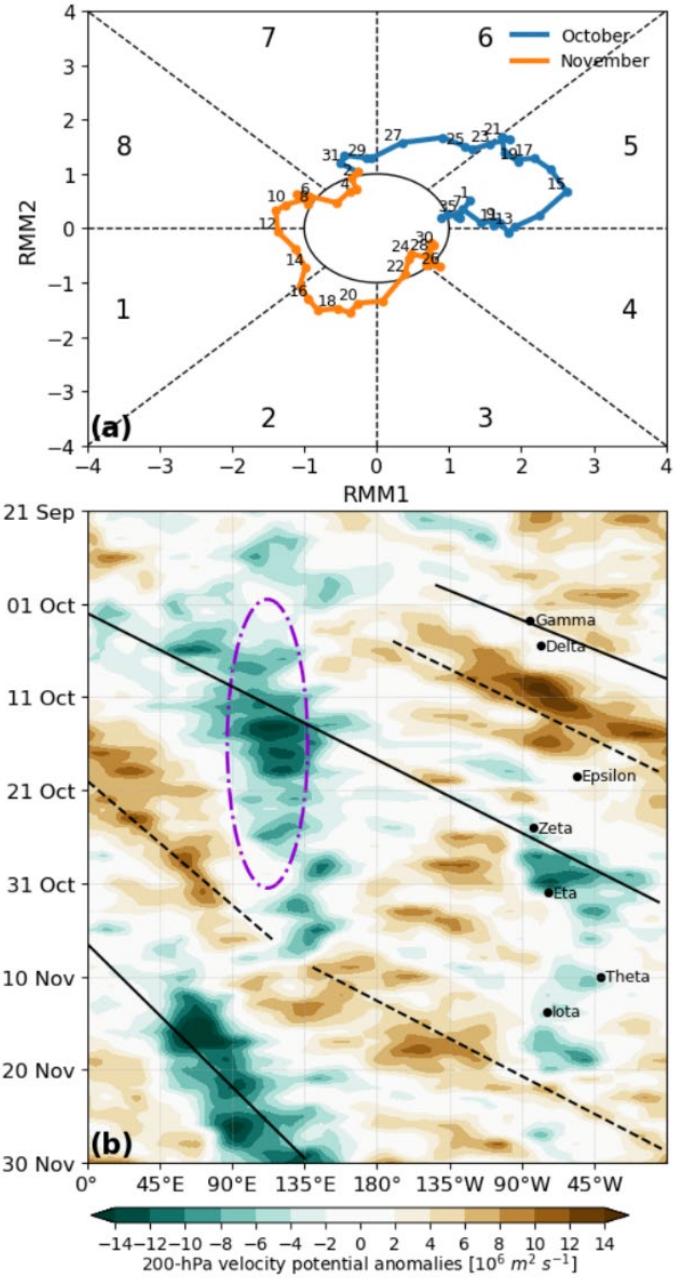

(a) Propagation of the Madden-Julian oscillation during Oct-Nov 2020 according to the Wheeler-Hendon (2004) index. (b) Hovmoller diagram of Oct-Nov 200 hPa velocity potential anomalies spanning the globe averaged over 5°S-5°N. Convectively-enhanced and convectively suppressed phases of the MJO are highlighted with solid and dashed lines, respectively. The relatively stationary enhancement of convection located around ~120°E is also highlighted with a dashed ellipse. The storms of interest to this study are denoted in the figure above as to where in the MJO they fell, with Gamma having positive 200 hPa velocity potential and Zeta and Iota having negative 200 hPa velocity potential.

Figure 4. Depiction of the MJO in October–November 2020. Source: Klotzbach et al. (2021).

2. Central American Gyre

Central American gyres (CAG) as defined by Papin et al. (2017) are "broad lower-tropospheric cyclonic circulations occurring near Central America […] that feature light wind cores, closed Earth-relative circulations, and widespread heavy precipitation." Though Central American Gyres can occur in the Caribbean Sea, the Gulf of Mexico, or the Eastern Pacific, the vast majority of them occur near or over the Central American mainland, as can be seen in Figure 5. This formation region is of importance to this study because its extent also includes the formation locations of the three storms being analyzed, namely Hurricanes Gamma, Zeta, and Iota, and one was observed to have directly interacted with the precursor of Zeta. The influence of such gyres on the formation of pouches and their subsequent tropical cyclones is not yet well understood.

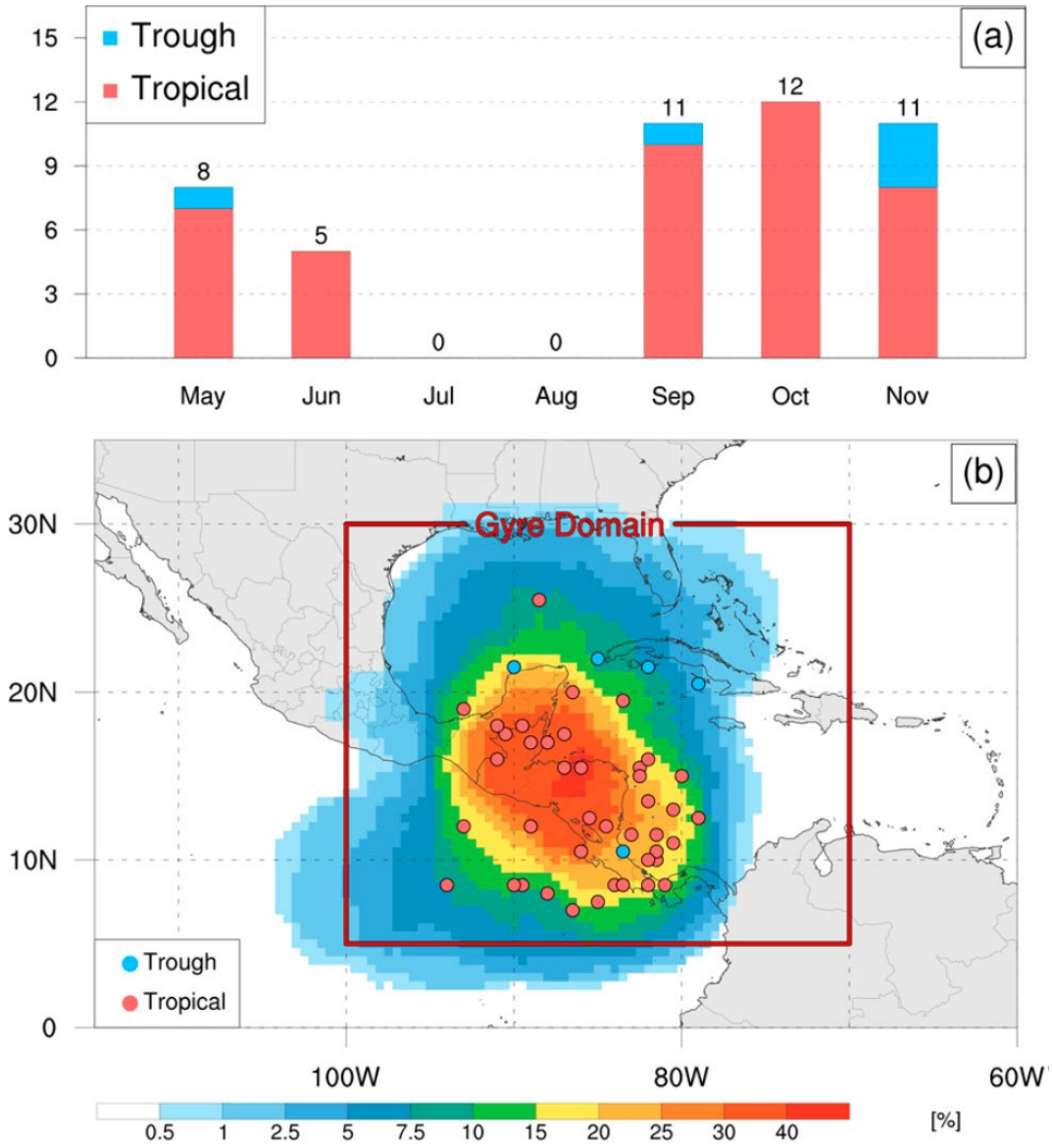

(a) Monthly CAG genesis frequency (1980-2010), where red and blue colors represent the number of CAGs classified as nonbaroclinic and baroclinic events, respectively. (b) CAG locations within domain, where shading denotes the probability of a CAG passing withing a 500-km radius of each grid point per season (May-November). Genesis location of individual nonbaroclinic and baroclinic CAGs are shown using red and blue dots, respectively.)

Figure 5. Depiction of formation locations and extent of CAGs 1980–2010. Source: Papin et al. 2017

3. Storms of Interest

The three storms chosen for this study are Hurricanes Iota, Gamma, and Zeta. All of these developed late in the Atlantic hurricane season in the Caribbean Sea within a span

of 60 days. Their tracks, both from this study and from the NHC, can be seen in Figure 6. The tracking of precursors produced by this study was able to extend the track for several days prior to formation.

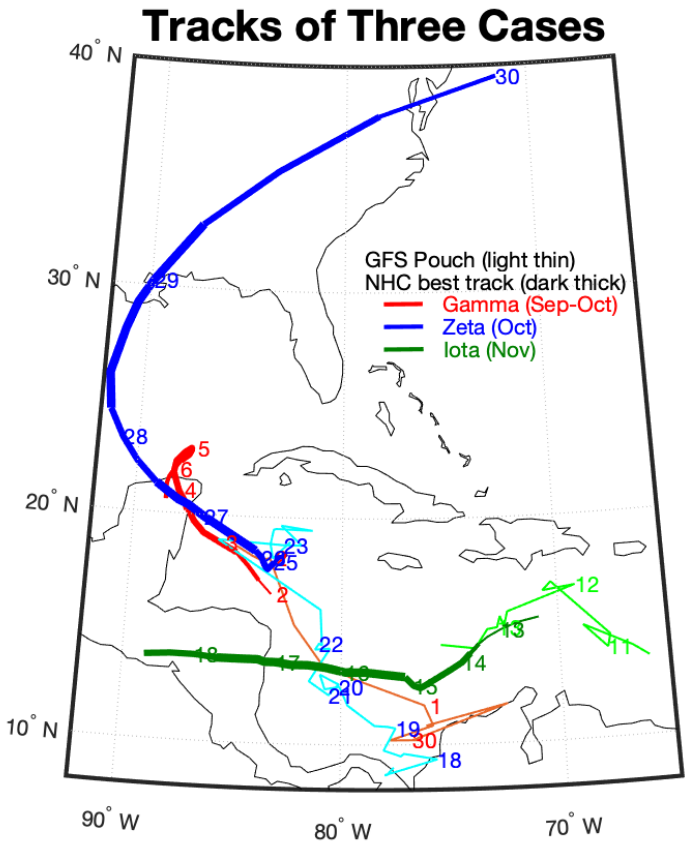

A depiction of the tracks for the three storms of interest, Hurricanes Gamma, Zeta, and Iota. The lighter colored part of each track represents the tracks produced by this study, and the darker colored part represents the official track from each storm's NHC report. The width of the track indicates the intensity of each storm at that point.

Figure 6. Depiction of tracks of storms of interest. Adapted from Latto (2021), Blake et al. (2021), and Stewart (2021).

a. Hurricane Iota

Hurricane Iota formed from a low-latitude African Easterly Wave (AEW) that crossed the Atlantic in November. The wave entered the Caribbean Sea on 8 November 2020, forming a tropical depression on 13 November 2020, and becoming Tropical Storm

Iota six hours later at 14N, 74.1W (Stewart 2021). Tropical Storm Iota underwent rapid intensification (RI) and overran the islands of Providencia and Santa Catalina as a Category 4 hurricane on the Saffir-Simpson Hurricane Wind Scale (SSHWS). Hurricane Iota proceeded westward overall, ultimately making landfall in Nicaragua and causing 67 direct deaths, 17 indirect deaths, 41 people missing and approximately $1.4 billion in damages across Central America, northern South America, and Mexico. Direct deaths are those whose cause of death is directly attributable to storms forces such as storm surge, wind, lightning, etc., whereas indirect deaths are attributable to things the storm caused but not directly part of the storm, such as electrocutions from downed power lines, house fires, CO2 poisoning form generators, etc. (Stewart 2021).

b. Hurricane Gamma

Hurricane Gamma began as an African easterly wave that crossed the Atlantic in late September, entering the Caribbean on 30 September 2020. It developed into a tropical depression on 2 October 2020 and became Tropical Storm Gamma 12 hours later at 18.4N, 85W (Latto 2021). Tropical Strom Gamma underwent rapid intensification, increasing its sustained wind speed from 35 to 65 knots in roughly 23 hours, and shortly thereafter made landfall on the Yucatan Peninsula as a Category 1 strength hurricane on 3 October 2020. (Latto 2021) Hurricane Gamma killed 6 people in Mexico, primarily due to rain and landslides (Latto 2021).

Hurricane Gamma is a good example of the rapidity in which tropical cyclones can form, intensify, and make landfall in the Caribbean Sea. In the space of 4 days, Hurricane Gamma experienced its entire life cycle, going from a tropical low, to a Tropical Depression (TD), to a Tropical Storm (TS), to a Hurricane, undergoing rapid intensification, landfalling, and dissipating (Latto 2021). Such short timelines cause serious difficulties and challenges for forecasters as well as the communities impacted, as there is often very little time to prepare for storm impact.

c. Hurricane Zeta

Hurricane Zeta had a complicated genesis sequence that will be explored more thoroughly later in this study. In brief, a series of factors, including an African easterly

wave, a mid-level trough, the MJO, a Central American Gyre and warm, moist flow from the southwest convolved to produce Hurricane Zeta. Hurricane Zeta became a tropical depression at 1200 UTC on 24 October 2020 and rapidly coalesced, becoming a tropical storm 12 hours later and becoming a hurricane 18 hours after that (Blake et al. 2021). Hurricane Zeta first made landfall on the Yucatan Peninsula on 27 October, losing strength, before entering the Gulf of Mexico as a tropical storm and re-intensifying in the favorable environment of the warm gulf. Hurricane Zeta underwent rapid intensification, going from 55 kt winds speeds to 100 kt wind speeds in 21 hours, before landfalling as a Category 3 Hurricane on the southeast Louisiana coast (Blake et al. 2021). Hurricane Zeta caused 5 direct deaths and 2 indirect deaths as well as approximately $4.4 billion in damages in the Unites States of America. Zeta's precursors also caused 2 indirect deaths and approximately $15 million in damages in Jamaica (Blake et al. 2021).

Hurricane Zeta is representative of the difficulties in forecasting and predicting storm formation in the Caribbean Sea. As the National Hurricane Center's report said, "the genesis of Zeta was complex" (Blake et al. 2021). There were multiple factors that led to the formation of Zeta, many of which were not being correctly represented in the numerical models the forecasters were using (Blake et al. 2021). The development of an understanding of the complex mechanics that create storms such as Zeta is a foundational reason for this study. Our overarching goal is to help advance the understanding of the formation of these late season storms in a way to benefit future forecasters.

THIS PAGE INTENTIONALLY LEFT BLANK

II. METHODOLOGY

A. THE POUCH PARADIGM AND ITS APPLICATION

This investigation of Caribbean-forming tropical cyclones was done within the premise of the Marsupial Paradigm (MP) as developed in Dunkerton et al. (2009) and further developed by Montgomery et al. (2012). For this investigation, Hurricanes Gamma, Zeta, and Iota were assessed in both Earth-relative and comoving frameworks using the same recursive process as Britton (2021). The goal of this analysis is to track the precursor (the pouch and other pre-pouch) structures to an earlier time to both learn the origin of the pouch and to better understand how the pouch formed in these specific storms in the Caribbean Sea. The formation processes documented will be compared against the typical formation pathway of a hurricane in the open-ocean Atlantic near and around the Main Development Region (Goldenberg and Shapiro 1996).

Global Forecast System (GFS) 6-hourly operational analyses with initialization times every day at 00 UTC, 06 UTC, 12 UTC, and 18 UTC with 0.25°, approximately 25 km, resolution were examined to determine the existence and location of a pouch. Investigation began from the time and location of formation as a tropical cyclone, as determined by the NHC from their post-storm reports. At this official formation time, the pouch was always very apparent with a distinct trough-critical latitude intersection and an obvious circulation at multiple levels in the GFS analyses. Previous analyses were then examined proceeding backwards through time every six hours to locate and plot the center of the pouch or pre-pouch disturbance by visual assessment based on the locations of the Okubo-Weiss (OW) center, the co-moving streamlines, the trough location, as well as the critical latitude. The process was then repeated with refined estimated storm speeds based off the known locations from the previous analysis, calculated with the Haversine formula (Inman 1835), which determines great-circle distance between two points based on their coordinates. The locations and speeds were then smoothed out to eliminate the discontinuities in tracking caused by the uncertainty of the center position. As pouches can be quite large geographically, there is room for significant errors in calculating their tracking speed based on where the visual inspection discerns the center. The smoothing of

the storm speeds over time allows for minimization of the impact of this error on the overall analysis. This retrospective examination was terminated when the early-stage precursor was so weak that no signal of a pouch was depicted in the GFS analysis. For instance, while the GFS may have depicted an African easterly wave, if the region had no circulation in the co-moving streamlines, and if the region had little to no OW organization, and no trough-critical latitude intersection, then no position was assigned. The pouch track was considered to start at the following (future) 6-hourly analysis time.

In this study, a pouch is an area of quasi-closed streamlines with centralized positive OW and cyclonic relative vorticity as well as an intersection between the critical latitude and the trough axis at any pressure level. A pouch is considered here to be fully formed when a pouch is exhibited at all four pressure levels (925, 850, 700, and 500 hPa), and the centers of the pouches at each level are stacked nearly vertically through these levels. A fully formed pouch helps promote deep convection and increased relative vorticity by shielding the inner area from the detrimental effects of a relatively dry environment.

Although analysis was done through four pressure levels (925, 850, 700, and 500 hPa), the visual selection of the pouch center was only dependent on the chosen tracking level at each time step. All three storms were tracked at the 850 hPa level because the precursor disturbance signal tended to be clearest at that level and for consistency in analysis, both within the analysis of each storm as well as in comparison to the other storms. Because all the storms formed in the same geographic area, as well as in roughly the same time period, it is unsurprising that their precursors were similar in structure and all trackable at the 850 hPa level. This also corresponds with the findings of Wang and Hankes (2013): When the formation occurs west of 60W it is generally more common for pouches to develop at 850 hPa and below.

The pouch tracking protocol produced outputs both in the form of visual plots of multiple variables, as well as area-averaged values of multiple variables and multiple levels, including the location, relative vorticity, OW, relative humidity, and two different calculations of vertical wind shear. Area-averages of these variables were calculated at

multiple pressure levels for both a 3°×3° (approximately 207 km x 198 km) and a 6°×6° box (approximately 414 km x 396 km) centered around the selected pouch center. While both regions were analyzed, the 3°×3° configuration was often the most useful as it focused directly on the pouch itself; however, the 6°×6 °box was also used in this study when necessary to illustrate specific phenomena. The aggregate of the area-average outputs for the whole tracking period were used to create the time-height and time series plots seen later in this study.

This study uses two different calculations of vertical wind shear, both of which are output by the pouch tracking protocol. The first is low-level vertical wind shear calculated by the difference in winds between the 850 and 500 hPa levels, then averaged over the 3°×3° or 6°×6° box. The second is deep vertical wind shear, which was calculated as the difference between winds at the 850 and 250 hPa levels and averaged over the 3°×3° or 6°×6° box. Both types of vertical wind shear have utility as the low-level wind shear can show disruptions at the low levels that can inhibit cyclogenesis and the deep vertical wind shear can show the effects of the upper-level jet and the vertical wind shear present throughout the air column.

For satellite analysis, infrared (IR) and visible imagery from the Geostationary Operational Environmental Satellite (GOES) system was compared with tracked positions of the precursors. The images were georeferenced using the Quantum Geographic Information System (QGIS 3.16 Hannover) software system to the WGS-84 global reference system and trimmed to match the size of the 3°×3° or 6°×6° box for comparison. The images were then analyzed in comparison to the output of the tracked positions.

B. VALIDATION

The locations and development of the storms as investigated by the comoving analysis was validated through a comparison of known conditions from the NHC's post-storm reports and satellite imagery. The progress and evolution of the precursor into a storm was verified through a comparison with time-stepped satellite imagery, which is useful in denoting the locations of most persistent deep convection. This satellite imagery

was geo-referenced, so that the tracked center at each time frame could be accurately compared to the depiction on the satellite image and compared with the tracked findings.

The tracks for each storm all started with the NHC position at tropical depression (TD) formation as stated in the post-storm reports by NHC forecasters Stewart (2021), Latto (2021), and Blake et al. (2021). The analyzed tracks of the precursors were compared to the stated atmospheric conditions that the NHC forecasters noted prior to storm formation, usually associated with the westward-moving African easterly wave. Because tracked positions were not determined by NHC for the time periods of interest *before* official formation, there remains the possibility for error as the AEWs are spatially very large and choosing a specific point to represent the "center" of a wave structure without an objective methodology inherently has the opportunity for error and uncertainty. For this study the "sweet spot," or the intersection between the trough axis and the critical latitude, is used as the tracked center of the pouch. It is advantageous to track the sweet spot as it has "qualitatively similar predictability as the track of a tropical cyclone" (Montgomery 2012). Previous work by Montgomery et al. (2010) shows that the sweet spot is the "preferred location for cyclogenesis." Therefore, since the sweet spot is the most likely spot to develop a tropical cyclone, it was what was tracked. Though there is still possibility for error in the track, using the sweet spot to track minimizes amount of human-introduced error present, as it gives a consistent target to observe over time.

Total Precipitable Water (TPW) content products from the University of Wisconsin Meteorology Department (University of Wisconsin – Madison 2021) provided the ability to compare the progression of the storm precursors to the pouch analysis and provide insight as to the movement and formation of these pouches and their subsequent TCs. The TPW product gives a clear indication of the state of moisture in the atmosphere at the times of interest in the areas where the pouches are forming and were tracked.

III. DATA AND RESULTS

Traditionally, hurricane forecasters track tropical cyclones from their point of formation as a tropical depression until their dissipation or their transition into extra-tropical storms. However, the focus of this study is on the pre-formation structures of Hurricanes Iota, Gamma, and Zeta. Consequently, this study will track the precursors through their various stages and delve into the mechanisms behind the formations of each storm system through discussion on the movement of atmospheric precursor structures as well as an analysis of how the local environment affected the formation of each storm.

A. IOTA

Of the three case studies presented in this thesis, the formation of Hurricane Iota was the most similar to that described by Dunkerton et al. (2009) of a so-called "wave-pouch" developing within a westward-moving tropical wave. This study will use Hurricane Iota's precursor as an example of what a standard pouch formation looks like within the guidance of the marsupial paradigm.

Iota formed from an African easterly wave that emerged off Africa on 30 October 2020 and crossed the Atlantic basin at low latitudes with disorganized convection (Stewart 2021). The wave came into the Caribbean along the coast of South America and moved northwestward over the Virgin Islands and Puerto Rico, growing in amplitude, increasing in steepness, and growing larger in the north-south directions, as it progressed (Stewart 2021). From the time the wave reached Hispaniola, the wave tracked more westward and slowed down. Around this time, fully formed Hurricane Eta was off the coast of Honduras, and a substantial peripheral ridge built to the southeast of Eta via Rossby wave dispersion due to the presence of Hurricane Eta in agreement with the work by Carr and Elsberry (1995). This peripheral ridge resulted in a west-southwest steering current for Iota's precursor. The GFS-determined track of the Iota precursor is shown in Figure 7, during which the disturbance evolved from an open wave entering the Caribbean, to a pouch forming on 00 UTC 11 November 2020, to a tropical depression at 12 UTC 13 November 2020 that became Tropical Storm Iota 6 hours later.

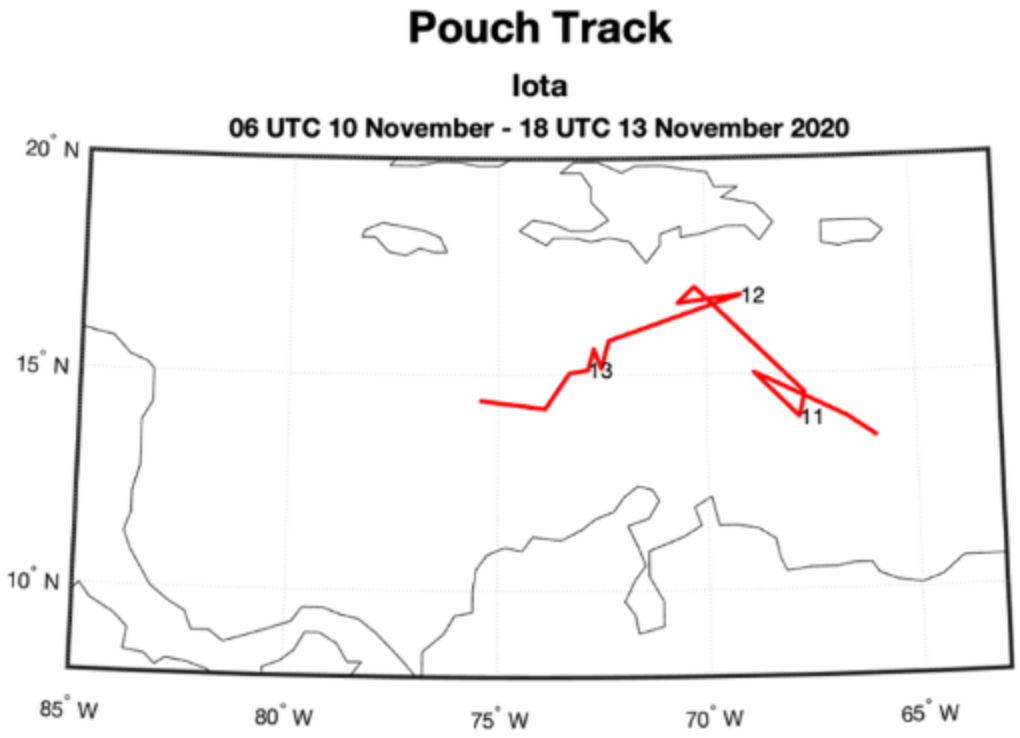

Depiction of the GFS analyzed track of Iota's precursor in the Caribbean Sea from 06 UTC 10 November 2020 to 18 UTC 13 November 2020. Points are determined every 6 hours at 00, 06, 12, and 18 UTC, with the date labelled to the immediate right of the 00 UTC position. The track clearly exhibits the precursor's movements to the west and then the south-west starting on 12 November as the precursor is influenced by the presence of Hurricane Eta (not depicted) prior to formation.

Figure 7. GFS analysis of track positions of Iota's precursor in the Caribbean Sea, November 2020.

Though Iota's precursor crossed the Atlantic Ocean as an open wave, a tropical wave in and of itself is not sufficient to generate a tropical cyclone; all the elements of tropical cyclone generation must be present, including a pouch as demonstrated in the MP (Dunkerton et al. 2009). The first time a pouch could be clearly observed in the tropical wave that became Iota was at 00 UTC 11 November 2020, as shown in Figure 8. The wave is clearly seen in both the Earth-relative and co-moving frames at all levels, but the only level that had a closed circulation was at 700 hPa in the storm-relative framework. This circulation was located at approximately 18°N, 69°W as marked in Figure 8 by the arrows on the OW plot (left). At 700 hPa, the closed circulation had concentrations of OW and cyclonic relative vorticity with peak values of at least 9×10^{-9} s^{-2} and 5×10^{-5} s^{-1} respectively.

There was a clear intersection of the trough axis and the critical latitude centered inside the pouch as marked by the thick black line and the purple line respectively. Though a pouch had not yet developed at the 925, 850, or 500 hPa levels, the relative vorticity in the open wave at the 925 hPa and 850 hPa levels was increasing at this time (not depicted).

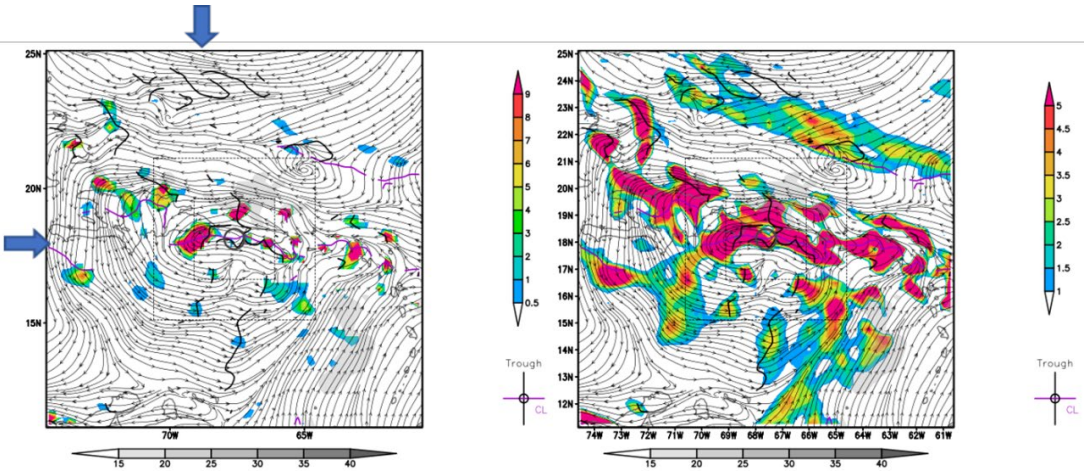

GFS analysis of OW (left) and relative vorticity (right) with 700 hPa streamlines in the precursor-relative frame of reference at 00 UTC 11 November 2020. The units for OW are $\times 10^{-9}$ s^{-2}, the units for relative vorticity are $\times 10^{-5}$ s^{-1}, and the gray colorbars below the plots represent wind speed in knots. The closed circulation at 700 hPa and areas of high OW and relative vorticity near the circulation center are discernible in the storm-relative frames and are marked with blue arrows.

Figure 8. GFS analysis of OW (left) and relative vorticity (right) at 700 hPa with streamlines at 00 UTC 11 November 2020

In the subsequent 24 hours, the precursor developed steadily with pouches being established at 850 hPa and 925 hPa. As can be seen in Figure 9, the pouches were not yet vertically aligned, but there was a closed circulation at the 700, 850, and 925 hPa levels, as well as concentrated OW and cyclonic relative vorticity in and around the center of each pouch. Additionally, the intersection of the trough axis and a critical latitude was analyzed at this point in the center of each pouch at the 700, 850, and 925 hPa levels. At the 850 and 925 hPa levels, there were also two separate pouches that each have their own established circulations, troughs, and critical latitudes. These pouches were located at approximately 16°N, 73°W and 18°N, 76°W and had maximum OW and relative vorticity values of 9×10^{-9} s^{-2} and 5×10^{-5} s^{-1} respectively. These lower-level pouches were quite small at this time,

and both fell within the borders of the larger pouch at 700 hPa, which was centered at 16°N, 72°W, although, the troughs and critical latitudes were again not fully aligned. There was little change in the size or intensity of the pouch at the 700 hPa level. However, the development in the pouches at 925 hPa and 850 hPa corresponded with the "bottom-up development" established in the Marsupial Paradigm (Dunkerton et al. 2009). Though the pouch at the 700 hPa level was the first to coalesce, it did not develop further until the pouches at the 925 and 850 hPa levels formed and intensified. The lower levels intensified and converged the vorticity first and then the 700 hPa pouch intensified, as will be seen later. At the 500 hPa level, there was a closed circulation and an established trough located approximately at 16°N, 70°W. The pouch had a peak OW value of at least 9×10^{-9} s^{-2} and a peak relative vorticity value of at least 5×10^{-5} s^{-1}, but the pouch was not developed enough to show the intersection of the critical latitude and the trough that is typical of a fully formed pouch. Additionally, the pouch structure was tilted to the east in the upper troposphere, with the sweet spot at 700 hPa centered approximately 160 km east of where the pouch at 850 hPa was centered. The sweet spot at 500 hPa was a further 110 km east of the 700 hPa sweet spot position. Although they were not fully aligned vertically, the outside boundaries of the circulations at each level were vertically aligned from 925 hPa through 700 hPa, and the 500 hPa level was stacked back to the east.

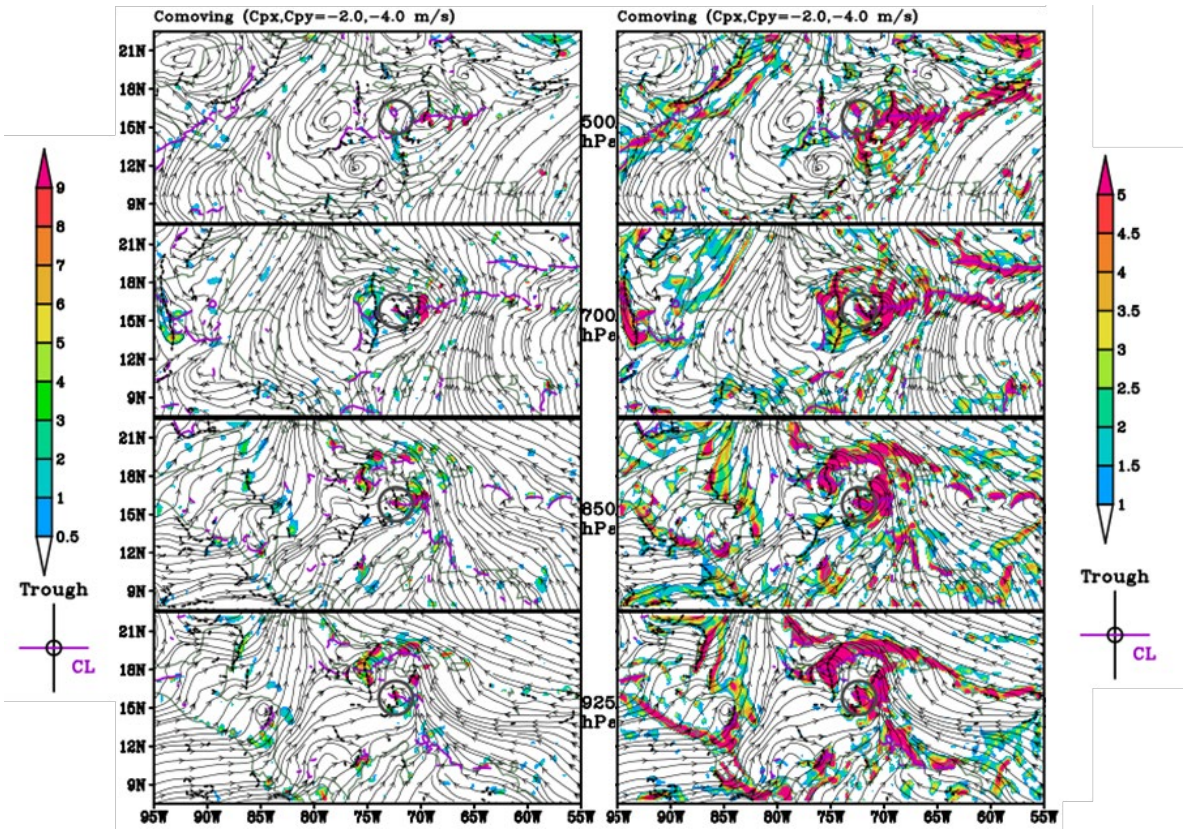

GFS analyses of Iota's precursor in the Caribbean Sea with OW (left) and relative vorticity (right) in a precursor-relative streamline depiction at 500, 700, 850, and 925 hPa (top to bottom) at 06 UTC 12 November 2020. The units for OW are $\times 10^{-9}$ s^{-2}, and the units for relative vorticity are $\times 10^{-5}$ s^{-1}. The precursor-relative model has a storm velocity of 2.0 m s^{-1} westward and 4.0 m s^{-1} southward. A pouch is clearly visible at 700 hPa, and the small pouches at 850 hPa and 925 hPa are seen, located directly below the pouch at 700 hPa. All the pouches have closed streamlines, a trough axis, a critical latitude, and high OW and relative vorticity.

Figure 9. GFS analysis of OW and relative vorticity at 500, 700, 850, and 925 hPa in the precursor-relative frame of reference at 06 UTC 12 November 2020

Over the next six hours, the precursor disturbance continued to organize, as can be seen in Figure 10. The disturbance was more vertically aligned, with the 925, 850, and 700 hPa levels becoming stacked. Furthermore, the small pouches at the 925 and 850 hPa levels had combined and consolidated to create a single larger and stronger pouch located near 15°N, 73°W that is aligned with the outer boundary of the pouch at 700 hPa, though the sweet spot of the pouch at 700 hPa remained further east at 15°N, 71°W. This consolidation and alignment process supports the "bottom-up" development viewpoint expected in the

MP (Dunkerton et al. 2009), as the lower levels were the ones experiencing development. As this consolidation occurred, the OW had increased at the low levels also, with peak OW of at least 9×10^{-9} s^{-2} covering a larger area than previously seen. This allowed for intensifying vortical development. The corresponding increase in cyclonic relative vorticity is plainly apparent at the 925 and 850 hPa levels, with a consolidation and increase in the areal coverage of the peak value of at least 5×10^{-5} s^{-1} of cyclonic relative vorticity found there. The pouch at 500 hPa, located near 51°N, 71°W, had also increased the areal coverage of the maximum OW value of 9×10^{-9} s^{-2} in the previous six hours. The pouch was still tilted eastward with height, with the 700 hPa sweet spot approximately 160 km east of the sweet spot at 850 hPa, and the 500 hPa sweet spot approximately 110 km east of the 700 hPa sweet spot. The pouch structure had developed as well, producing closed streamlines in the pouch-relative reference. That the lower levels were strengthening and aligning first agrees with the work of Dunkerton et al. (2009) as a key portion of the development of a tropical cyclone.

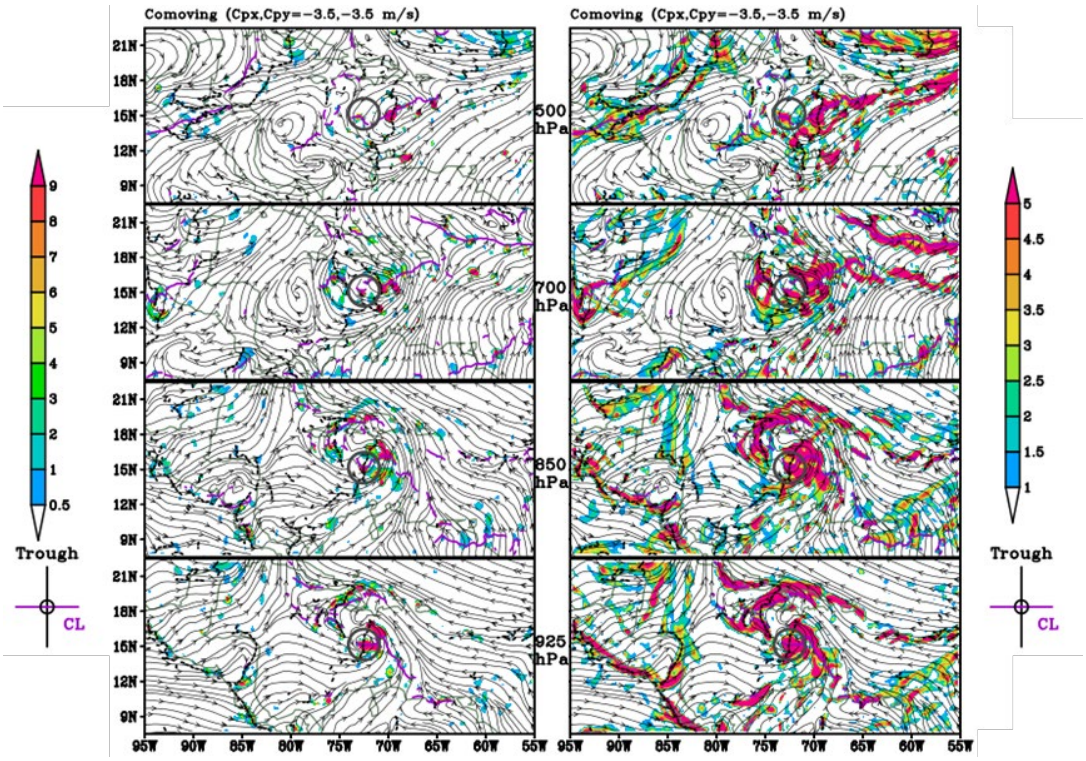

Like Figure 9, except at 12 UTC 12 November 2020. The precursor-relative model has a precursor velocity of 3.5 m s^{-1} westward and 3.5 m s^{-1} southward. Pouches at 925 hPa and 850 hPa are clearly defined and vertically aligned. The pouch at 700 hPa is also well developed but centered slightly further east (although the pouch itself is largely aligned with the lower levels). The pouch at 500 hPa is developing in the storm-relative framework with closed streamlines, centralized OW, centralized relative vorticity, and a crossing trough axis and critical latitude.

Figure 10. GFS analysis of OW (left) and relative vorticity (right) at 500, 700, 850, and 925 hPa in the storm-relative frame of reference at 12 UTC 12 November 2020

Following on from the previous time period, the precursor continued to align, deepen, and develop. As can be seen in Figure 11, six hours later, the precursor disturbance established pouches at all levels that were nearly vertically aligned. The pouches at 925 and 850 hPa were located approximately at 16°N, 73°W, while the pouches at 700 and 500 hPa are centered near 16°N, 72°W. Though strongest in the lower levels, all the analyzed levels have increased their areal coverage of peak OW value at or above 9×10^{-9} s^{-2}. Additionally, the coverage of the maximum relative vorticity value of 5×10^{-5} s^{-1} has increased and condensed around the sweet spot at all analyzed levels. Although official formation as a tropical depression was still 18 hours after this, all the elements were in

place for a tropical cyclone to form. The pouch was fully formed, atmospheric circulations were vertically aligned, and the traditional six elements of tropical cyclone formation were present. The convection continued building as Iota organized into a fully formed tropical cyclone.

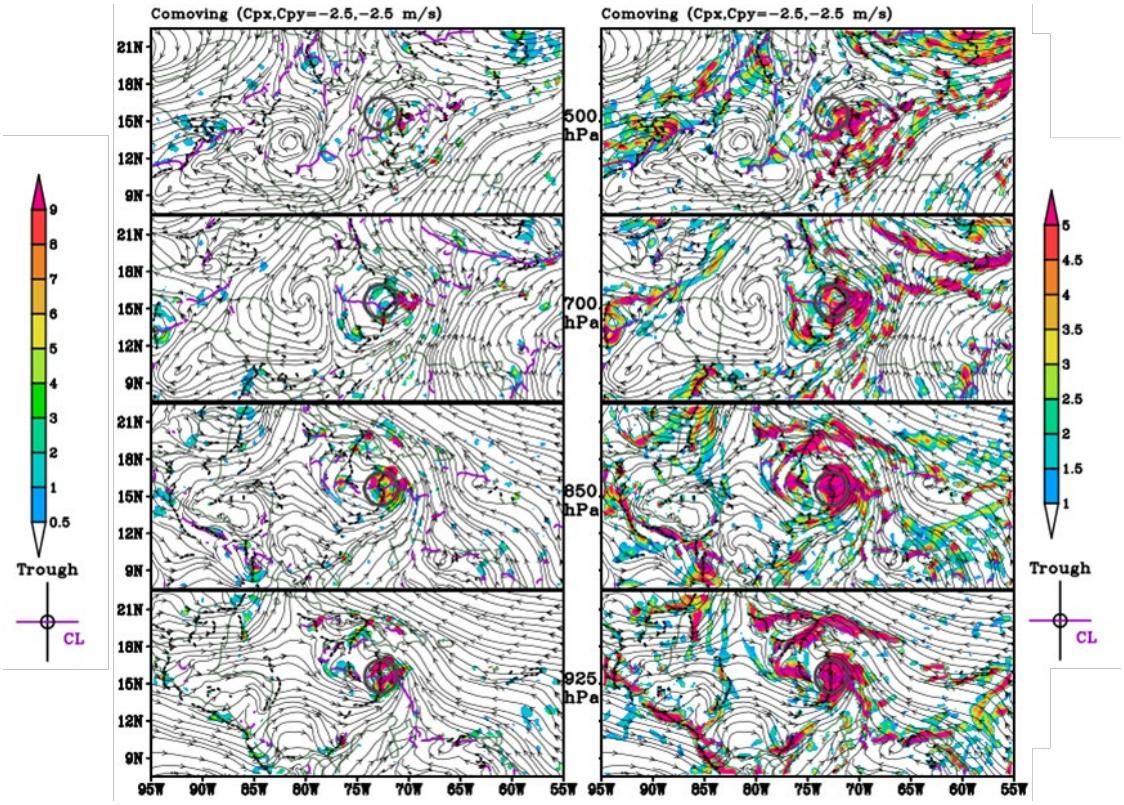

Like Figure 9, except at 18Z 12 November 2020. Pouches are fully developed at every level, and the 500 hPa pouch continues to move more in alignment with the lower levels. Relative vorticity and OW have increased significantly at all levels promoting the growth of deep convection throughout the air column and facilitating TC development.

Figure 11. GFS analysis of OW (left) and relative vorticity (right) at 500, 700, 850, and 925 hPa in the storm-relative frame of reference at 18 UTC 12 November 2020

The formation of the pouch, and ultimately the storm Iota over time is clearly illustrated in the time-height plots of Figure 12, which show the time evolution of the area-averaged OW and relative vorticity, respectively, through the tropospheric column in the 3°×3° box centered on the tracked sweet spot. A pouch was first seen at 00 UTC 11

November 2020, marked by the green vertical lines in Figure 12, which occurred before significant amounts of OW and relative vorticity were depicted by GFS. The first occurrence of multi-level pouches occurred at 06 UTC 12 November 2020 immediately before the OW and relative vorticity increased, implying a possible connection. The OW in the lower levels increased by 8×10^{-9} s^{-2} in the span of the 24 hours on 12 October 2020. This occurred in conjunction with the development of the lower-level pouches previously outlined and the appearance of a fully formed pouch at 18 UTC 12 November 2020, marked by the purple vertical lines in Figure 14. Although the first pouch was observed at the 700 hPa level, that pouch did not develop until after the pouches at 925 and 850 hPa consolidated. The way that the low levels built their pouches first is also observable in Figure 12: The levels below 700 hPa clearly developed relatively high levels of OW and relative vorticity before the levels above 700 hPa.

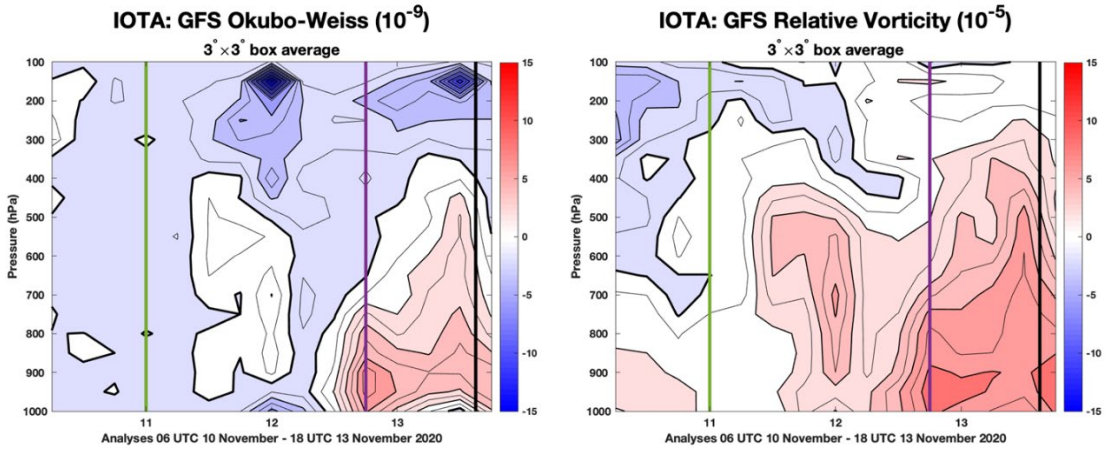

GFS analysis of OW (left) and relative vorticity (right) in the area surrounding Iota's precursor at over time. The x axis represents time period the precursor was tracked from 06 UTC 10 November to 18 UTC 13 November. The y axis is height as represented by pressure in hPa levels. The intensity of each variable is indicated by the colors with respect to either color bar. The green vertical line represents the time a pouch was first identified at 00 UTC 11 November 2020, the purple vertical line represents the time the pouch was fully formed at 18 UTC 12 November 2020, and the black line represents the first NHC advisory at 15 UTC 13 November 2020. It is apparent in both plots that there was an initial burst of organizational spin occurring late on 11 November, with a significant increase in both OW and relative vorticity in the second half of 12 November into 13 November as the storm organizes and forms.

Figure 12. GFS analysis of OW and relative vorticity as time vs. height plots for Iota's precursor

A series of GOES-16 imagery coincident with the previously presented GFS analyses depicts the gradual organization of convection about the Iota precursor pouch center in the 3°×3° box (Figure 13). The first two times, 00 UTC on November 11 and 06 UTC on November 12, are IR images; the second two times, 12 and 18 UTC on 12 November 2020, are visible images. Though there were cold cloud tops visible at 00 UTC 11 November 2020 (Figure 13, upper left), they were disorganized and not coherent. The effects of these smaller, air-mass thunderstorms can be seen in Figures 12 and 14, as after they occurred, the relative vorticity and relative humidity increased, but they were not strong or organized enough to prime the upper levels of the troposphere for sustained convection yet. The presence of the cold cloud tops visible at 12°N, 72°W at 06 UTC 12 November 2020 (Figure 13, upper right) correspond with the effects of deep convection seen at 12 UTC 11 November 2020 to 06 UTC 12 November 2020 in Figures 12 and 14. The visible images at 12 and 18 UTC 12 November 2020 (Figure 13, lower left and right respectively) show the growth of the centralized cloud cover at 15°N, 72°W as the pouch formed fully at 12 UTC 12 November (Figure 13, lower left) and sustained deep convection began. The low-level swirl of the developing storm is apparent in the visible imagery as the precursor organizes into a fully-fledged tropical cyclone.

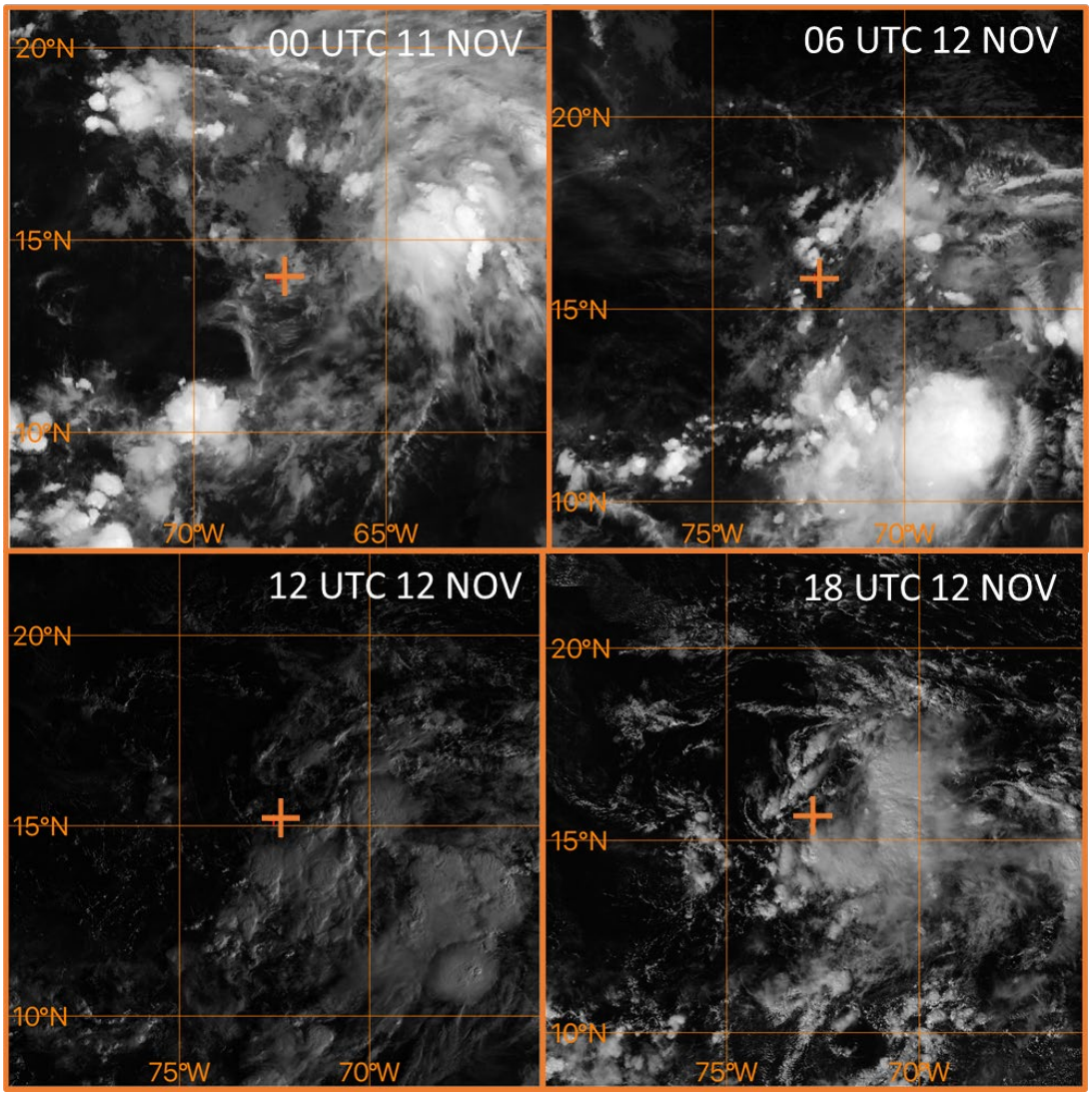

GOES IR and visible satellite imagery of Iota's precursor at the times of interest centered on the GFS tracked position. 00 UTC 11 November and 06 UTC 12 November are IR images while 12 and 18 UTC 12 November are visible images. The tracked center (sweet spot) is represented by an orange cross. The imagery depicts the increase in convection over time, which is especially apparent at 12 UTC and 18 UTC 12 November 2020 when the pouch structure began to align vertically and became a promotive environment for TC formation.

Figure 13. GOES IR and visible imagery of the GFS tracked positions at various times of interest for Iota's precursor

Throughout the time that Iota's precursor was building into a tropical cyclone, the environment surrounding the disturbance was generally favorable for development. As previously mentioned, Klotzbach et al. (2021) demonstrated that the late-season Caribbean

and Gulf of Mexico in 2020 was extremely favorable for tropical cyclone development in a general climatological sense. In particular, the sea surface temperature was anomalously high compared to climatological averages and helped support a thermodynamically favorable environment for tropical cyclone formation. During this time, the sea surface temperatures in the Caribbean contributing to creating the third highest ACE for October-November since 1979 (Klotzbach 2021), providing a thermodynamically favorable environment for tropical cyclone formation. Additionally, the environment through which Iota's precursor travelled had favorable relative humidity (RH) for development of convection and further organization (Figure 14). As can be seen in Figure 14, prior to 11 November 2020 the relative humidity was very high at low levels with values in excess of 80% below 800 hPa. The upper levels were drier with values between 30 and 80% above 800 hPa. The relative humidity dramatically increased after 12 UTC on 11 November 2020 with relative humidity values approaching 90% throughout the air column. This increase of mid-level atmospheric moisture coincided with a significant increase in vertical mass flux during the same time, going from 0 kg m^{-2} s^{-1} to 5 kg m^{-2} s^{-1}. This increase is indicative of a significant increase in deep convection occurring at that time. These analyses suggest that the deep convection moistened the upper levels, priming them for further organization and development, which can be seen occurring on 13 November 2020.

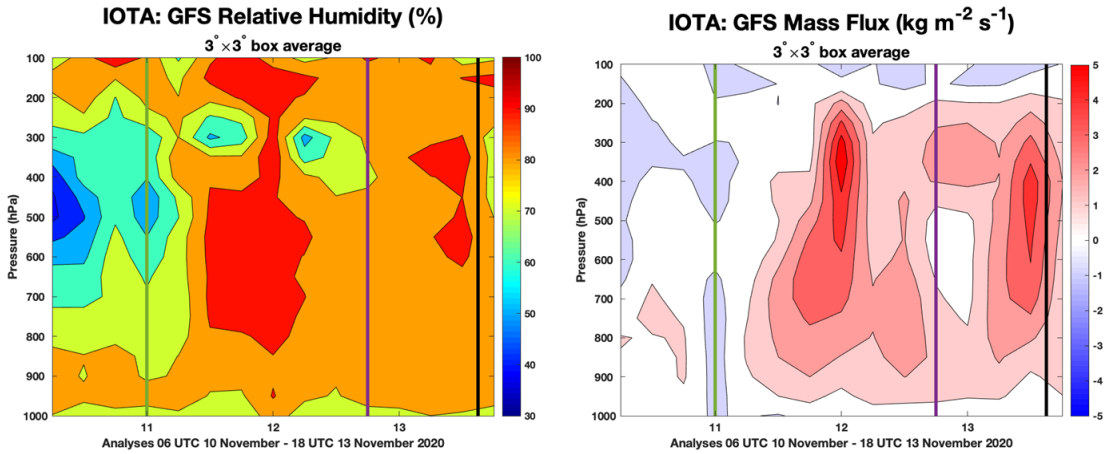

Similar to Figure 12, except for RH (left) and vertical mass flux (right). It is apparent in both plots that there was a significant increase in both relative humidity and vertical mass flux throughout the troposphere in the second half of 11 November into 12 November, indicating the presence of deep convection and an improvement in the overall organization of the precursor disturbance.

Figure 14. GFS analysis of relative humidity and vertical mass flux as time vs. height plots for Iota's precursor

Seven variables that affect formation of a tropical cyclone are examined over time in Figure 15 using 3°×3° and 6°×6° box area-averages centered on the sweet spot of the pouch. Deep-level vertical wind shear, as represented by the blue curve in the lower right plot in Figure 15, decreased from greater than 13 m s^{-1} early on 11 November 2020 to less than 10 m s^{-1} in the span of a day. Such a high value of deep-level vertical wind shear is known to be inhibitive of the formation process, so it is unsurprising that the OW and relative vorticity, as depicted in the upper left panel of Figure 15, do not substantially increase until the vertical wind shear decreases. Additionally, an increase in the deep vertical wind shear in the 6°×6° box can be seen on 11 November 2020 (dashed blue line in the lower right panel of Figure 15) as the precursor neared the southern side of Hispaniola. During this time, the low-level winds encountered a combination of a tropical upper tropospheric trough and upper-level outflow from Hurricane Eta (not depicted) which was located to the north and west of Iota's precursor in the Gulf of Mexico. The precursor did not move far enough north for this region of increased deep-layer vertical wind shear to affect the 3°×3° box or the precursor's development.

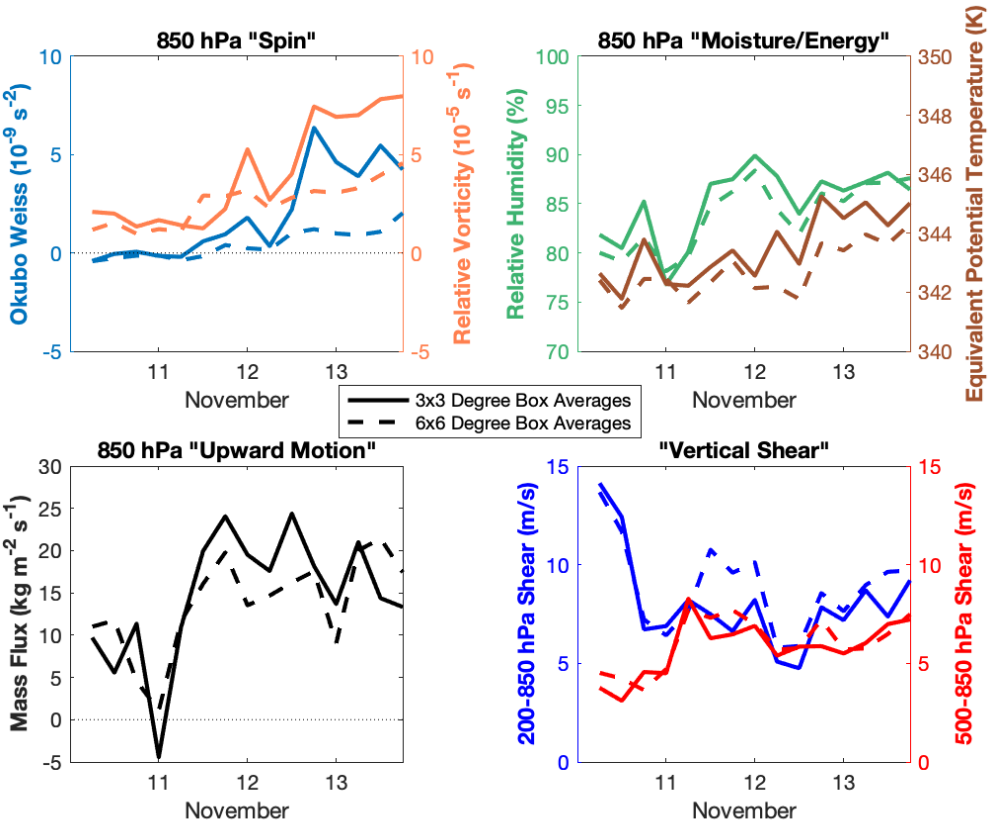

GFS Analysis of spin (upper left), moisture (upper right), upward motion (lower left), and vertical wind shear (lower right) in the area surrounding Iota's precursor at over time. The x axes for each plot represent time period the precursor was tracked from 06 UTC 10 November to 18 UTC 13 November with the respective variable shown as a time series. The formation of the pouch can be clearly matched to the increase in spin seen in the upper left panel as well as the increase in upward motion seen in the lower left. The presence of deep layer vertical wind shear, as represented by the blue line in the lower right panel, is apparent early on 11 November, and the decrease in that vertical wind shear directly precedes the formation of the pouches and the increase seen in OW and relative vorticity.

Figure 15. GFS analysis of Iota's precursor for spin, moisture, upward motion, and vertical wind shear as time series plots

In summary: The formation of Iota was fairly straightforward and can be seen as a progression from an open wave, to a pouch, building in the lower levels, into a tropical depression, and on into a tropical storm. Iota's formation exhibits many characteristics described in the Marsupial Paradigm, with a fully developed pouch structure that is observable in the co-moving framework 18 hours before its official formation time as a tropical depression.

B. GAMMA

The second case investigated is Hurricane Gamma. Gamma had an interesting evolution, as while there was a tropical wave associated with its formation, Gamma was in part affected by the vorticity produced by the South American landmass as well as the wave. In addition, the formation sequence includes a vorticity "roll-up" as outlined in the Marsupial Paradigm.

Gamma formed from a tropical wave that came off Africa on 21 September 2020 moved westward across the Atlantic at low latitude, entering the Caribbean Sea on 27 September 2020 and continuing into the western Caribbean Sea on 30 September 2020 (Latto 2021). As will soon be suggested, the wave encountered a low-level vorticity pouch coming off the coast of Colombia and Venezuela on 29 September 2020, which in addition to the AEW led to the formation of a tropical depression at 06 UTC on 2 October 2020 and became Tropical Storm Gamma at 18 UTC on the same day (Latto 2021). As can be seen in Figure 16, the vorticity pouch associated with Gamma can be tracked back to the South American landmass for several days prior to formation. There was a long-lived vorticity "strip" that developed at low levels in the southwest Caribbean Sea, which became the vorticity pouch for Gamma. This strip of vorticity "rolled-up," meaning that it went from a long east-west oriented strip of relative vorticity through a reorientation along a north-south axis and, finally, condensed into a single, central point of relative vorticity. Although the open wave can also be tracked back further in time as it crossed the Atlantic Ocean (not depicted), the low-level vorticity necessary to build the cyclone is associated with the interaction with this low-level vorticity structure. The track is extremely variable in the day after moving off the coast due to the presence of multiple small OW centers at that time. The highest point of OW was tracked through the period of confusion on 30 September 2020, but as time proceeded forward, the OW center that contributed to Gamma's precursor became clear on 1 October 2020.

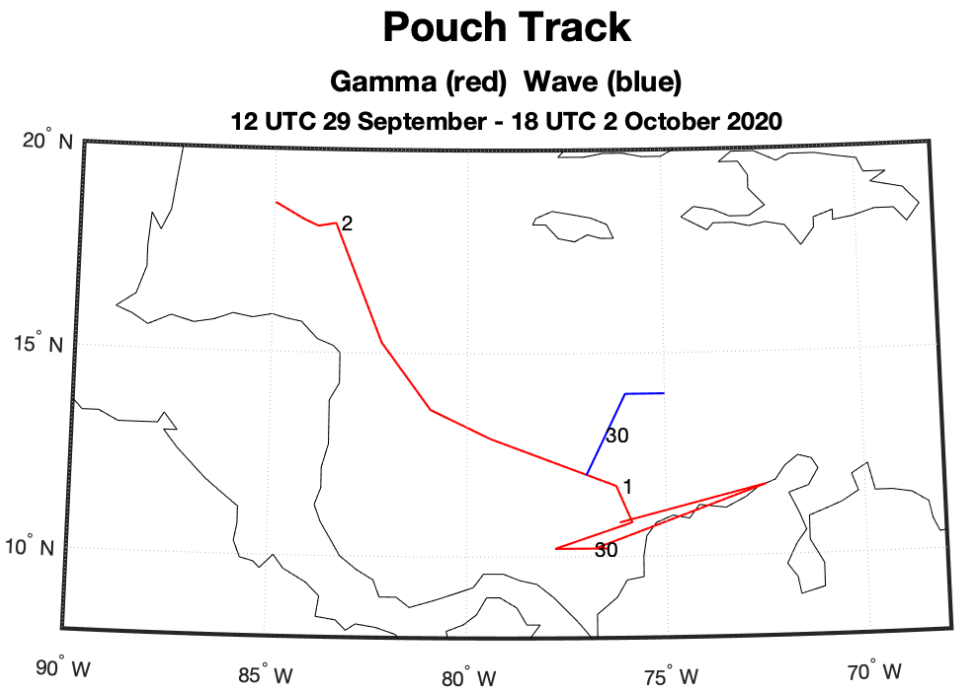

Depiction of the GFS analyzed track of Gamma's precursor in the Caribbean Sea from 12 UTC 29 September 2020 to 18 UTC 2 October 2020. Points are determined every 6 hours at 00, 06, 12, and 18 UTC, with the date labelled to the immediate right of the 00 UTC position. The red line represents the precursor pouch associated with the vorticity strip. The blue line represents the movement of the identified precursor wave prior to its interaction with the low-level vorticity strip and roll-up into a low-level pouch. The track clearly exhibits the precursor's movements to the northwest from 18 UTC 30 September 2020 onwards. The back-and-forth movement of the track on 30 September 2020 is indicative of the difficulty in attributing a specific OW center as the center of a nascent pouch when the vorticity is scattered throughout the area.

Figure 16. GFS analysis of track positions of Gamma's precursor in the Caribbean Sea, September-October 2020.

Although there is a clear input signal from the African easterly wave that crossed the Atlantic, the precursor did not develop until it started interacting with the low-level cyclonic vorticity structure coming from the Colombian coast. The first time a pouch was observed was at 12 UTC 29 September 2020 in the vicinity of 11°N, 77°W. This quasi-pouch extended downwards from 850 hPa through 925 hPa, indicating that the development originated at low levels. This structure had fully closed streamlines in the

precursor-relative view, but in the Earth-relative framework, it was still an open circulation at this point in time. Additionally, the tropical wave was clear in the Earth relative view, but it was an open wave without a closed circulation. This open tropical wave was located east of the low-level pouch at 12 UTC 29 September 2020 (not depicted). There was a significant amount of cyclonic relative vorticity associated with the vorticity strip structure, as depicted in Figure 17. The cyclonic relative vorticity was especially concentrated in a long "vorticity strip" located roughly along the latitude line of 11°N between 64° and 77°W. The vorticity strip is characterized by a core strip of 5×10^{-5} s^{-1} values of relative vorticity that can be seen in the right plot of Figure 17. The sweet spot of the pouch at 850 hPa is the western terminus of the vorticity strip. This vorticity strip was very persistent and was observable through multiple forecast periods. However, as can be seen in the left plot of Figure 17, there were few areas of peak OW values in comparison to the size of the vorticity strip due to the straining processes in the areas. There were intermittent clusters of OW values of greater than or equal to 9×10^{-9} s^{-2}, but there was comparatively less maximum OW in coverage than relative vorticity in the area of the vorticity strip. Nevertheless, there was a clear, though small, OW center within the precursor-relative pouch.

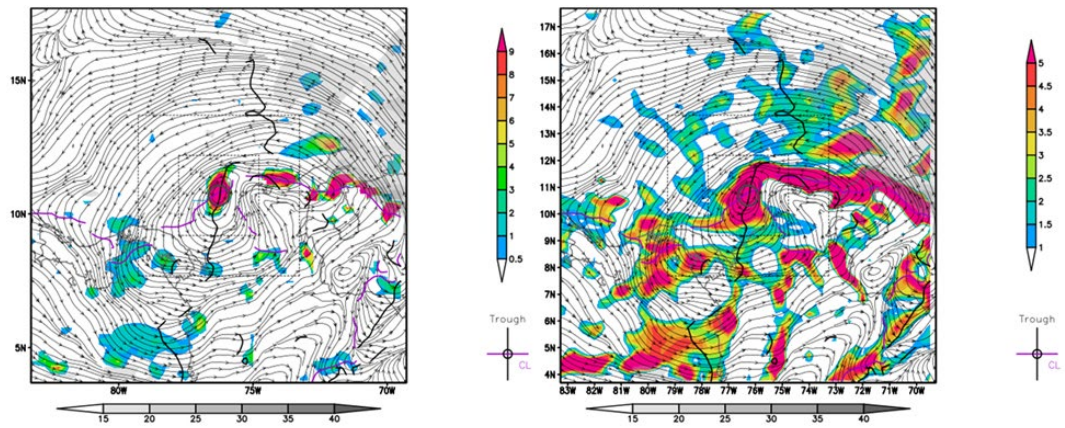

GFS analysis of OW (left) and relative vorticity (right) with 850 hPa streamlines in the precursor-relative frame of reference at 12 UTC 29 September 2020 with the disturbance moving at 4 m s^{-1} westward. The units for OW are $\times 10^{-9}$ s^{-2}, the units for relative vorticity are $\times 10^{-5}$ s^{-1}, and the gray color bars below the plots represent wind speed in knots. The closed circulation at 850 hPa and areas of high OW and relative vorticity near the circulation center are clearly visible in the precursor-relative frames.

Figure 17. GFS analysis of OW (left) and relative vorticity (right) at 850 hPa with streamlines at 12 UTC 29 September 2020

This low-level quasi-pouch feature seen on 29 September 2020 did not develop for several days, until the tropical wave moved in from the east and began to align with the low-level structure. Instead of building itself and moving west and north as would be expected of a burgeoning tropical cyclone, the low-level pouch oscillated within the southwest corner of the Caribbean between Colombia and Panama and did not develop in intensity or vertical depth for 30 hours. At 18 UTC 30 September 2020, as can be seen in Figure 18, the vorticity strip previously located along 11°N between 69° and 77°W had begun to "roll-up" similarly to several precursors studied by Dunkerton et al. (2009). The vorticity strip at this time was located between 12° and 15° N and 65° and 79° W, with the western terminus at the sweet spot of the low-level pouch at approximately 12°N, 79°W. The vorticity strip maintained an overall high coverage of peak cyclonic relative vorticity with the value of at least 5×10^{-5} s^{-1}. The strip was still primarily oriented east-west, but there was a very clear movement and concentration of relative vorticity around the low-level pouch structure when compared with previous forecast periods. At the same time, the open tropical wave which had previously traversed the Atlantic basin aligned vertically above the low-level structure geographically, as can be seen in Figure 16. The interaction

of the tropical wave and the low-level structure appeared to give the precursor disturbance complex the impetus for development.

Prior to this event, neither structure showed significant indications of developing. The low-level structure, though full of relative vorticity at the peak value of at least 5×10^{-5} s^{-1} in the strip, showed no interaction with the upper levels and the wave was not carrying significant relative vorticity with it. By 18 UTC 30 September 2020 the streamlines in the upper levels, particularly at 700 hPa had begun to establish a circulation directly above the lower-level circulations at 12°N, 79°W as the wave moved into vertical alignment with the lower-level pouch, which can be seen in Figure 18. These streamlines in the Earth-relative frame corresponded to the separate streamlines that were previously observed as belonging to the tropical wave (not depicted), and at this point they were oriented in such a way that they are coincident with the streamlines of the lower-level pouches at 12°N, 79°W. Although the pouch at 700 hPa was not fully enclosed yet, it is clear that the precursor was becoming more organized. At 18 UTC 30 September 2020 is also when Gamma's precursor begins moving to the northwest. This movement, as can be seen in Figure 16, accelerated as it developed, and it continued in that direction through formation.

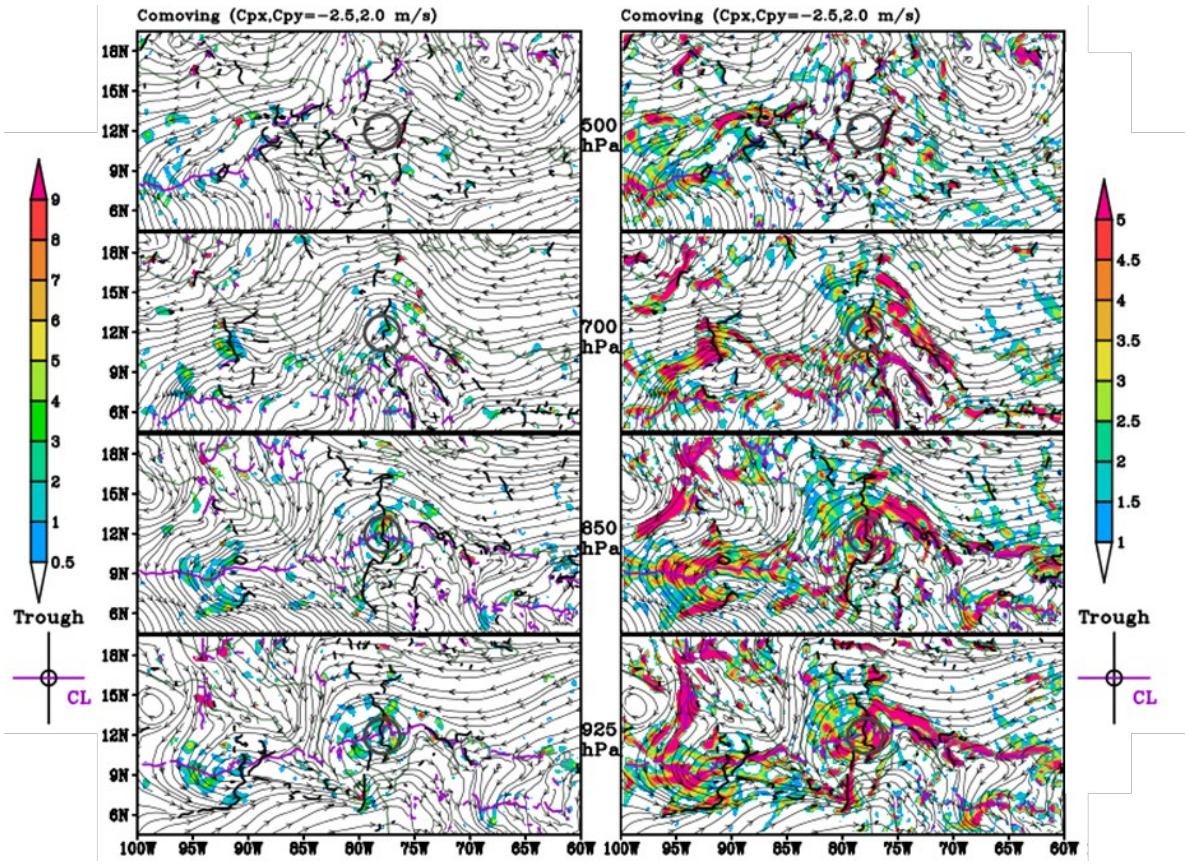

GFS analyses of Gamma precursor in the Caribbean Sea with OW (left) and relative vorticity (right) in a precursor-relative depiction at 500, 700, 850, and 925 hPa (top to bottom) at 18 UTC 30 September 2020. The precursor-relative model has a velocity of 2.5 m s^{-1} westward and 2 m s^{-1} northward. The units for OW are $\times 10^{-9}$ s^{-2}, and the units for relative vorticity are $\times 10^{-5}$ s^{-1}. The pouch is clearly visible at 925 and 850 hPa with closed streamlines and a crossing trough and critical latitude. The wave at 700 hPa has moved directly above the pouches at 925 and 850 hPa. The vorticity in the area is beginning to condense within the circulation from the "vorticity strip" formation it had previously demonstrated.

Figure 18. GFS analysis of OW and relative vorticity at 500, 700, 850, and 925 hPa in the precursor-relative frame at 18 UTC 30 September 2020

Over the subsequent 18 hours after the wave came into alignment with the lower-level pouches, the wave and the lower-level quasi-pouch structures amalgamated into a single atmospheric disturbance. The precursor complex had continued to consolidate and roll up at the lower levels as well as built the circulations and pouches in the upper levels. As can be seen in Figure 19, by 12 UTC 1 October 2020 there were clear pouches at 925 and 850 hPa, and there was a small, but fully enclosed pouch at 700 hPa, all centered

approximately at 13°N, 81°W. At the 500 hPa level, there were indications of a pouch starting to form at 15°N, 81°W, but the circulation was not yet fully enclosed, and the trough axis was not crossing the critical latitude as seen at the other levels. Additionally, it can be clearly seen that the vorticity strip associated with the lower-level pouch structure had reoriented from the east-west direction to the north-south direction along 81°W. The peak relative vorticity in this vorticity roll-up appears to be associated with the distortion of the pouch at 925 and 850 hPa. The streamlines surrounding the pouch were very distorted, especially on the northern end, having an almost pointed appearance. The lower-level pouch was elongated along the north-south axis of the trough along 81°W, primarily to the north of the sweet spot at 13°N, 81°W. What had previously been the western terminus of the vorticity strip had changed to the southern terminus with the roll-up. The elongation of the pouch along the trough axis was a deviation from the more typical circular shape of a cyclonic gyre pouch in a typical developing easterly wave (Dunkerton et al. 2009). The elongation of the pouch directly corresponded the reorientation of the vorticity within the circulation, implying a connection to the vorticity roll-up. The OW center of the pouch remained firmly at the sweet spot where the trough axis and critical latitude cross with high values of relative vorticity at 5×10^{-5} s^{-1}. The sweet spot also had a small spot of peak OW at or above 9×10^{-9} s^{-2}. According to the Marsupial Paradigm, further development of the disturbance was then expected.

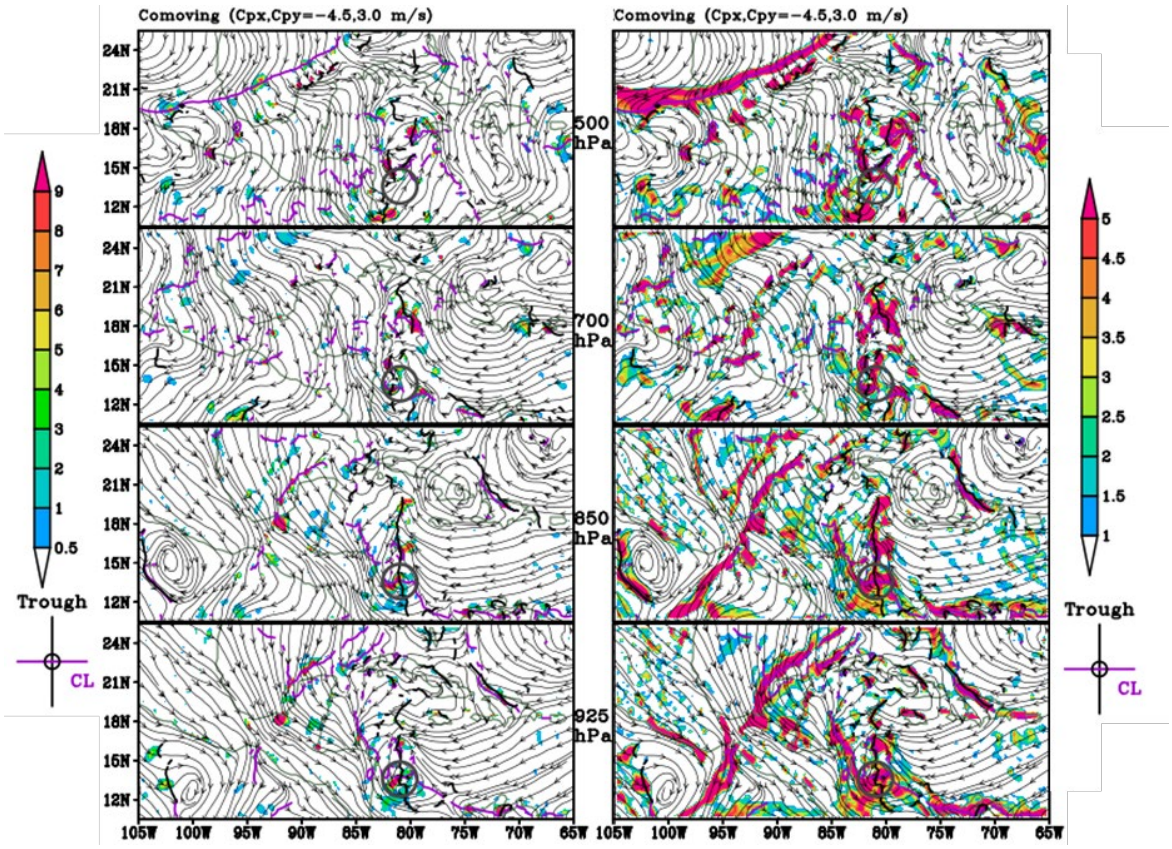

Like Figure 18, except at 12 UTC 01 October 2020. The precursor-relative model has a precursor velocity of 4.5 m s^{-1} westward and 3.0 m s^{-1} northward. Pouches at 925, 850, and 700 hPa levels are clearly defined. The streamlines at 500 hPa are starting to circulate but have not yet become fully enclosed. The vorticity strip at lower levels has reoriented in the north-south direction vs. the east-west orientation that it previously had, and the pouch circulations at all levels has become elongated to the north and south in conjunction with the vorticity strip reorientation.

Figure 19. GFS analysis of OW (left) and relative vorticity (right) at 500, 700, 850, and 925 hPa in the precursor-relative frame of reference at 12 UTC 01 October 2020

Over the following six hours, Gamma's precursor continued to consolidate and organize. As shown in Figure 20, by 18 UTC 1 October 2020 there were pouches at all levels centered on 17°N, 83°W, with closed cyclonic circulations, centralized OW with a peak value of at least 9×10^{-9} s^{-2}, centralized cyclonic relative vorticity with a peak value of at least 5×10^{-5} s^{-1}, and a clearly established intersection of the critical latitude and trough axis. Gamma's precursor at this point had developed a fully established pouch structure with vertical alignment from the surface through 500 hPa. The vorticity roll-up had also

continued from the previous time period. Though the pouch is fully established, it is still elongated in the north-south direction along the trough axis, albeit it is less prominent than the previous time period. The roll-up process was ongoing, and the vorticity was continuing to centralize itself to the pouch.

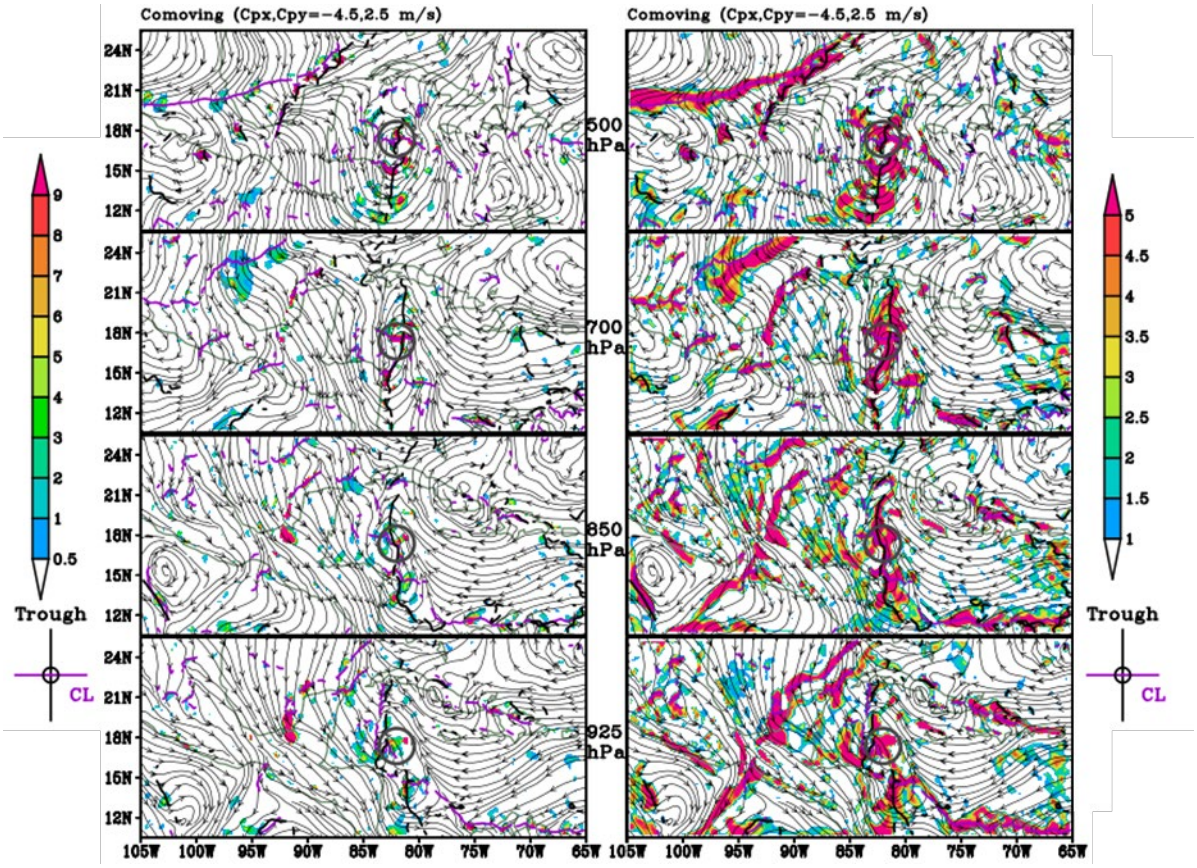

Like Figure 18, except at 18 UTC 01 October 2020. The precursor-relative model has a precursor velocity of 4.5 m s^{-1} westward and 2.5 m s^{-1} southward. Pouches at all levels are clearly defined and vertically aligned. The pouches remain somewhat elongate along the north-south axis, but they all have closed streamlines, centralized OW and relative vorticity, and an intersection of the critical latitude and trough axis.

Figure 20. GFS analysis of OW (left) and relative vorticity (right) at 500, 700, 850, and 925 hPa in the storm-relative frame of reference at 18 UTC 01 October 2020

In the subsequent 12 hours, Gamma's precursor continued to consolidate and develop into a tropical depression. By 06 UTC 2 October 2020 the relative vorticity roll-up process had largely completed with the vorticity concentrated in the center of the pouch

with a value of 5×10^{-5} s^{-1} and the streamlines concentrated from their elongated position along the trough axis into a more circular structure. The OW at this time has also grown in its areal coverage at the peak value of at least 9×10^{-9} s^{-2} around the sweet spot of the pouch at 18°N, 84°W. This is also the time period when the precursor officially became a tropical depression (Latto 2021), and it continued to develop very rapidly into a tropical storm within 12 hours from this point in time. The fully developed pouch can clearly be seen at all levels in Figure 21.

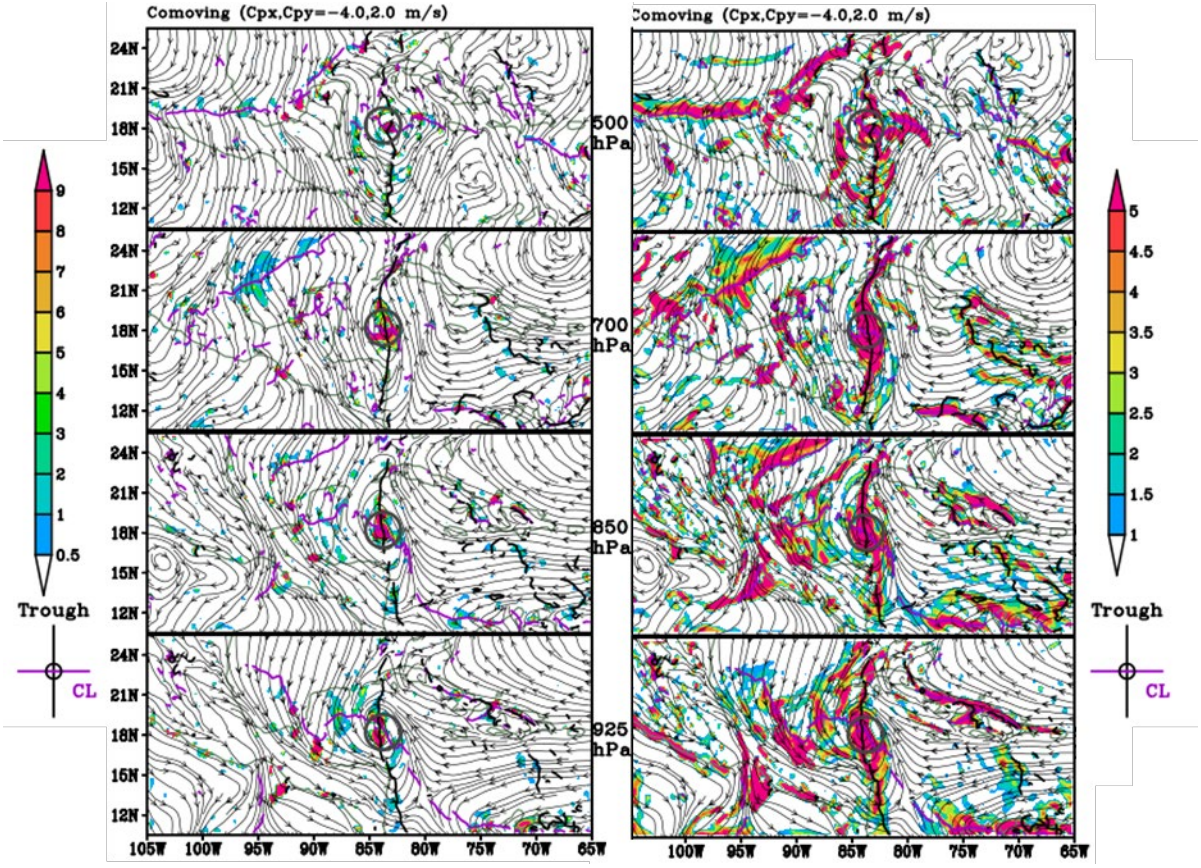

Like Figure 18, except at 06 UTC 02 October 2020. The precursor-relative model has a precursor velocity of 5.0 m s^{-1} westward and 3.5 m s^{-1} northward. Pouches at all levels are clearly defined and vertically aligned. The roll-up has completed at this point as the relative vorticity has centralized within the pouches and the streamlines have normalized to the more typical circular structure.

Figure 21. GFS analysis of OW (left) and relative vorticity (right) at 500, 700, 850, and 925 hPa in the storm-relative frame of reference at 06 UTC 02 October 2020

The evolution of Gamma's precursor is visible when observed over time, such as in Figure 22. Though there was a large amount of vorticity in the area early in the development, especially at low levels, there were low values of OW in the region inhibiting the growth of the disturbance. This is especially clear in the time-height plots in Figure 22. The tropical wave came into vertical alignment with the low-level pouch as suggested by the increase in relative vorticity at the 700 hPa level at 18 UTC 30 September 2020. The vorticity roll-up and elongation of the pouch in the north-south direction are evident by the decrease in OW and relative vorticity on 1 October 2020 in the 3°×3° region. However, this temporary decrease in OW and relative vorticity is not evident in the 6°×6° frame. This is because the reorientation of the low-level vorticity from the long east-west oriented strip along the north-south trough axis advected part of the vorticity (and consequently the OW) outside the 3°×3° frame. The subsequent consolidation of the pouch meant it was fully formed at 06 UTC 2 October 2020, marked by the purple vertical lines in Figure 22. The burst of convective activity facilitated by that pouch that built Hurricane Gamma is also apparent as the significant increase of OW and vorticity that occurred from 2 October 2020 onwards.

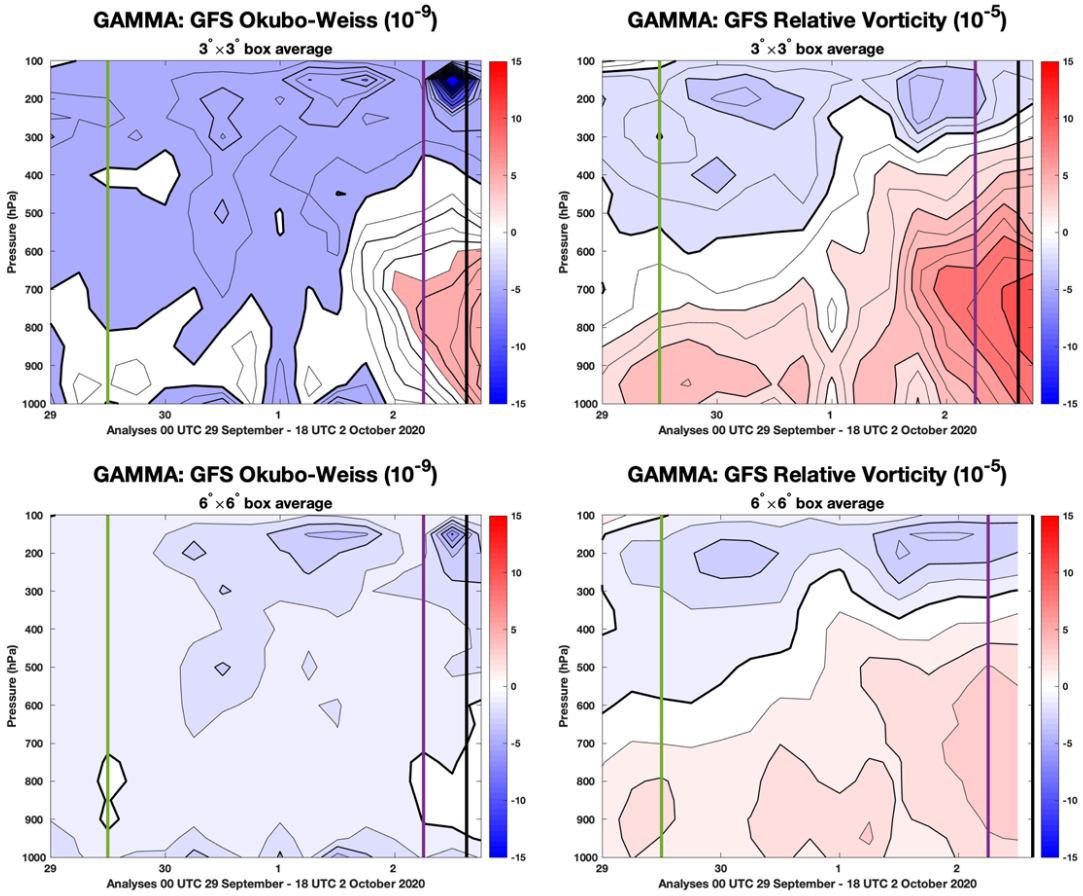

GFS analysis of OW (left) and relative vorticity (right) in the area surrounding Gamma's precursor at over time in 3°×3° view (top) and 6°×6° view (bottom). The x axis represents time period the precursor was tracked from 00 UTC 29 September to 18 UTC 02 October. The y axis is height as represented by pressure in hPa levels. The intensity of each variable is indicated by the colors with respect to either color bar. The green vertical line represents the time a pouch was first identified at 12 UTC 29 September 2020, the purple vertical line represents the time the pouch was fully formed at 06 UTC 2 October 2020, and the black line represents the first NHC advisory at 15 UTC 2 October 2020.The vorticity roll-up and elongation of the pouch along a north-south axis is clear as the decrease in OW and relative vorticity seen on 01 October 2020 in the 3°×3° view but not in the 6°×6°. The completion of the vorticity roll-up and centralization of the pouch is apparent as the increase in OW and relative vorticity seen on 02 October 2020.

Figure 22. GFS analysis of OW and relative vorticity as time vs. height plots for Gamma's precursor

The quick progression of Gamma's precursor is also visible in GOES satellite imagery during the times of interest (Figure 23). In the space of roughly 36 hours, the precursor flow structure evolved from an incoming tropical wave coming into alignment with the low-level pouch (Figure 23, upper left) to rolling up the vorticity strip (Figure 23,

upper right) to an elongated, but fully formed pouch (Figure 23, lower left) to sustained convection and formation as a tropical depression (Figure 23, lower right). The tropical wave came into alignment with the low-level vorticity strip at 18 UTC 30 September 2020 (Figure 23, upper left), and the lack of organized convective activity was evident in the visible satellite imagery. The start of the sustained deep convection at 12 UTC 1 October 2020 (Figure 23, upper right) was evidenced by the presence of cold cloud tops in the IR imagery by the bright white areas, that indicate the presence of cold temperatures at that time. The consolidation of relative vorticity and consequent organization of the disturbance can be inferred in the increased central cloud cover in the visible imagery at 18 UTC 1 October 2020 (Figure 23, lower left) and the increased cold cloud tops at the core of the disturbance at 06 UTC 2 October 2020 (Figure 23, lower right). The cold cloud tops visible at 06 UTC 02 October 2020 (Figure 23, lower right) indicate the presence of deep convection, and the beginnings of the characteristic swirl of a tropical cyclone was evident.

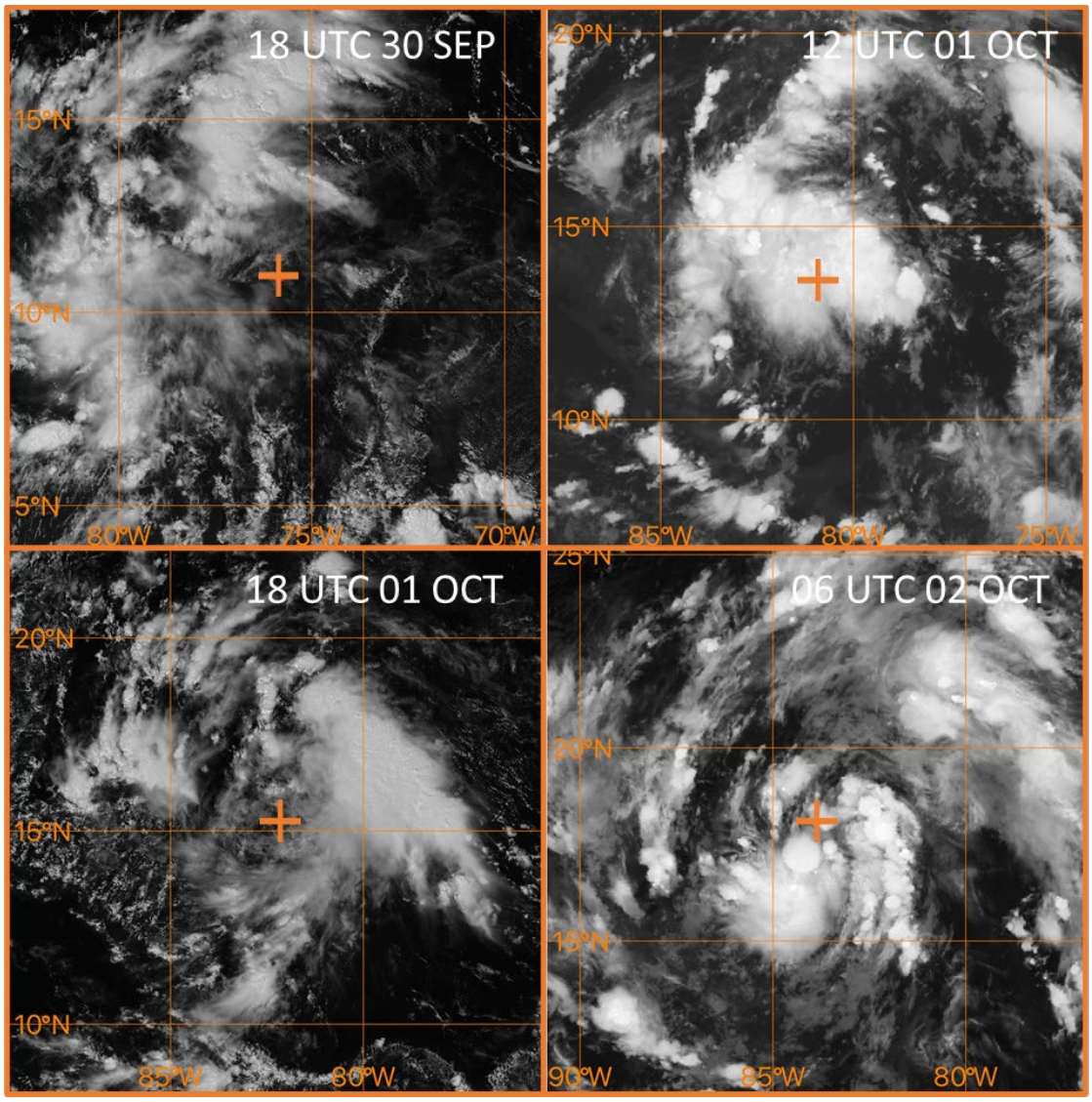

GOES IR and visible satellite imagery of Gamma's precursor at the times of interest centered on the GFS tracked position. 18 UTC 30 September and 18 UTC 01 October are visible images while 12 UTC 01 October and 06 UTC 02 October are IR images. The tracked center (sweet spot) is represented by an orange cross. The imagery depicts the increase in convection over time, which is especially apparent at 06 ITC 02 October 2020 when the vorticity roll-up completed, and the storm is designated a tropical depression.

Figure 23. GOES IR and visible imagery of the GFS tracked positions at various times of interest for Gamma's precursor

The growth of Gamma's precursor is also clear in the relative humidity and vertical mass flux time-height plots (Figure 24). As can be seen in Figure 24, there is an increase in vertical mass flux on 30 September 2020 going from 0 to 5 kg m^{-2} s^{-1} in the upper levels

and then dying down to 1 kg m^{-2} s^{-1} after the convective plume had passed. This means that there was deep convection occurring at that time, because a high value of vertical mass flux is an indication of convection, as convection is marked by air moving vertically through the column. That vertical mass flux occurs throughout the air column means that deep convection is occurring, which moistens the upper troposphere, bringing the relative humidity values from 40% to near 90% in the upper levels. This convective plume complex coincided with the tropical wave vertically aligning with the low-level pouch. However, this convection was not sustained and died out as the vorticity roll-up continued at low levels and reoriented itself along the trough axis. This is apparent in the decrease in both relative humidity and vertical mass flux seen on 1 October 2020, as the relative humidity returns to around 65% and the vertical mass flux subsides to 0 kg m^{-2} s^{-1} (Figure 24). The ensuing consolidation of the pouch and the building into the upper levels of the troposphere are also evident from the notable increase in both relative humidity and vertical mass flux seen during the latter part of 1 October 2020 and continuing as the pouch became fully formed at 06 UTC 2 October 2020, marked by the purple vertical lines in Figure 24, the deep convection became sustained, and the disturbance deepened into a tropical depression.

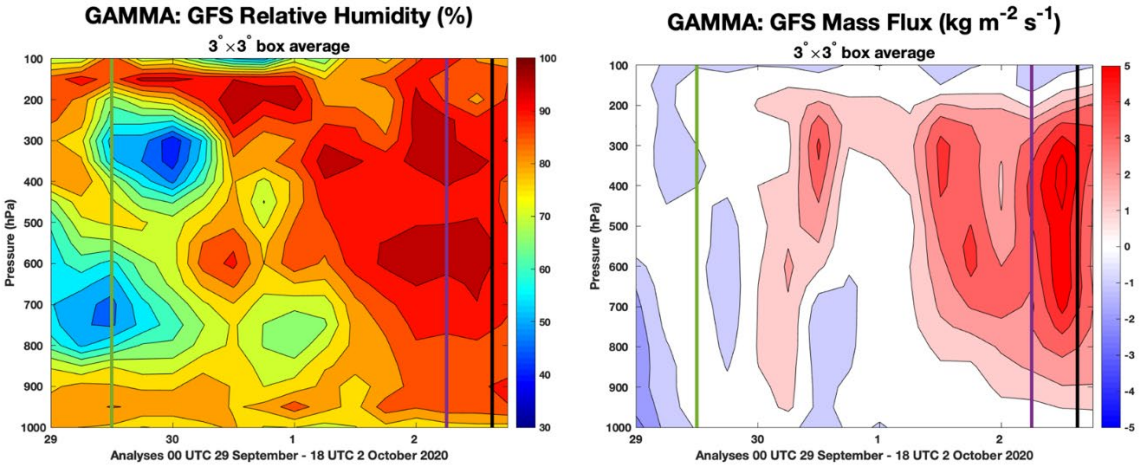

Similar to Figure 22, except for RH (left) and vertical mass flux (right) in the 3°×3° box. Initial convection associated with incoming wave is evident on 30 September 2020. The subsequent relative vorticity roll-up and elongation of the pouch along a north-south axis is apparent in the decrease in vertical mass flux and RH seen on the latter half of 30 September 2020 and throughout 01 October 2020. The following formation of a deep cyclonic pouch as the wave became aligned with the low-level pouch, deep convection, and formation of a TD are clear in the increase in both RH and vertical mass flux in the second half of 01 October 2020 into 02 October 2020.

Figure 24. GFS analysis of relative humidity and vertical mass flux as time vs. height plots for Gamma's precursor

Looking at the progression of Gamma's precursor over time, it is possible to observe these events. The tropical wave becoming aligned with the low-level pouch can be seen in the decrease of area-averaged deep vertical wind shear on 30 September 2020, decreasing from 10 m s^{-1} to 5 m s^{-1}. (Figure 25). The vorticity roll-up can be observed in the dip in OW, relative vorticity, relative humidity, equivalent potential temperature, and vertical mass flux on 1 October 2020 (Figure 25). The formation of the pouch and deepening of the disturbance into a tropical depression is marked by the increase in OW, relative vorticity, relative humidity, and vertical mass flux on 2 October 2020, with the OW increasing past 10×10^{-9} s^{-2} and the relative vorticity increasing past 10×10^{-5} s^{-1} (Figure 25). There is an anomalously high value of deep vertical wind shear value of roughly 13 m s^{-1} at 00 UTC 1 October 2020 in both the 3°×3° and 6°×6° averaging regions that corresponds to a tropical upper tropospheric trough (TUTT) that briefly interacts with the area of interest for one forecast period. This interaction may have had a mildly deleterious effect on the precursor's formation, but it clearly did not inhibit the formation process.

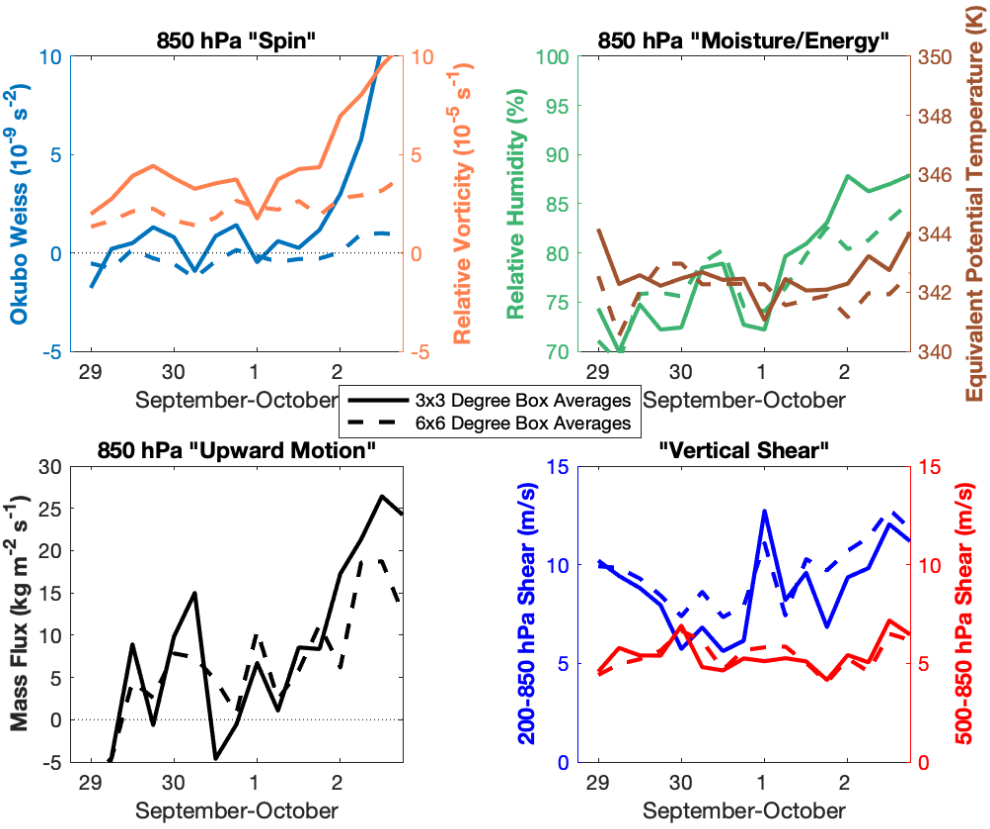

GFS Analysis of spin (upper left), moisture (upper right), upward motion (lower left), and vertical wind shear (lower right) in the area surrounding Gamma's precursor over time. The x axes for each plot represent time period the precursor was tracked from 18 UTC 30 September to 18 UTC 02 October with the respective variable shown as a time series. The presence of vorticity is evident throughout the time period. The incoming tropical wave's alignment corresponded with a decrease in deep vertical wind shear, but it was not until the vorticity roll-up was complete and a pouch was formed that the OW, relative vorticity, and vertical mass flux notably increased, indicating that the disturbance had reached TD stage.

Figure 25. GFS analysis of Gamma's precursor for spin, moisture, upward motion, and vertical wind shear as time series plots

In summary: the progression of Gamma's precursor was unique in that the NHC-identified precursor tropical wave interacted with a low-level vorticity pouch that formed off the coast of South America. Also, the vorticity strip precursor disturbance experienced a vorticity roll-up as discussed in Dunkerton et al. (2009). The formation of the storm, though unique and difficult to forecast, conforms to the Marsupial Paradigm.

C. ZETA

Hurricane Zeta had a very complicated genesis sequence. While the initial disturbance came from an African easterly wave, the originating wave differed from the previous cases in that it profoundly interacted with a Central American Gyre in the hours leading up to the formation of Tropical Storm Zeta.

The African easterly wave that contributed to the formation of Zeta exited Africa in early October and traversed the Atlantic at a low latitude as an open tropical wave (Blake et al. 2021). The wave then tracked westward along the northern coast of South America from Guyana to Colombia. It entered the Caribbean Sea and began interacting with the local environment 18 October 2020. In the Caribbean Sea, the wave formed an initial pouch within the wave. As can be seen in Figure 26, the precursor disturbance moved off the northern coast of Southern America and then encountered a low-level structure in the form of the Central American Gyre (not depicted) on 21 October 2020. The encounter slowed the precursor's advance as well as facilitated the formation of a tropical cyclone. The precursor became a tropical depression at 12 UTC 24 October 2020, and Tropical Storm Zeta formed at 00 UTC 25 October 2020 in the Caribbean Sea, east of Nicaragua and south of Jamaica.

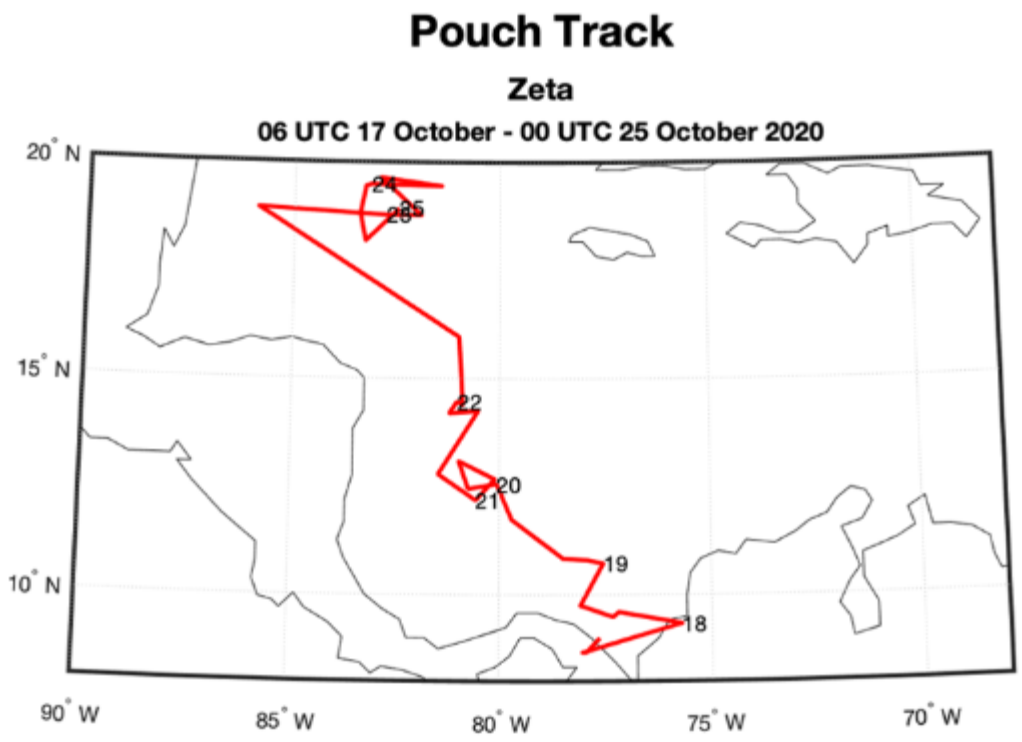

Depiction of the GFS analyzed track of Zeta's precursor in the Caribbean Sea from 06 UTC 17 October 2020 to 00 UTC 22 October 2020. Points are determined every 6 hours at 00, 06, 12, and 18 UTC, with the date labelled to the immediate right of the 00 UTC position. The track shows the movement of the AEW to the northwest from 00 UTC 18 October 2020 until it slows and remains nearly stationary for a period on 20–21 October 2020 before interacting with a CAG on 21–23 October 2020 and forming on 25 October 2020.

Figure 26. GFS analysis of track positions of Zeta's precursor in the Caribbean Sea, October 2020.

A tropical wave crossing the Atlantic and interacting with the northern South American coastline is not unusual, even if it does not always result in the formation of a tropical cyclone. A pouch is still necessary for a tropical cyclone to develop. The first time that a pouch for Zeta's precursor can be seen in GFS 6-hourly analyses is at 12 UTC 18 October 2020 when the disturbance is just off the coast of Colombia, as can be seen in Figure 27. The pouch is clearly evident at 850 hPa with closed streamlines surrounding an intersection of a trough and critical latitude at approximately 10°N, 78°W. This sweet spot also has high values of centralized OW and relative vorticity, with peak values of at least 9×10^{-9} s^{-2} and of 5×10^{-5} s^{-1} respectively. At this time there were also the beginnings of a

pouch at 925 hPa (not depicted), with centralized OW and relative vorticity in circulation, but the streamlines had not yet closed.

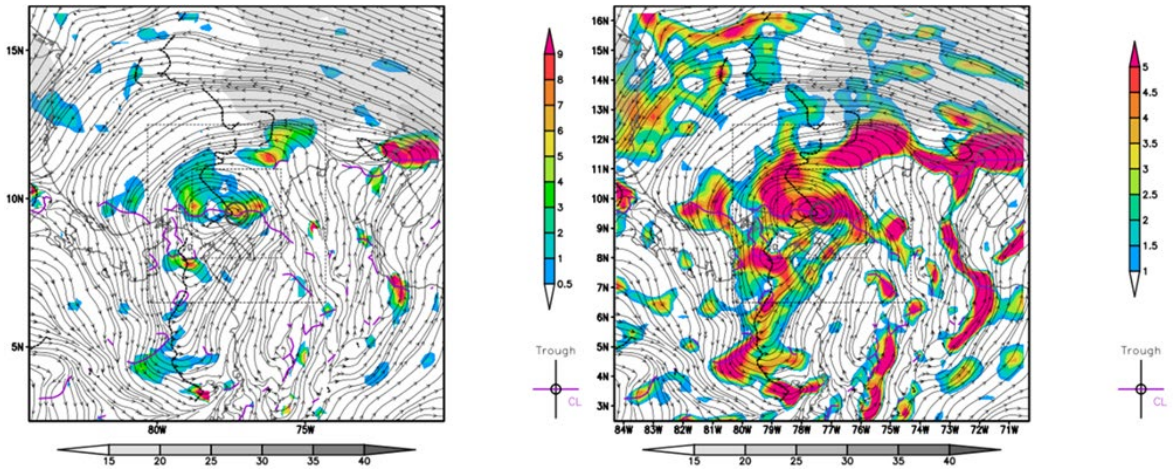

GFS analysis of OW (left) and relative vorticity (right) with 850 hPa streamlines in the precursor-relative frame of reference at 12 UTC 18 October 2020 with the disturbance moving at 1 m s^{-1} westward and 0.5 m s^{-1} southward. The units for OW are $\times 10^{-9}$ s^{-2}, the units for relative vorticity are $\times 10^{-5}$ s^{-1}, and the gray colorbars below the plots represent wind speed in knots. The closed circulation at 850 hPa and areas of high OW and relative vorticity near the circulation center are discernible in the precursor-relative frames.

Figure 27. GFS analysis of OW (left) and relative vorticity (right) at 850 hPa with streamlines at 12 UTC 18 October 2020

After this first depiction, the wave-pouch, which extended downward from 850 hPa through the 925 hPa level, proceeded northwestward until it encountered the low-level circulation of a Central American Gyre at 06 UTC 21 October 2020. In Figure 28, the relatively small wave-pouch is depicted east of Nicaragua at 12°N, 81°W with peak values of at least 9×10^{-9} s^{-2} of OW and of 5×10^{-5} s^{-1} of relative vorticity. The quasi-stationary Central American Gyre is clearly visible in the both the Earth-relative and precursor-relative frameworks as a large low-level circulation centered over the Yucatan peninsula near 20N, 87W that spans from the Bay of Campeche to Honduras with large areal coverage of peak OW values of 9×10^{-9} s^{-2} or more and peak relative vorticity values of 5×10^{-5} s^{-1} or more. The CAG was clearly defined at 925 and 850 hPa, but it did not reach into the upper atmosphere (not depicted), which is consistent with the CAG as outlined by Papin et al.

(2017). As the incoming wave-pouch and the CAG were both located in the lower levels, they were beginning to interact with each other at this time.

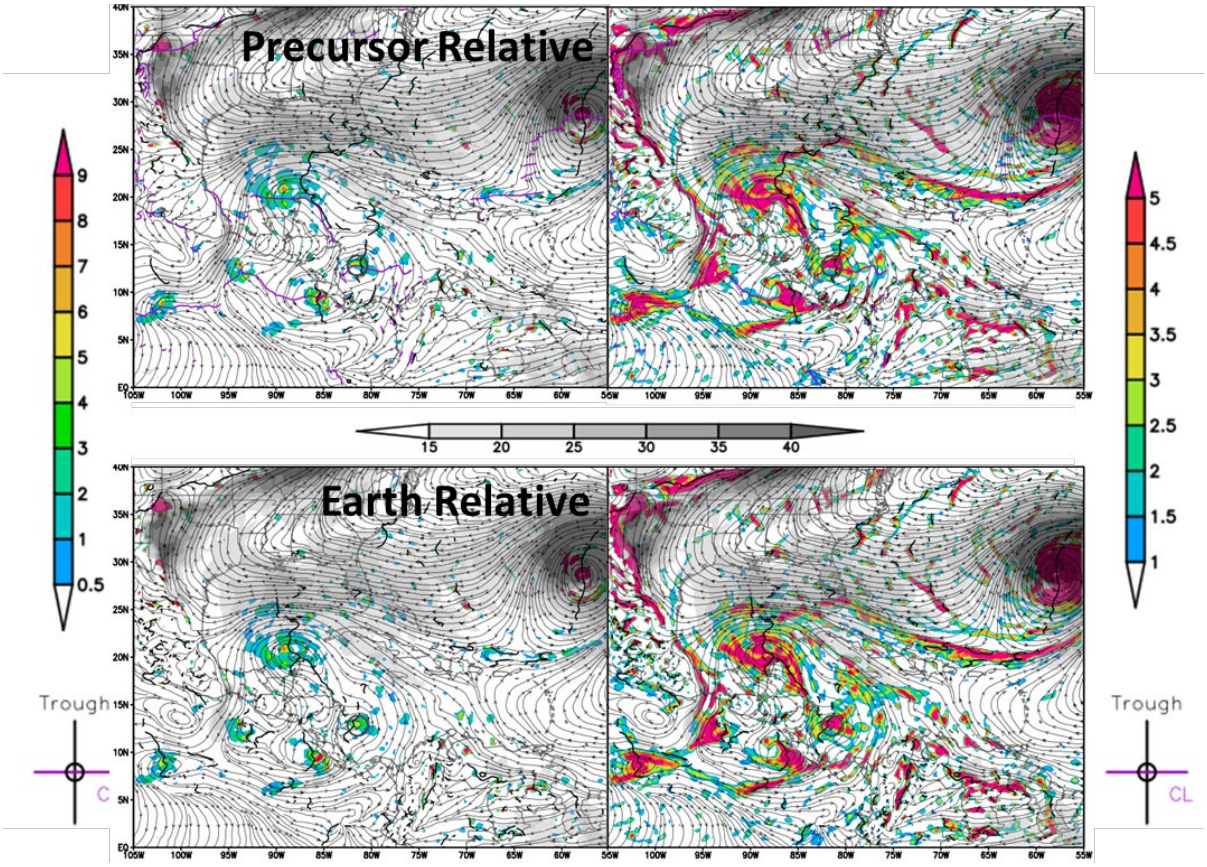

GFS analysis of OW (left) and relative vorticity (right) with 850 hPa streamlines in the precursor-relative and Earth-relative frames of reference at 06 UTC 21 October 2020 with the disturbance moving at 1 m s^{-1} eastwards and 1 m s^{-1} northwards. The units for OW are $\times 10^{-9}$ s^{-2}, and the units for relative vorticity are $\times 10^{-5}$ s^{-1}. The CAG is apparent as the large close circulation centered over the Yucatan Peninsula, and the wave pouch was well-defined as the smaller circulation located between Nicaragua and Panama. That they were closed separate entities is clear in the Earth-relative frame, while it is apparent that they were beginning to interact in the precursor-relative framework.

Figure 28. GFS analysis of OW (left) and relative vorticity (right) at 850 hPa with streamlines at 06 UTC 21 October 2020

Twelve hours following the initial interaction of the wave-pouch and the CAG, the two proceeded to integrate, becoming one large circulation. This circulation stretched from 15°-23°N to 82°-93°W and included the both the areas previously covered by either the Central American Gyre or the wave-pouch. At the beginning of this integration phase, the

circulation had two distinct centers of OW and relative vorticity. However, as the systems merged, the vorticity became more generalized throughout the entire large circulation with values ranging from 1×10^{-5} s^{-1} to 5×10^{-5} s^{-1} and an increased areal coverage of the relative vorticity from the relatively centered depiction 12 hours prior (Figure 28). At 18 UTC 21 October (Figure 29), twelve hours after the merger initiation, the two circulations had become lobes of a single larger circulation. Additionally, the relative vorticity had dispersed throughout the new larger circulation, although the maximums were still distinct and separate from each other and located where the previous centers of the CAG and wave-pouch were at approximately 20°N, 87°W, and 15°N, 82°W respectively. Another indication of the interaction was that the disturbance became stationary during the time that the circulations were condensing and reorganizing into one singular circulation. This effect can be seen in Figure 26 as the time around 21 October 2020 where the track appears to circle in place.

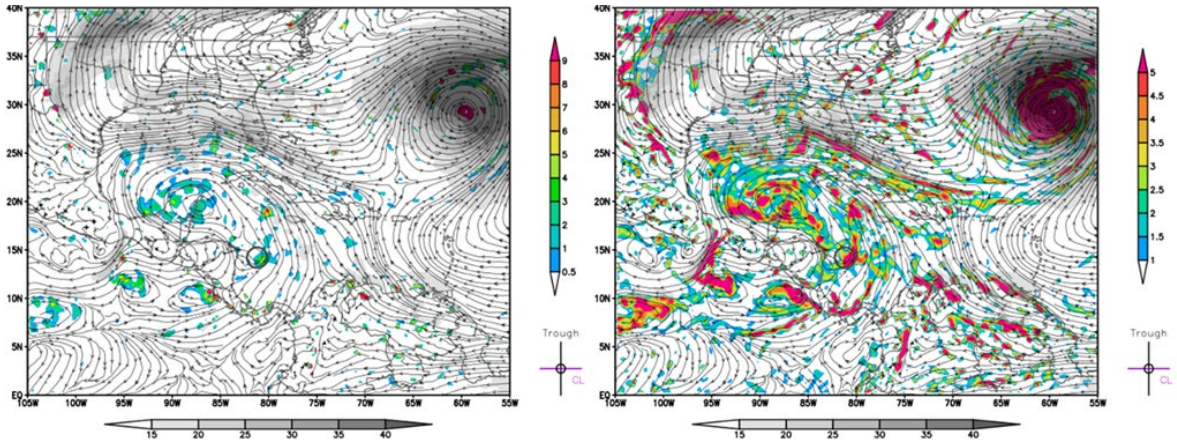

GFS analysis of OW (left) and relative vorticity (right) with 850 hPa streamlines in the precursor-relative frame of reference at 18 UTC 21 October 2020 with the disturbance stationary. The units for OW are $\times10^{-9}$ s^{-2}, the units for relative vorticity are $\times10^{-5}$ s^{-1}, and the gray colorbars below the plots represent wind speed in knots. The circulations of the CAG and wave pouch have merged to become a single circulation, although features of the previous circulations, such as vorticity and OW centers are still evident. The circulations have not yet fully integrated themselves, and a full-formed pouch for the whole circulation was not evident at this time.

Figure 29. GFS analysis of OW (left) and relative vorticity (right) at 850 hPa with streamlines at 18 UTC 21 October 2020

The wave-pouch and CAG continued to consolidate around a central point within the new larger circulation, at approximately 18°N, 83W, forming a single, much larger pouch. This was an axisymmetrization, such as described by Montgomery and Kallenbach (1997). By 00 UTC 23 October (Figure 30), approximately 42 hours after the circulations begin to merge, a single large but cohesive pouch to the east of Nicaragua. Though the pouch itself was still significantly larger than what has been typically seen in the other storms, the OW and vorticity were becoming increasingly more centralized, as seen in the 925 and 850 hPa levels, with peak values for OW of 4×10^{-9} s^{-2} and of 5×10^{-5} s^{-1} or higher for relative vorticity (Figure 30). This consolidation, particularly of vorticity, is an indication of the increasing organization of the precursor. Additionally, the beginnings of a pouch at 700 hPa can be seen at 19°N, 82°W, although the streamlines were not yet closed. This is the first indication that the lower-level pouch circulations were building into the upper levels of the atmosphere.

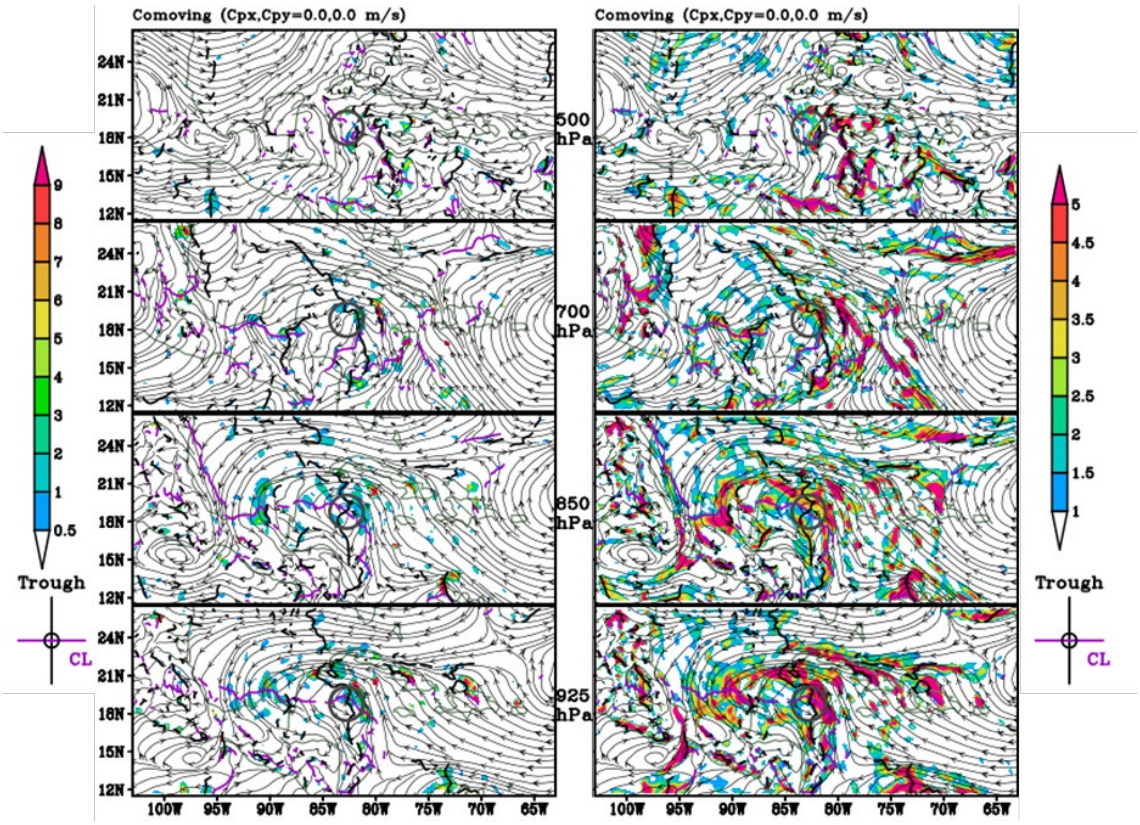

GFS analyses of Zeta precursor in the Caribbean Sea with OW (left) and relative vorticity (right) in a precursor-relative depiction at 500, 700, 850, and 925 hPa (top to bottom) at 00 UTC 23 October 2020. The precursor-relative model has a stationary storm velocity. The units for OW are $\times 10^{-9}$ s^{-2}, and the units for relative vorticity are $\times 10^{-5}$ s^{-1}. The pouch is clearly visible at 925 and 850 hPa with closed streamlines and a crossing trough and critical latitude. The OW and vorticity had condensed at 925 and 850 hPa, though there was still a significant amount of vorticity dispersed throughout the pouch.

Figure 30. GFS analysis of OW and relative vorticity at 500, 700, 850, and 925 hPa in the precursor-relative frame of reference at 00 UTC 23 October 2020

Over the following twelve hours, Zeta's precursor pouch built and extended upward through 500 hPa (Figure 31). All levels exhibited clear circulations with fully closed streamlines, centralized OW and relative vorticity, and well-defined intersections of troughs and critical latitudes located at 20°N, 83°W. Regions of positive relative vorticity, which 12 hours prior had still been widely dispersed throughout the large pouch at 925 and 850 hPa, had coalesced around the new center of the pouch creating a central area at the sweet spot of relative vorticity with a value of 5×10^{-5} s^{-1}. This sweet spot also had a peak value of at least 9×10^{-9} s^{-2} of OW, an increase from 12 hours prior. This new pouch center

that emerged was not directly aligned to either of the previous centers of the wave pouch or the CAG, but instead grew in the space between them, southeast of where the center of the gyre was and northwest of where the wave-pouch was. The vortices had merged, and the pouch as a whole had axisymmetrized. By this point in the process, the larger pouch had compressed to a size comparable with the other storms observed in this study. Though the pouch at 500 hPa was located slightly southeast of the lower pouches at 19°N, 82°W, the disturbance is vertically aligned for the most part. The vertical alignment of the pouches and the increasing centralization of the relative vorticity are indicators that the precursor was organizing as a pre-formation TC, even though Zeta was still 24 hours prior to becoming a tropical depression. The bottom-up development of Zeta's precursor matches the Marsupial Paradigm, though the process prior to the final pouch development was more complicated involving the merger of the wave-pouch with the CAG.

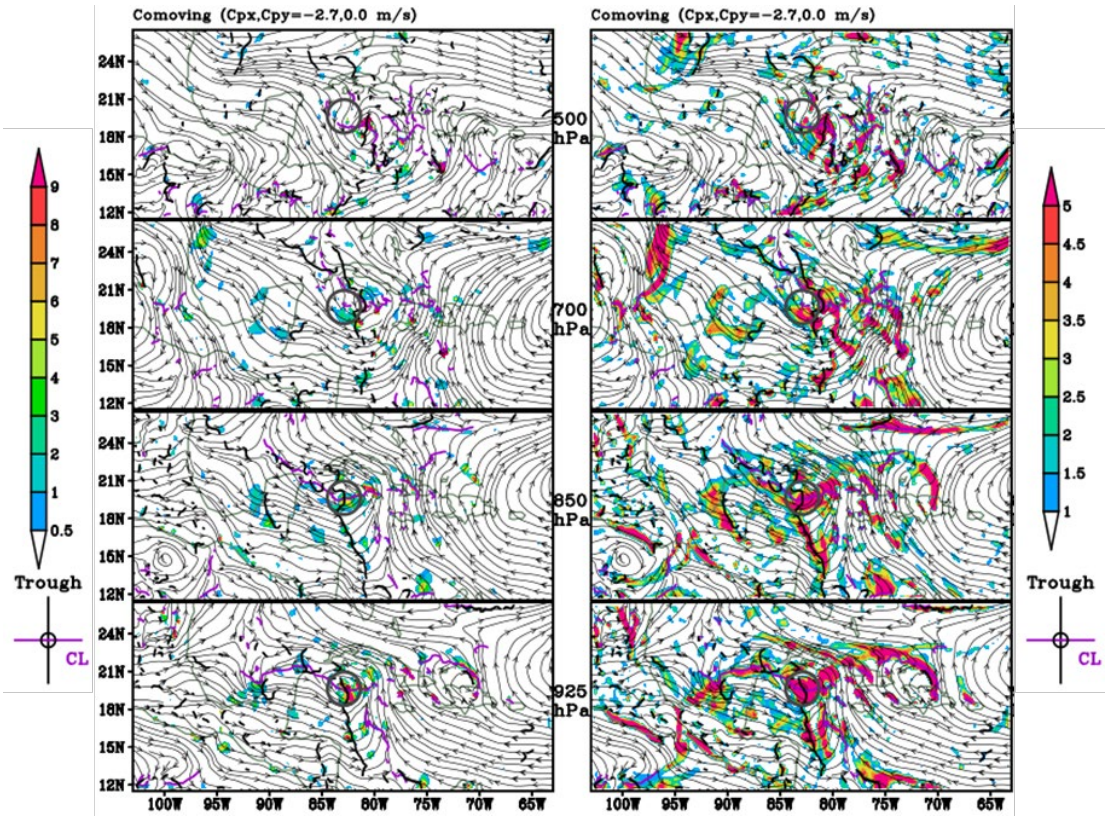

Like Figure 30, except at 12 UTC 23 October 2020. The precursor-relative model has a precursor velocity of 2.7 m s^{-1} westward. Pouches at all levels are clearly defined. The pouches at 925, 850, and 700 hPa are vertically aligned, while the pouch at 500 hPa is displaced to the east. The vorticity has become centralized and the size of the pouches at 925 and 850 hPa have condensed down to a more typical size for storm formation.

Figure 31. GFS analysis of OW (left) and relative vorticity (right) at 500, 700, 850, and 925 hPa in the precursor-relative frame of reference at 12 UTC 23 October 2020

The evolution of Zeta's precursor over time can be seen in Figure 32. Figure 32 depicts the OW and relative vorticity of the pouch associated with wave the until 06 UTC on 21 October 2020 when the wave-pouch began to interact with the CAG. From that point onwards, the precursor was considered to include the both the wave-pouch and the CAG. As Figure 32 shows, there were significant amounts of low-level cyclonic vorticity in the area with values of more than 5×10^{-5} s^{-1} below 700 hPa, but the OW was low prior to the interaction with values around 0×10^{-9} s^{-2} below 700 hPa between 17 October 2020 and 22 October 2020. Given the presence of positive OW centers at the sweet spots at the same time, this means that there were values of OW inside the 3°×3° box that were negative, and

that these negative values had enough areal coverage to bring the area-average of the box down to 0×10^{-9} s^{-2} in the lower levels.

The dispersion and reconsolidation of the vorticity into the large pouch created from both the wave-pouch and the CAG can be clearly seen as the decrease in OW and relative vorticity on 21–22 October 2020, from 0×10^{-9} s^{-2} to -2×10^{-9} s^{-2} for OW and from 2×10^{-5} s^{-1} to -2×10^{-5} s^{-1} in the upper levels for relative vorticity. The consolidation and growth of the pouches throughout the troposphere can be seen as the increase in OW and relative vorticity after the pouch was fully formed at 12 UTC 23 October 2020, marked by the purple vertical lines in Figure 32, into 24 October 2020, increasing from 0×10^{-9} s^{-2} to 4×10^{-9} s^{-2} for OW and 0×10^{-5} s^{-1} to 6×10^{-5} s^{-1} for relative vorticity (Figure 32).

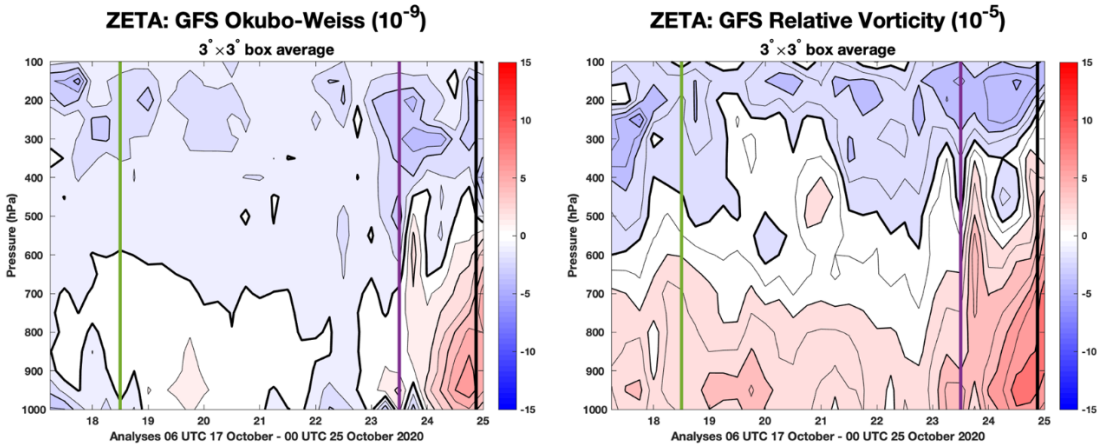

GFS analysis of OW (left) and relative vorticity (right) in the area surrounding Zeta's precursor at over time. The x axis represents time period the precursor was tracked from 06 UTC 17 October to 00 UTC 25 October. The y axis is height as represented by pressure in hPa levels. The intensity of each variable is indicated by the colors with respect to either color bar. The green vertical line represents the time a pouch was first identified at 12 UTC 18 October 2020, the purple vertical line represents the time the pouch was fully formed at 12 UTC 23 October 2020, and the black line represents the first NHC advisory at 21 UTC 24 October 2020. These plots are associated with the pouch from the incoming wave prior to the interaction between the wave-pouch and the CAG on 21 October. The presence of the vorticity at low levels in the area is evident in the right plot. The consolidation of the wave pouch and the CAG can be clearly seen as the decrease in both OW and relative vorticity on 21–22 October. The subsequent formation of the cohesive pouch system and consolidation of the vorticity within the CAG into the Zeta's precursors pouch is apparent as the increase in both OW and relative vorticity on 24 October, prior to the formation of Zeta at 12 UTC 24 October 2020 and becoming a TS at 00 UTC 25 October 2020.

Figure 32. GFS analysis of OW and relative vorticity as time vs. height plots for Zeta's precursor

The evolution of Zeta's precursor can also be observed in satellite pictures. In Figure 33, the precursor is depicted at the times of interest in GOES-16 IR and visible imagery. The progression of the precursor can be seen as through the selected times of interest. In chronological order, the wave-pouch and the CAG began interacting at 06 UTC 21 October 2020 (Figure 33, upper left), the OW and relative vorticity dispersed throughout the new combined pouch from the wave-pouch and the CAG 12 hours later (Figure 33, upper right), the new larger pouch consolidated and began building from the lower levels 30 hours after that (Figure 33, lower left), and the precursor pouch became fully established at all levels and sustained deep convection began 12 hours following that (Figure 33, lower right).

As the wave-pouch and CAG interact and merge 06 UTC 21 October 2020 through 00 UTC 23 October 2020 (Figure 33 upper left and right), there were not large convective plumes during this process, only scattered plumes of convective activity throughout the 3°×3° box, which was consistent with the widespread distribution of relative vorticity throughout the larger merged pouch. The presence of cold cloud tops at 00 UTC 23 October 2020 (Figure 33, lower left) corresponds to the time period when the merged pouch had become a fully formed pouch and had compacted down to a size more typical of tropical cyclone precursors. It also corresponds to the start of sustained convection. The effects of the sustained convection can be seen in the IR imagery at 12 UTC 23 October 2020 (Figure 33, lower right), with the increased central coverage of the cold cloud tops suggesting the presence of deep convection near the central core of the disturbance, which also was the sweet spot. The beginnings of the cyclonic swirl are also visible in the 12 UTC 23 October 2020 IR imagery, approximately 24 hours prior to the disturbance being named a tropical depression.

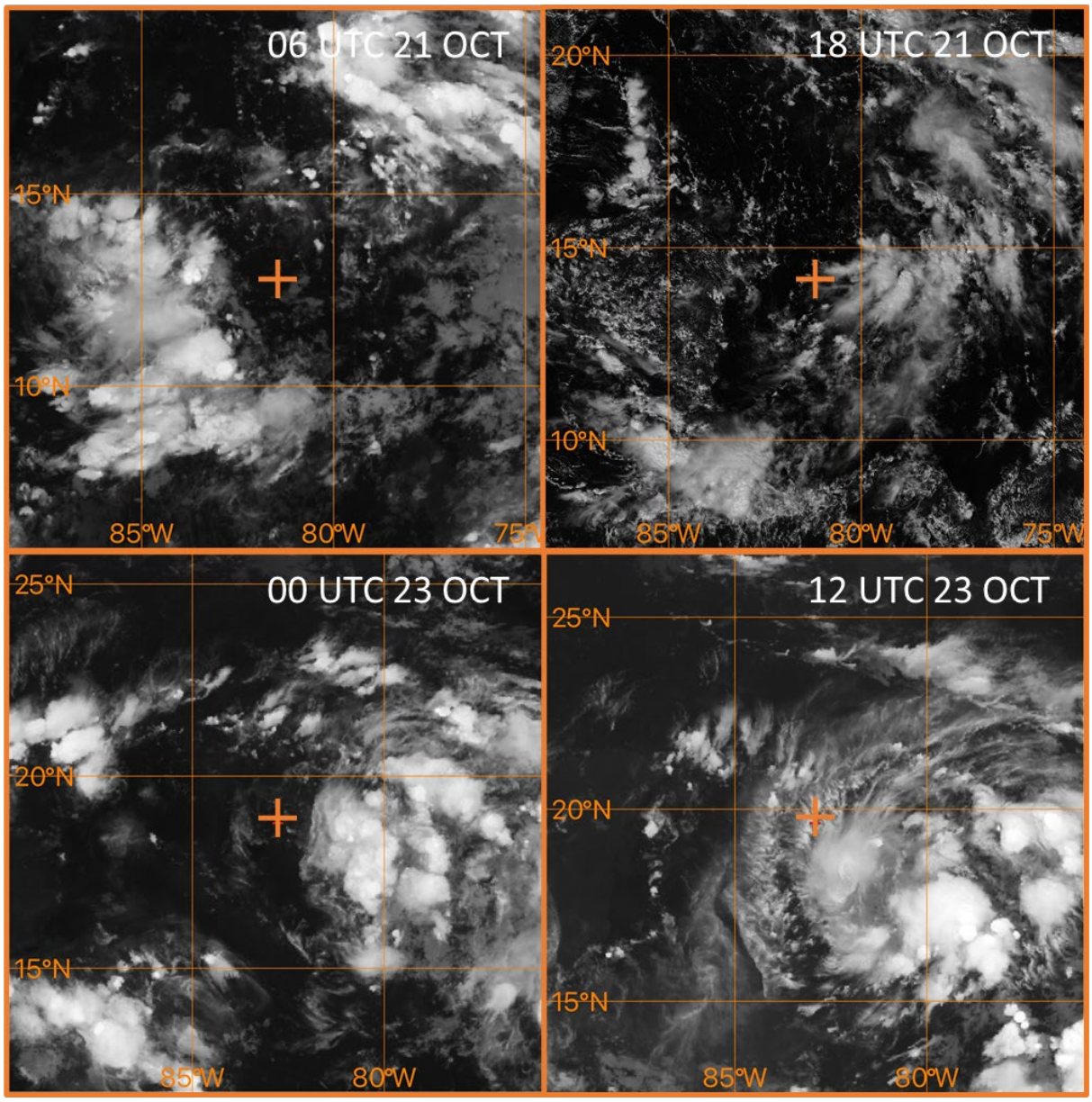

GOES IR and visible satellite imagery of Zeta's precursor at the times of interest centered on the GFS tracked position. 06 UTC 21 October, 00 UTC 23 October, and 12 UTC 23 October are IR images while 18 UTC 21 October is a visible image. The tracked center (sweet spot) is represented by an orange cross. The imagery depicts the progression of the precursor from the initial interaction of the wave pouch and the CAG in the upper left panel at 06 UTC 21 October to the dispersion of vorticity throughout the new larger pouch in the upper right at 18 UTC 21 October to the building of the pouch from the lower levels in the lower left panel at 00 UTC 23 October and ending with the fully established pouch at all levels in the lower right at 12 UTC 23 October. Though there were intermittent plumes of convection throughout the formation process, deep convection was not sustained until 12 UTC 23 October.

Figure 33. GOES IR and visible imagery of the GFS tracked positions at various times of interest for Zeta's precursor

Though the environment in the southwestern Caribbean Sea was overall conducive to tropical cyclone formation, Zeta's precursor did not form a tropical cyclone until the consolidation of the wave-pouch and the CAG into the single precursor pouch was complete. This is demonstrated in Figure 34. There was a clear diurnal signal of convection in the vertical mass flux associated with the wave-pouch as the areas of high vertical mass flux of 2 kg m^{-2} s^{-1} seen in Figure 34, occurring every day and alternating with time periods of negative vertical mass flux, are indicative of convective plumes, and the pattern seen here is diurnal in nature. Despite this cyclical convective development, it did not develop sustained convection until after the amalgamation was complete on 23 October 2020. This is mirrored in the relative humidity seen over time, as the convective plumes, seen as the alternating areas of 40% and 70% relative humidity, periodically moisten the upper atmosphere, the atmosphere cyclically dried out again once the convection had died down. Additionally, the interaction between the wave-pouch and the CAG is visible as the decrease in relative humidity and vertical mass flux occurring on 21–22 October 2020. The relative humidity in the upper levels decreased from 90% to 60% and the vertical mass flux peaks caused by the convective plumes on those days do not reach as high into the atmosphere, not extending above 300 hPa. Sustained deep convection started on 23 October 2020 and was marked by relative humidity of 80% or more through the majority of the atmospheric column. This coincided with the pouch becoming fully formed at 12 UTC 23 October 2020, marked by the purple vertical lines in Figure 34. These deep convective periods possessed levels of vertical mass flux greater than 3 kg m^{-2} s^{-1}. The start of sustained deep convection correlated well with the establishment of a fully formed pouch at all levels and matches the increase in relative humidity available in the upper atmosphere. The foregoing characteristics indicate that the formation of a tropical depression was imminent. Indeed, the disturbance became a tropical depression 24 hours later.

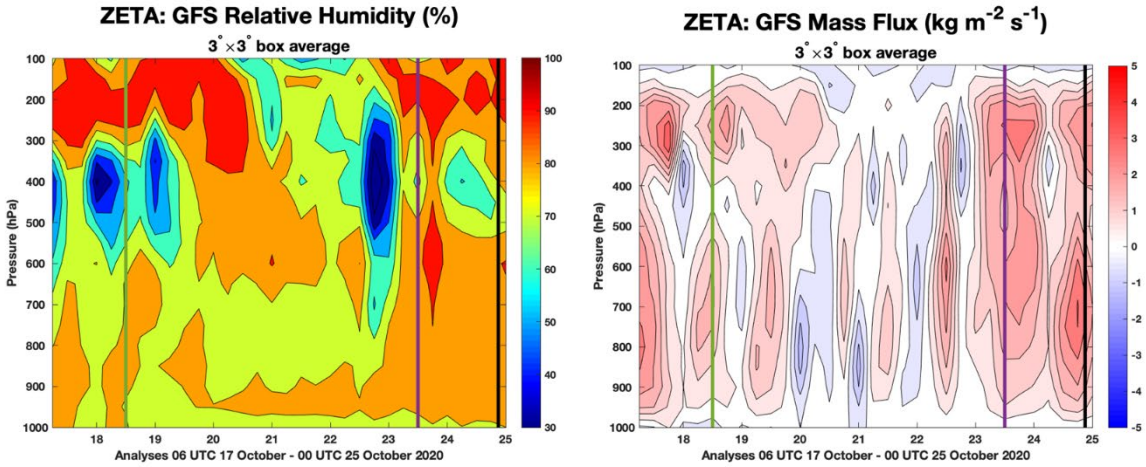

Similar to Figure 32, except for RH (left) and vertical mass flux (right). The diurnal cycle of intermittent convection is clear in the vertical mass flux plot, and it correlates with the moistening of the atmosphere seen in the relative humidity. The effects of the amalgamation of the wave-pouch and the CAG can be seen as the decrease in RH over 21–22 October, with the increase in vertical mass flux and RH corresponding to the formation of the precursor pouch on 23 October prior to Zeta forming as a TD at 12 UTC 24 October 2020.

Figure 34. GFS analysis of relative humidity and vertical mass flux as time vs. height plots for Zeta's precursor

The evolution of Zeta's precursor disturbance can be seen also when the data is consolidated and graphed as a simple time series (Figure 35). The integration of the wave-pouch and the CAG is apparent in the relative humidity, equivalent potential temperature, vertical mass flux, and deep vertical wind shear plots as they dip on 21–22 October 2020 followed by an increase, signaling the building of the pouch that became Tropical Storm Zeta. The relative humidity and equivalent potential temperature show the diurnal cycling of the convective plumes as the atmosphere in turn moistens and dries out in relation to the convection. However, the trend of this convective activity shows a decrease of the area-average from 17 October 2020 into 21 October 2020 of roughly 10% in relative humidity and 4°K in equivalent potential temperature as the gyre and the pouch interact and merge. The formation of the merged pouch afterwards on 23 October 2020 is also clear as the relative humidity and equivalent potential temperature trend upwards in their diurnal cycling, with a gain of roughly 12% relative humidity and 4°K in equivalent potential temperature in the 3°×3° and 6°×6° box area-averages. The diurnal cycling of the convection is clearly visible in the vertical mass flux time series, as well as the start of the

sustained deep convection on 23 October 2020 with the upward trend of the vertical mass flux gaining roughly 10 kg m^{-2} s^{-1} over four days from 22 October 2020 to 25 October 2020. The decrease in the deep vertical wind shear of approximately 7 m s^{-1} from 17 October 2020 to 21 October 2020 accompanied the merger of the wave-pouch and the gyre. Subsequently, both types of vertical wind shear gained roughly 5 m s^{-1} as the pouch became fully organized and facilitated the start of sustained deep convection in the precursor from 23 October 2020 to 25 October 2020. The consolidation of the pouch is clear in all the plots as the final increase across all variables immediately before Zeta forms, when the pouch firmly establishes itself and the necessary ingredients for a tropical cyclone amass.

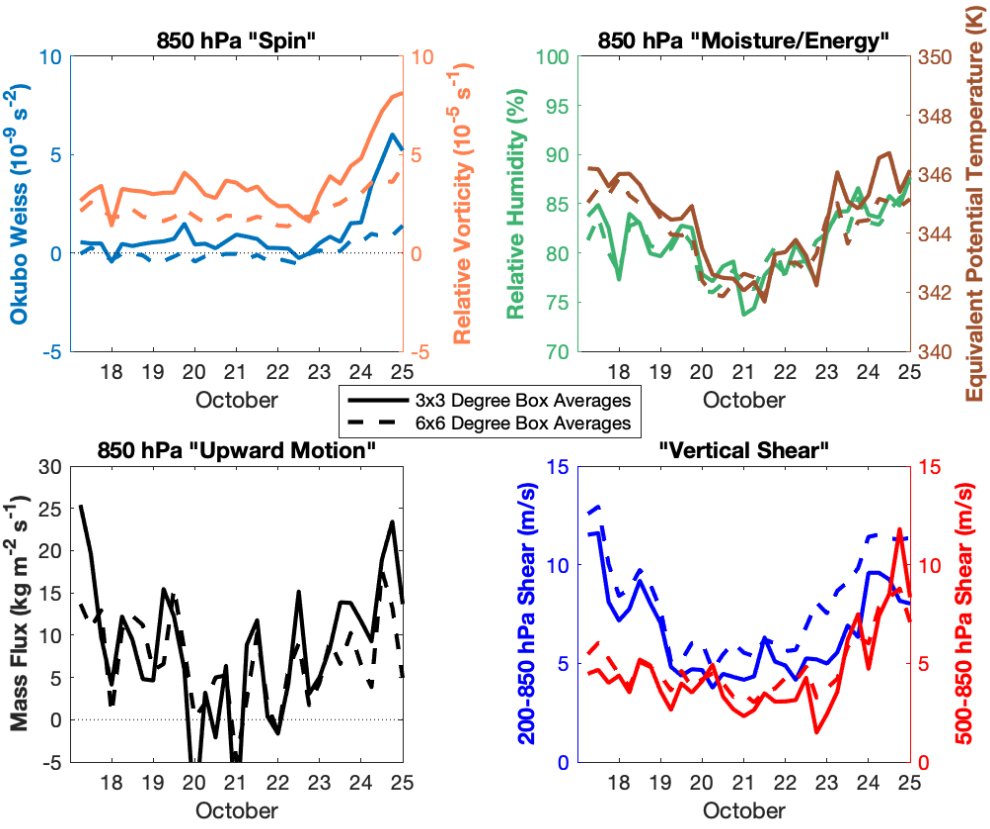

GFS Analysis of spin (upper left), moisture (upper right), upward motion (lower left), and vertical wind shear (lower right) in the area surrounding Zeta's precursor over time. The x axes for each plot represent time period the precursor was tracked from 06 UTC 17 October to 00 UTC 25 October with the respective variable shown as a time series. The interaction of the wave-pouch and CAG is visible as the dips in RH, equivalent potential temperature, and vertical mass flux on 21–22 October, with the building of the new pouch visible as the increase in all variables from 23 October 2020 onwards.

Figure 35. GFS analysis of Zeta's precursor for spin, moisture, upward motion, and vertical wind shear as time series plots

In summary: although the formation sequence of Hurricane Zeta was complex, involving principally two different atmospheric circulation structures, the precursor disturbance did clearly exhibit a fully formed pouch structure in the days prior to formation. For this, and other reasons, the formation aligned within the descriptions of the Marsupial Paradigm.

THIS PAGE INTENTIONALLY LEFT BLANK

IV. CONCLUSIONS

Tropical cyclones are a both a danger to ships and shore infrastructure and a challenging problem for forecasters. The Marsupial Paradigm seeks to expand the bevy of knowledge available to forecasters and to give them the tools to understand the processes that govern the formation of tropical cyclones. The Marsupial Paradigm gives the framework to understand how a pouch protects the nascent tropical cyclone from the deleterious effects of environmental vertical wind shear and dry air entrainment while nurturing the growth of deep convection within. This allows the disturbance to deepen and grow until it becomes self-sustaining as a tropical cyclone.

The three storms examined in this study, though showcasing different methods of formation, all adhere to the tenets of the Marsupial Paradigm. Although, these storms formed in the Caribbean Sea, they can still be analyzed and tracked within the same framework that has been used on storms that form in open ocean. That the storms formed within such close geographical boundaries and such a tight time frame make them ideal to analyze and compare as they have more similarities in their backgrounds than differences. They all formed within the southwest side of the Caribbean Sea late in the traditional Atlantic hurricane season in 2020. They all had a tropical wave associated with their formations. They all formed in relatively quick fashion, and after formation, all three storms experienced a rapid intensification period (Blake et al. 2021, Latto 2021, Stewart 2021). These three storms usefully illustrate how their similarities, small differences can make marked contributions to tropical cyclone formation.

Hurricane Iota was the most typical storm analyzed. Heeling close to the principles outlined in the Marsupial Paradigm, Iota formed in a way that would be typically expected of an Atlantic hurricane. Iota developed from an African Easterly wave that traversed the Atlantic Ocean, entered the extremely warm waters of the Caribbean, developed a pouch, and formed into a hurricane. Iota also had a pouch at 700 hPa early on, which correlates with the work of Wang and Hankes (2013), who found that for disturbances that come from waves off Africa, even though the development occurred in the lower levels. It is this formation structure that aligns with the “bottom-up” hypothesis of the Marsupial Paradigm.

Iota demonstrated a classic tropical cyclone formation and aligned very closely with the Marsupial Paradigm.

Hurricane Gamma, contrastingly, developed from the interaction of a tropical wave with a low-level vorticity strip that rolled up in the formation process. This is a formation type that was also outlined by Dunkerton et al. (2009) in the Marsupial Paradigm. The low-level vorticity strip reoriented itself from an east-west orientation to a north-south orientation along the trough axis and was then pulled into the center of the pouch as the prelude to tropical cyclone formation. But it was not solely the roll-up that led to the formation of Gamma, because at the same time that the vorticity strip was rolling up, the tropical wave that had previously entered the Caribbean Sea was aligning itself directly over the sweet spot of the pouch that was associated with the vorticity roll-up. It is difficult to speculate on whether either disturbance would have resulted in a tropical cyclone formation on its own, but the interaction of the two directly led to the formation of Gamma in this instance. Either way, both the vorticity roll-up and formation from a tropical wave are cases that are known by and described by the Marsupial Paradigm, and the pouch structure that became Gamma was quite evident. So, the Marsupial Paradigm appears qualitatively to help understand the formation of Hurricane Gamma.

Hurricane Zeta had the most unusual formation circumstances, forming from the interaction of a tropical wave-pouch with a Central American Gyre. Although the effects of a Central America Gyre were not explicitly discussed by Dunkerton et al. (2009), the Marsupial Paradigm is still accurate when the gyre is viewed as a pouch.

Though it was rather larger than the pouches studied previously, the gyre exhibited all the characteristics of a low-level pouch, such as a closed circulation and an intersection of the critical latitude and trough axis with centralized peak levels of OW and relative vorticity, though it did not extend vertically past 850 hPa. Thus, the formation of Zeta can still be explained with the Marsupial Paradigm, especially in regard to the low-level development of the wave-pouch and the subsequent interaction of the wave-pouch and the Central American Gyre as essentially having occurred between two pouches.

Although the Marsupial Paradigm was originally designed for the more common open ocean-forming storms in the Atlantic, there is value in its application to storms that form in other source regions, such as the Caribbean Sea. The Marsupial Paradigm can be used in the Caribbean Sea to improve operational forecaster's dynamical kinematic understanding of the flow field, which can improve their ability to analyze possible areas of development in a timely and accurate manner. The pouch structures seen in this study developed relatively quickly, but the ability to identify which disturbances may become destructive tropical cyclones should enable the communities that live in the Caribbean Sea and the Gulf of Mexico more time to prepare for their impact.

A. OPERATIONAL IMPACT AND SUMMARY

Operationally, the Marsupial Paradigm, with its co-moving view, gives forecasters the ability to enhance their understanding of the atmosphere in near-real time with forecast products. This viewpoint provides context to their satellite observations and can improve their forecasts by showing where a likely tropical cyclone may form. The Marsupial Paradigm can be used in conjunction with the current dynamical models in use for forecasting tropical cyclones to provide additional analysis of forecast development areas. This can lead to the ability to discriminate tropical waves that will develop from tropical waves that do not on the order of hours to days. This is especially important for source regions, such as the Caribbean Sea, that are notoriously hard to forecast. While this study is not a complete review of every storm to come from the Caribbean Sea during the 2020 or other seasons, there are a few key points that may prove useful in follow-on work.

1. An incoming tropical wave may or may not develop into a tropical cyclone, but there must be a pouch that facilitates that development. This pouch may come from the wave itself or from an outside feature that interacts with the wave.

2. The vorticity strip seen in Gamma is not an atypical phenomenon, as similar formations were observed in the work by Dunkerton et al. (2009). This phenomenon may contribute to the formation of Caribbean tropical cyclones by adding to the vorticity available to the disturbance, and further

building pouches in the vertical associated with interacting tropical waves. A sign of such an occurrence is a vorticity roll-up.

3. Central American Gyres are known phenomena in the Caribbean Sea. The low-level vorticity they possess may contribute to and enhance the formation of an incoming tropical wave into a tropical cyclone, as seen with Zeta. Tracking the interaction between such gyres and tropical waves could lead to enhanced early forecasting of tropical depressions in this region.

B. OPPORTUNITIES FOR FUTURE WORK

The formation region of the Caribbean Sea is unusual in that it is not as common a place to form as the open Atlantic Ocean. When combined with the fact that much of previous hurricane formation research was focused on the open ocean and more northerly areas, there is much work to be done on the way that storms form in the Caribbean. Although this study delved into the particulars of three storms in the late season Caribbean of 2020, there are many more storms from the same formation area to research, both from the 2020 season and prior seasons. A more robust catalogue of storms that formed in the Caribbean would allow for a more comprehensive comparison and collection of data on how common each of these formation types is.

The concept of the vorticity roll-up as it relates to tropical cyclone formation is not new, but it is an area where more research and data could be of value. A concerted effort to identify areas, such as the northern tip of Colombia, that produce vorticity streamers in the tropics might lead to a valuable comparison on the formation of pouches and their subsequent tropical cyclones on a more global scale. This could then be used to expand the understanding and utilization of the Marsupial Paradigm.

Similarly, regarding the role of vorticity roll-up phenomenon, the effects of the Central American Gyre and other similar gyres, such as monsoon gyres may provide a useful opportunity for further research. Do other gyres in tropical areas enhance the development as analyzed in the case of Zeta? Is there a baseline mechanism that can be applied to many different areas across the world? These are questions that have not yet

been, to my knowledge, answered, but perhaps in the future may be answered with further research.

Finally, there is much work to be done in order to operationalize the Marsupial Paradigm and make it available to tropical forecasters. Initially, access to the co-moving framework and tracking protocols could allow forecasters to see precursors develop in near-real time. With the auto-tracker currently employed by the Montgomery Research Group, it only analyzes the 00 UTC GFS run each day. Improvements could be made to both the speed and capacity of the programming to run automatically more often than one a day. As time goes on, and more data sets are analyzed, the pouch-tracking algorithm may also be improved to provide better discrimination between those pouches that develop and those that do not. Another leap towards operationalization would be to develop a way to determine the sweet spot of a pouch from real-world observations vice solely GFS forecasts. This currently is unfeasible without flying an instrumented plane through the disturbance, which is costly, inefficient, and difficult to do due to lack of available assets. In the future, however, such a tool, such as reusable long-distance drone, could provide observational data to build the Marsupial Paradigm and allow for future forecasters to build a track of a potential tropical cyclone earlier.

THIS PAGE INTENTIONALLY LEFT BLANK

APPENDIX. TOTAL PRECIPITABLE WATER PRODUCTS

Total precipitable water content products from the University of Wisconsin – Madison (2021) were used in the analysis, but not included in the main body of this paper. These products were accessed at: http://tropic.ssec.wisc.edu/real-time/mtpw2/product.php?color_type=tpw_nrl_colors&prod=global2&timespan=24hrs&anim=html5. The primary method of viewing these products was as a video, as it provides a continuity between forecast periods and is an easy-to-use visual way to compare positions in time. This appendix includes a few snapshots in time of important events in the formation of each storm as a demonstration in lieu of the videos used in the analysis.

A. IOTA

Tracking Iota's precursor with the TPW products began at 00 UTC 30 October 2020 and went until 18 UTC 13 November 2020. The video depicts the tropical waves travel across the Atlantic Ocean and the formation of Iota. Figure 36 is a still image of the tropical wave crossing the Atlantic at 19 UTC 3 November 2020.

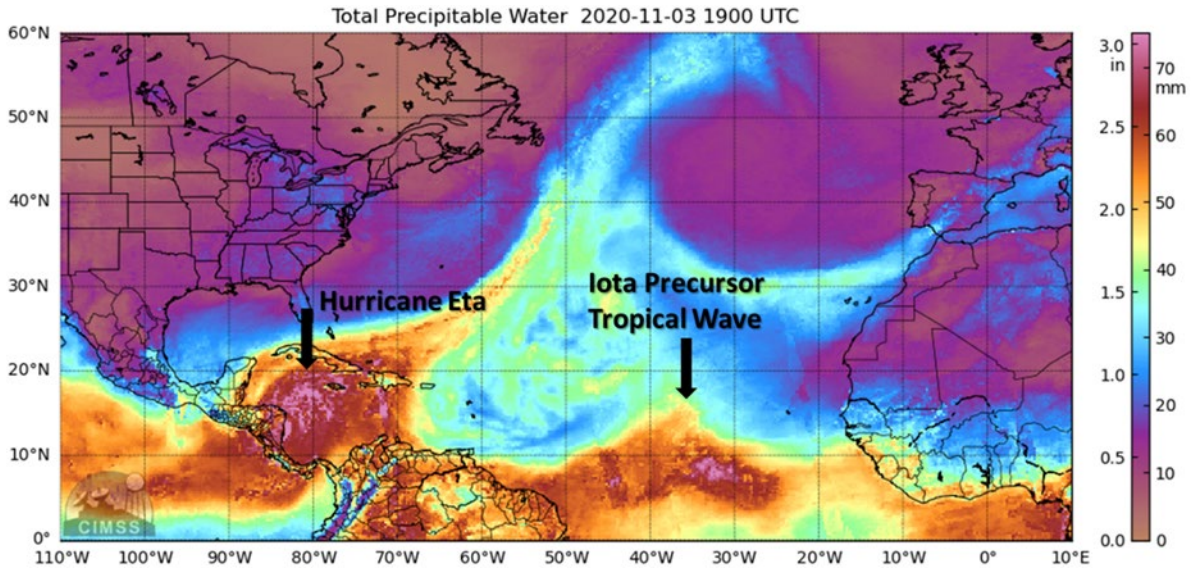

Depiction of the TPW at 19 UTC 03 November 2020. The tropical wave is visible at low latitudes in the Mid-Atlantic, and Hurricane Eta is visible in the Caribbean Sea.

Figure 36. TPW product of Iota's precursor at 19 UTC 03 November 2020.

Iota formed directly from a tropical wave without any interaction with other atmospheric vortical structures. Figure 37 shows Iota's precursor 16 hours before formation as a tropical depression. It is clearly defined and visible in the Caribbean Sea.

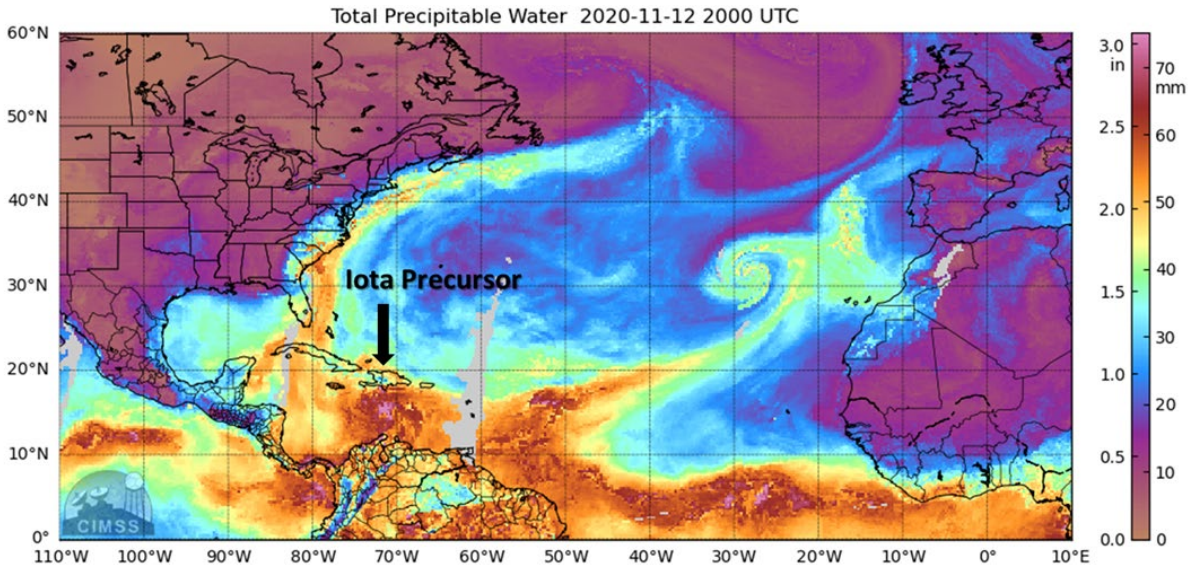

Depiction of the TPW at 20 UTC 12 November 2020. Iota's precursor is clear in the Caribbean Sea. This is 16 hours prior to formation as a tropical depression.

Figure 37. TPW product of Iota's precursor at 20 UTC 12 November 2020.

B. GAMMA

Tracking of Gamma's precursor with TPW products covered the time period from 00 UTC 21 September 2020 to 15 UTC 1 October 2020. Figure 38 shows the tropical wave associated with Gamma's formation traversing the Caribbean Sea at 00 UTC 29 October 2020.

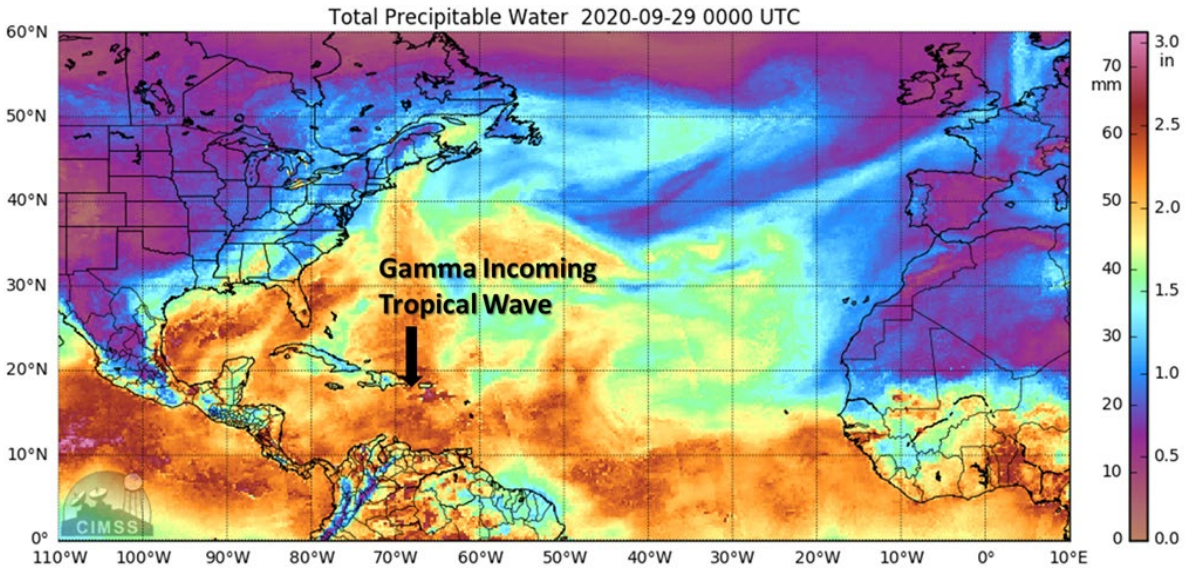

Depiction of the TPW at 00 UTC 29 September 2020. The tropical wave associated with Gamma's precursor is visible in the Caribbean Sea.

Figure 38. TPW product of Gamma's precursor at 00 UTC 29 September 2020.

The incoming tropical wave in the Gamma case interacted with a low-level strip of vorticity off the coast of Panama and Colombia before coalescing as a tropical depression. Figure 39 depicts Gamma at the time that it formed as a tropical depression at 18 UTC 2 October 2020.

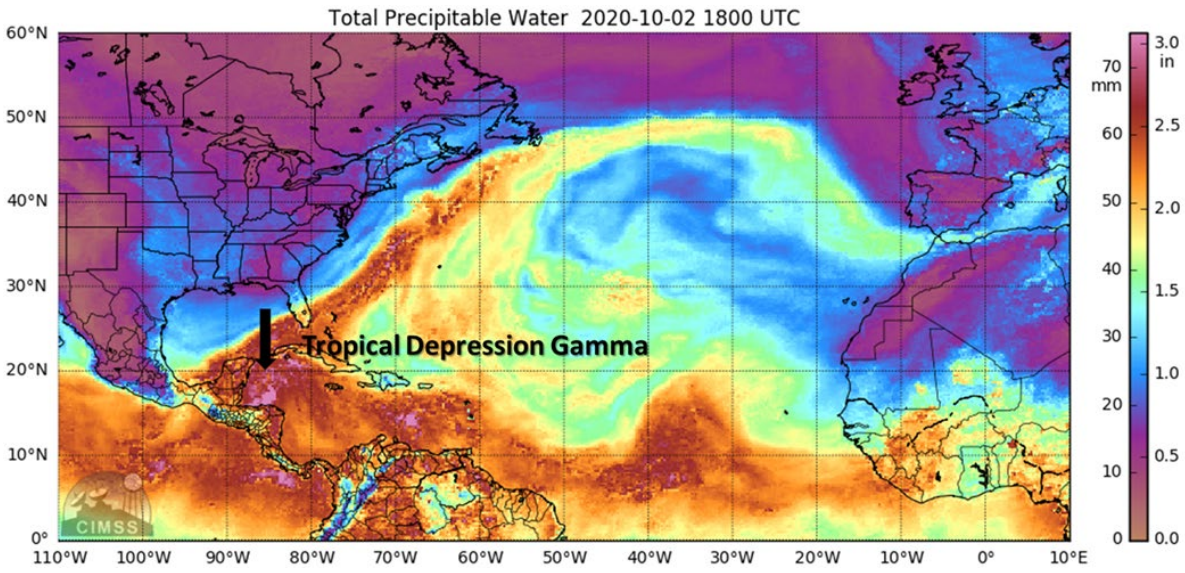

Depiction of the TPW at 18 UTC 02 October 2020. Tropical Depression Gamma can be seen as the area in the Caribbean Sea with the most TPW content.

Figure 39. TPW product of Gamma's precursor at 18 UTC 02 October 2020.

C. ZETA

Tracking of Zeta's precursor with TPW products covered the time period from 00 UTC 15 October 2020 to 21 UTC 24 October 2020. The tropical wave associated with Zeta's precursor can be seen in Figure 40.

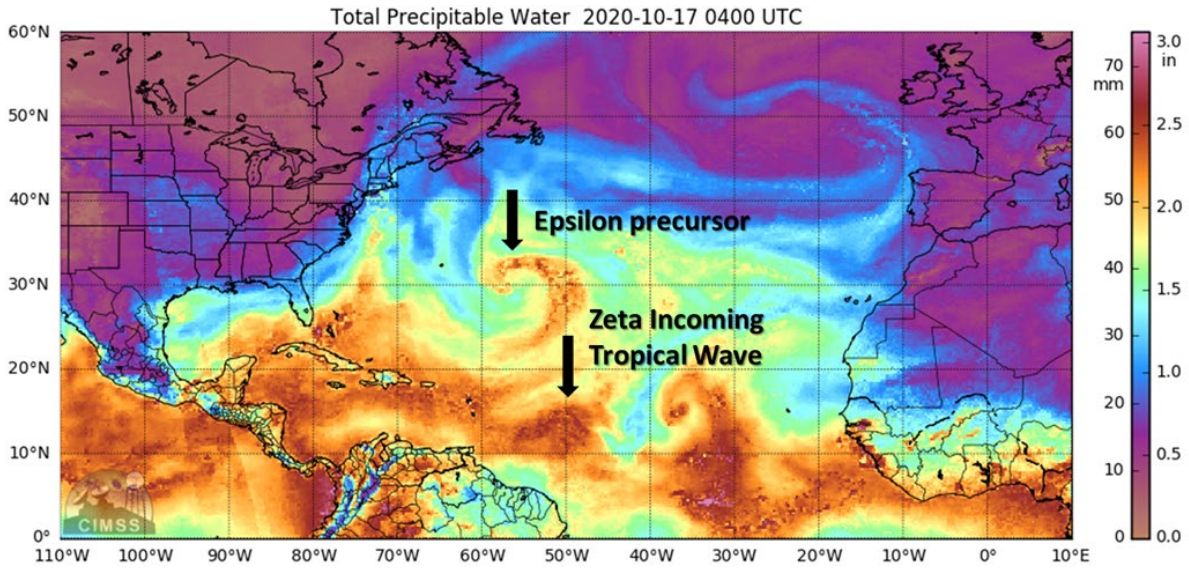

Depiction of the TPW at 04 UTC 17 October 2020. The tropical wave associated with Zeta's precursor is clearly visible in the low-latitude Mid-Atlantic. The pouch structure that would be Epsilon is visible in the Mid-Atlantic at approximately 30°N, 56°W.

Figure 40. TPW product of Zeta's precursor at 04 UTC 17 October 2020.

Zeta's formation was caused by an interaction between an incoming tropical wave and a low-level Central American Gyre in the southwestern Caribbean Sea. This was a prolonged interaction, taking several days, but a still of it can be seen in Figure 41 at 03 UTC 21 October 2020. The area of high TPW in the Caribbean Sea contains both the incoming wave and the Central American Gyre, which are not distinguishable from each other in this product. Nevertheless, the area of high TPW does correlate with the area of relative vorticity and OW that was consolidated into Zeta.

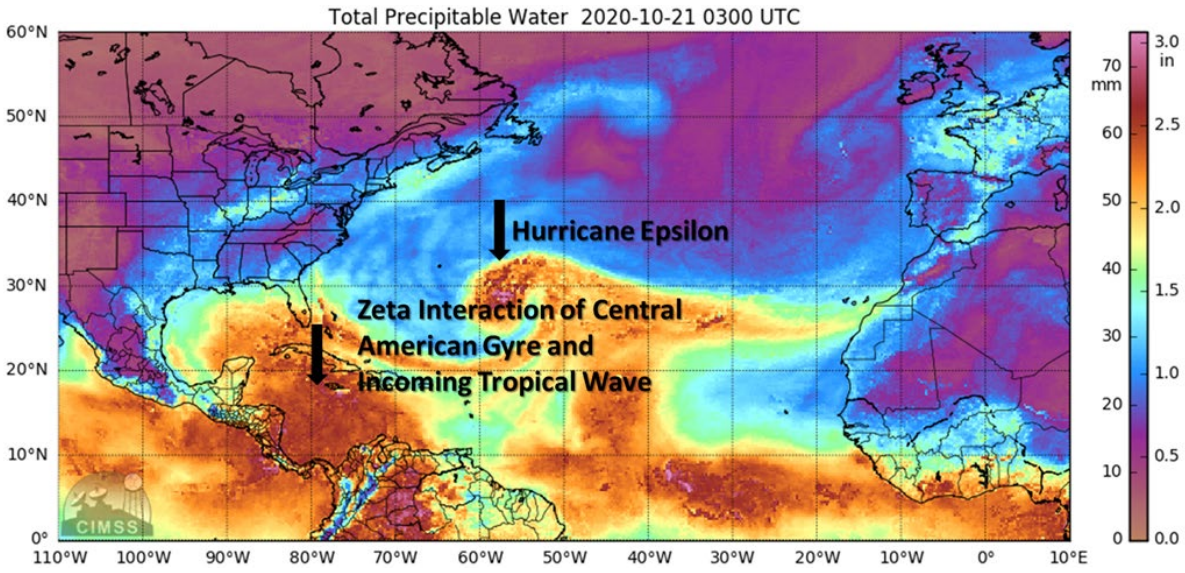

Depiction of the TPW at 03 UTC 21 October 2020. The tropical wave and Central American Gyre that interact to become Zeta are visible as the area of high TPW in the Caribbean Sea, although the two elements are indistinguishable from each other in this view. Hurricane Epsilon is clearly visible in the Mid-Atlantic at approximately 30°N, 58°W.

Figure 41. TPW product of Zeta's precursor at 03 UTC 21 October 2020.

Zeta's precursor consolidated the effects of both the Central American Gyre and the pouch associated with the incoming tropical wave to become Zeta. This can be seen in Figure 42 as the area of high TPW in the Bay of Campeche represents the Tropical Depression Zeta. Figure 42 is at 14 UTC 24 October 2020, approximately two hours after becoming a tropical depression.

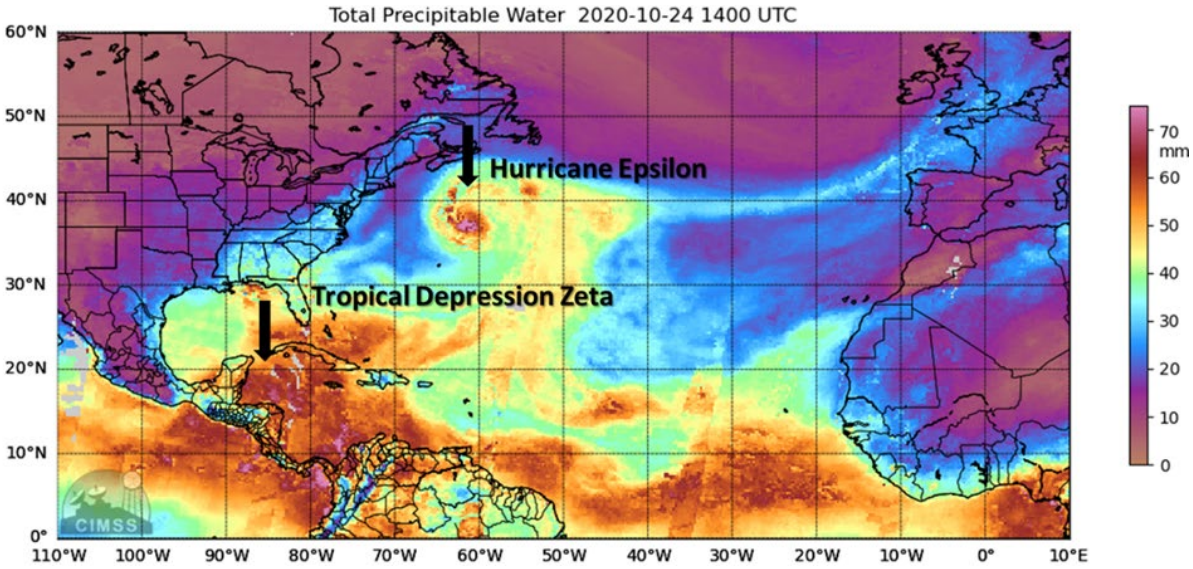

Depiction of the TPW at 14 UTC 24 October 2020. Tropical Depression Zeta is clearly visible in the Bay of Campeche. Hurricane Epsilon is clearly visible in the Mid-Atlantic at approximately 38°N, 62°W.

Figure 42. TPW product of Zeta's precursor at 14 UTC 24 October 2020.

THIS PAGE INTENTIONALLY LEFT BLANK

LIST OF REFERENCES

American Meteorological Society, 2012, "Velocity Potential." Glossary of Meteorology, https://glossary.ametsoc.org/wiki/Velocity_potential.

American Meteorological Society, 2014, "Vorticity." Glossary of Meteorology, https://glossary.ametsoc.org/wiki/Vorticity.

Beven, J. L., R. Berg, and A. Hagen, 2019: Hurricane Michael (AL142018). National Hurricane Center Tropical Cyclone Report, 86 pp, https://www.nhc.noaa.gov/data/tcr/AL142018_Michael.pdf

Blake, E., R. Berg, and A. Hagen, 2021: Hurricane Zeta (AL282020). National Hurricane Center Tropical Cyclone Report, 56 pp, https://www.nhc.noaa.gov/data/tcr/AL282020_Zeta.pdf

Britton, S., 2021: An exploration of the Marsupial paradigm in developing African easterly waves from 2020: Josephine, Isaias, and Laura. M.S. Thesis, Dept. of Meteorology, Naval Postgraduate School, 108 pp, http://hdl.handle.net/10945/67674 .

Bove, M. C., J. B. Elsner, C. W. Landsea, X. Niu, and J. J. O'Brien, 1998: Effect of El Niño on U.S. Landfalling Hurricanes, Revisited, *Bull. Amer. Meteor. Soc*., **79**, 2477–2482, https://doi.org/10.1175/1520-0477(1998)079%3C2477:EOENOO%3E2.0.CO;2.

Carr, L. E. and R. L. Elsberry, 1995: Monsoonal interactions leading to sudden tropical cyclone track changes. *Mon. Wea. Rev.* 123, 265–289, https://doi.org/10.1175/1520-0493(1995)123<0265:MILTST>2.0.CO;2

Dunkerton, T. J., M. T. Montgomery, and Z. Wang, 2009: Tropical cyclogenesis in a tropical wave critical layer: easterly waves. *Atmos. Chem. Phys.,* 9, 5587–5646.

Elsberry, R. L., W. M. Frank, G. J. Holland, J. D. Jarrell, and R. L. Southern, 1985: A global view of tropical cyclones. Office of Naval Research, 57 pp.

Goldenberg, S. B., and L. J. Shapiro, 1996: Physical mechanisms for the association of El Niño and West African rainfall with Atlantic major hurricane activity. *J. Climate*, **9**, 1169–1187, https://doi.org/10.1175/1520-0442(1996)009%3C1169:PMFTAO%3E2.0.CO;2.

Gray, W. M. 1975: Tropical Cyclone Genesis. CSU-ASTP-234, 121 pp, http://hdl.handle.net/10945/32587

Gray, W. M., 1984: Atlantic Seasonal Hurricane Frequency. Part I: El Niño and 30 mb Quasi-Biennial Oscillation Influences, *Mon. Wea. Rev*., **112**, 1649–1668, https://doi.org/10.1175/1520-0493(1984)112%3C1649:ASHFPI%3E2.0.CO;2.

Inman, J. W., 1835: *Navigation and Nautical Astronomy for the Use of British Seamen.* C. and J. Rivington, 260 pp.

Klotzbach, P. J., 2010: On the Madden-Julian Oscillation-Atlantic hurricane relationship. *J. Climate,* 23, 282–293, https://doi.org/10.1175/2009JCLI2978.1

Klotzbach, P. J., and Coauthors, 2021: A hyperactive end to the Atlantic hurricane season: October-November 2020. *Bull. Amer. Meteor. Soc.,* https://doi.org/ 10.1175/BAMS-D-20-0312.1.

Latto, A. S., 2021: Hurricane Gamma (AL252020). National Hurricane Center Tropical Cyclone Report, 20 pp, https://www.nhc.noaa.gov/data/tcr/ AL252020_Gamma.pdf

Montgomery, M. T., and R. J. Kallenbach, 1997: A theory for vortex rossby-waves and its application to spiral bands and intensity changes in hurricanes. *Q. J. Roy. Met. Soc.,* **123**, 435–465, https://doi.org/10.1002/qj.49712353810.

Montgomery, M. T., L. L. Lussier III, R. W. Moore, and Z. Wang, 2010: The genesis of Typhoon Nuri as observed during the Tropical Cyclone Structure 2008 (TCS-08) field experiment – Part 1: The role of the easterly wave critical layer. *Atmos. Chem. Phys.*, **10**, 9879–9900. https://doi.org/10.5194/acp-10-9879-2010.

Montgomery, M. T., and Coauthors, 2012: The pre-Depression Investigation of Cloud-Systems in the Tropics (PREDICT) Experiment: Scientific Basis, New Analysis Tools, and Some First Results. *Bull. Amer. Met. Soc.*, **93**: 153–172, https://doi.org/10.1175/BAMS-D-11-00046.1.

Papin, P. P, L, F. Bosart, and R. D. Torn, 2017: A climatology of Central American gyres. *Mon. Wea. Rev.,* **145**, 5, 1983–2000, https://doi.org/10.1175/MWR-D-16-0411.1

Reeves, M. M., 2019: Tyndall AFB continues rebuild effort one year after Hurricane Michael, United States Air Force, 1, https://www.af.mil/News/Article-Display/ Article/1985948/tyndall-afb-continues-rebuild-effort-one-year-after-hurricane-michael/.

Rice, D., 2008: Storm alert: ‘Pouches’ protect embryonic hurricanes, USA Today, 1.

Stewart, S. R., 2021: Hurricane Iota (AL312020). National Hurricane Center Tropical Cyclone Report, 48 pp, https://www.nhc.noaa.gov/data/tcr/AL312020_Iota.pdf

United States Senate, 2018: United States Navy and Marine Corps readiness, *115th Cong*. Washington, D.C., United States Congress, 1–109, https://www.congress.gov/115/chrg/CHRG-115shrg42873/CHRG-115shrg42873.pdf.

University of Wisconsin – Madison, 2021: Real-time Product View: Total Precipitable Water, Accessed 15 October 2021, http://tropic.ssec.wisc.edu/real-time/mtpw2/product.php?color_type=tpw_nrl_colors&prod=global2&timespan=24hrs&anim=html5.

Wang, Z., I. Hankes, 2013: Characteristics of tropical easterly wave pouches during tropical cyclone formation. *Mon. Wea. Rev.*, **142**, 626–633, jttps://doi.org/10.1175/MWR-D-13-00267.1

Williams, I. N., and C. M. Patricola, 2018: Diversity of ENSO events unified by convective threshold sea surface temperature: A nonlinear ENSO index. *Geophys. Res. Lett.*, **45**, 9236–9244. https://doi.org/10.1029/2018GL079203.

THIS PAGE INTENTIONALLY LEFT BLANK

INITIAL DISTRIBUTION LIST

1. Defense Technical Information Center
   Ft. Belvoir, Virginia

2. Dudley Knox Library
   Naval Postgraduate School
   Monterey, California